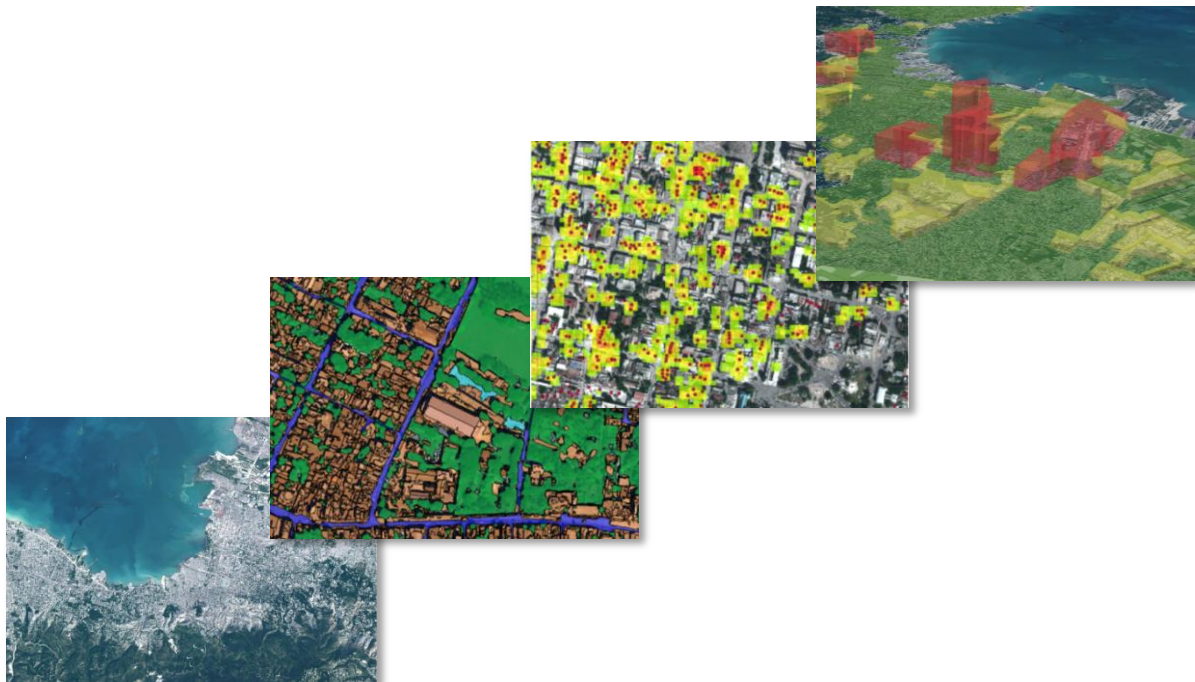




Diploma Thesis

**Rapid Mapping for Earthquake Disasters-
A Team-based Method for Visual Damage Assessment
Using Optical VHSR Satellite Data**



by
Stefan Klett

The cover illustration shows starting from the lower left corner:

Satellite Image of Port-au-Prince and Carrefour (source: GeoEye-1 – 13.10.2010, true colour display, ground resolution 0.5 m)

Object-based Classification Result (supporting information of a subset in Carrefour, source: Own illustration)

Kernel Density Estimation of Visual Damage Assessment (results of the focus groups in central Port-au-Prince, source: Own illustration)

3-D rendered Visualisation of Damage Assessment (extruded city blocks indicate damage count, source: Own illustration)

Eberhard Karls University of Tuebingen

Institute of Geography

–

Chair of Physical Geography and GIS

Diploma Thesis

**Rapid Mapping for Earthquake Disasters-
A Team-based Method for Visual Damage Assessment
Using Optical VHSR Satellite Data**

Submitted in June 2011 by:

Stefan Klett

SUPERVISORS:

1. Supervisor: Prof. Dr. Volker Hochschild (University of Tuebingen)
2. Supervisor: Dr. Tobias Schneiderhan (Centre for Satellite Based Crisis Information, DLR)

*The great jazz ensemble has talent and a shared vision,
but what really matters is that the musicians know how
to play together*

Peter M. Senge, *The Fifth Discipline*, 1990

Restriction note

This thesis contains internal and confidential information of the German Aerospace Centre (DLR). The transmission of the entire thesis, or parts of its content, as well as reproductions or copies – also in digital form – is strictly prohibited. Exemption clauses are subject to permission in written form of the German Aerospace Centre and the author.

Sperrvermerk

Die vorliegende Arbeit beinhaltet interne vertrauliche Informationen des Deutschen Zentrums für Luft- und Raumfahrt e.V.. Die Weitergabe des Inhalts der Arbeit, im Gesamten oder in Teilen, sowie das Anfertigen von Kopien oder Abschriften – auch in digitaler Form – sind grundsätzlich untersagt. Ausnahmen bedürfen der schriftlichen Genehmigung des Deutschen Zentrums für Luft- und Raumfahrt e.V. und des Autors.

Acknowledgements

First and foremost I want to express my gratitude to Dr. Tobias Schneiderhan for being my secondary supervisor and giving me the possibility to write my thesis at the Centre for Satellite Based Crisis Information. He gave me the chance to get insights into backgrounds and coherences of international humanitarian aid. In addition, his scientific input and remarks were of particular value for the thesis. I am equally grateful to Prof. Dr. Volker Hochschild who agreed to be my primary supervisor. His confidence and support in a position for me as an assistant instructor and tutor in the Geography Department at the University of Tübingen. I would also like to thank him for promoting the cooperation with DLR.

I should also like to thank Dr. Sandro Martinis of ZKI for valuable advice and support concerning eCognition environment and implementation of the architect solution. Similarly I want to thank André Twele of ZKI for very useful advice in the area of remote sensing, especially in image processing. And I am grateful to the whole ZKI-team for the privilege of being part of it and the contribution to the statistical analysis.

I would like to thank Dr. Hannes Taubenböck, Dr. Thomas Esch and Dr. Thorsten Andresen of DLR for their consultation, help and scholarly debates.

Thank you to my colleague Felix Reinsch, who supported me with technical advice for the implementation of object-based classification, and to Andre Kalia for vast and fruitful discussions on your balcony and further input that enriched this thesis. And to all the other guys of BV-Labor.

I want to thank my correctors Antonia Herzog, Friederike Hubschneider and Paul Kahle who showed me the fine art of English writing.

I am particularly grateful to my parents, who gave me sufficient freedom to walk my way and shape my own personality. I would also like to express my gratitude to my brothers, without whose support I would have been deprived of this unique chance.

Thank you Lise for your selfless endorsement. Your moral assistance and mental support are unrivalled. Moreover I thank you for making me laugh and appreciate every day.

Contents

Restriction note	I
Acknowledgements	II
Contents	III
List of Figures.....	V
List of Tables	VII
Acronyms and Abbreviations.....	VIII
1 Introduction	1
1.1 The Research Challenge	5
1.2 Objectives.....	6
1.3 Thesis Outline.....	7
2 Fundamentals and State of the Art	9
2.1 Study Area and Data	9
2.2 The Earthquake Event	11
2.2.1 Earthquakes	11
2.2.2 Actual Situation.....	13
2.3 Fundamentals of Remote Sensing.....	15
2.3.1 High Resolution Sensors – Principles and State of the Art.....	17
2.3.2 Digital Image Processing	19
2.4 Digital Classification Procedures.....	19
2.4.1 Pixel-based Image Analysis.....	19
2.4.2 Object-based Image Analysis	20
2.4.3 Object-based Accuracy Assessment	23
2.5 Building Detection using Remote Sensing Methods.....	24
2.6 Visual Interpretation of Remote Sensing Data	26
2.7 Earth Observation and Disaster Management	28
2.8 Fundamentals of Team-based Methods.....	31
3 Rapid Mapping.....	33

3.1	User Requirements for Map Products	36
3.2	Usability of Different Sensors and Resolutions for EQ Emergency Response/ damage assessment	38
3.3	Damage Assessment.....	40
3.3.1	The Case of Haiti.....	44
3.3.2	Limitations of Remote Sensing for EQ Damage Assessment.....	46
4	A Team-based Method for Damage Assessment	50
4.1	Supporting Information	53
4.2	Developing a Team-based Method	57
5	Visualisation of Damaged Buildings.....	62
5.1	Illustration Facilities	64
5.2	Spatial Relations of Data Representation	69
6	Results and Discussion.....	72
6.1	Rapid Mapping	72
6.2	Team-based Method.....	73
6.2.1	Classification	74
6.2.2	Accuracy Assessment	78
6.2.3	Developing a Team-based Method.....	81
6.3	Visualisation	87
7	Conclusion and Outlook.....	93
7.1	Conclusions.....	93
7.2	Outlook.....	94
	References.....	96
	Internet Resources	103
	Declaration	104
	Appendix	A

List of Figures

Figure 1.1: Number of fatalities by type of event and by region 1970-2010.....	1
Figure 1.2: Cumulative damage from disasters scaled by GDP 1970 to 2008.....	2
Figure 1.3: Exposure to earthquakes and cyclones from 2000 until 2050.....	2
Figure 1.4: Satellite-based damage assessment map of Port-au-Prince, Haiti.....	4
Figure 2.1: Study area Port-au-Prince, Haiti.....	10
Figure 2.2: Seismic waves spread out into all directions from the seismic centre.....	11
Figure 2.3: Tectonically setting of the Hispaniola Island.....	12
Figure 2.4: Complete destruction of a concrete building in Haiti.....	13
Figure 2.5: Population movement out of Port-au-Prince as of 24 January 2010.....	14
Figure 2.6: IDP camp in Port-au-Prince.....	15
Figure 2.7: Spectral characteristics of energy sources, atmospheric transmittance and common remote sensing systems.....	16
Figure 2.8: Problems with VHSR satellite data.....	18
Figure 2.9: Three-dimensional feature space for multi-spectral classification.....	20
Figure 2.10: Modular framework for an object-oriented urban land-cover classification....	22
Figure 2.11: Iteration process of visual interpretations.....	27
Figure 2.12: Operational loop of the International Charter on Major Disasters.....	30
Figure 3.1: Trends in number of reported events.....	33
Figure 3.2: Disaster Management Cycle.....	34
Figure 3.3: Rapid Mapping workflow of ZKI.....	36
Figure 3.4: Pre- and post-disaster comparison of a collapsed building in Carrefour.....	38
Figure 3.5: Classification of damage to masonry buildings according to the EMS.....	41
Figure 3.6: Damage assessment workflow.....	42
Figure 3.7: Detailed damage assessment map of Port-au-Prince.....	45
Figure 3.8: Still intact roofs of a settlement in Port-au-prince hide crushed sidewalls from the interpreter.....	47
Figure 3.9: Comparison of an aerial photograph and a ground photograph of the EQ in Kobe/Japan in 1995.....	47
Figure 3.10: Examples of middle storey collapse resulting from the EQ in Kobe/Japan in 1995.....	48
Figure 4.1: Comparison of machine-based and manual interpretation.....	50
Figure 4.2: Communication between action and rule-set.....	54
Figure 4.3: GUI of the eCognition architect action library.....	55
Figure 4.4: Scale parameters used for hierarchical classification of image objects on a subset of the GeoEye-1 image.....	56

Figure 4.5: Spectral thresholds of selected classes in the modified GUI of the eCognition feature space plot	57
Figure 4.6: Multi-temporal analysis using the swipe tool	59
Figure 5.1: Timeline of damage assessment maps in response to the Haiti EQ.....	64
Figure 5.2: Damage assessment maps of Port-au-Prince/Carrefour	68
Figure 5.3: Distorted data representation caused by interpolation.....	69
Figure 5.4: Illustration facilities and comparison of block-based damage estimation	70
Figure 6.1: OBIA classification of Carrefour using the architect solution.....	75
Figure 6.2: Classification example of a GeoEye-1 subset in Carrefour, Haiti.....	76
Figure 6.3: Illustrative examples of common problems for OBIA in the Haiti case	78
Figure 6.4: Over-segmentation due to patch-work roofs and chimneys	80
Figure 6.5: Comparison of MPAR values.	81
Figure 6.6: Kernel density of interpretation results	83
Figure 6.7: Normal distribution probability density function of interpretation results.....	85
Figure 6.8: Multi-user data management for team-based damage assessment	86
Figure 6.9: Presentation of single house damages in an interactive PDF	88
Figure 6.10: Comparison of grid-based and block-based damage assessment.....	89
Figure 6.11: Block-based quantitative damage assessment of Carrefour.....	90
Figure 6.12: Combined qualitative and quantitative representation of damage numbers utilising three-dimensional extrusion of city blocks	91

List of Tables

Table 2.1: Basic characteristics of most commonly used current VHSR sensors	18
Table 3.1: User requirements for earthquake emergency response within the SAFER framework.....	37
Table 3.2: Sensor dependent damage recognition in comparison to UNOSAT/WB/JRC ..	39
Table 6.1: Selected thresholds used for object-based classification.....	77
Table 6.2: Thematic accuracy of GeoEye-1 data classification	79
Table 6.3: Thematic accuracy of WorldView-II data classification	79

Acronyms and Abbreviations

CNES	Centre National d'Études Spatiales (French Space Agency)
COPUOS	Committee On the Peaceful Uses of Outer Space
CRED	Centre for Research on the Epidemiology of Disasters
DEM	Digital Elevation Model
DFD	Deutsches Fernerkundungsdatenzentrum (German Remote Sensing Data Centre)
DLR	Deutsches Zentrum für Luft- und Raumfahrt e.V. (German Aerospace Centre)
EMS	European Macroseismic Scale
EO	Earth Observation
EQ	Earthquake
ERCS	Emergency Response Core Service
ESA	European Space Agency
FTP	File Transfer Protocol
GDP	Gross Domestic Product
GIS	Geographic Information Systems
GMES	Global Monitoring for Environment and Security
GMT	General Mean Time
GSD	Ground Sampling Distance
GUI	Graphical User Interface
HSR	High Spatial Resolution
IDP	Internally Displaced Person
IFOV	Instantaneous Field Of View
INSPIRE	Infrastructure for Spatial Information in Europe

ISDR	International Strategy for Disaster Reduction
ISO	International Standards Organization
JRC	European Commission Joint Research Centre
K	Kappa Coefficient
KDE	Kernel Density Estimation
LIDAR	Light Detection And Ranging
M	Magnitude
MINUSTAH	Mission des Nations Unies pour la Stabilisation en Haïti (United Nations Stabilisation Mission in Haiti)
MPAR	Mean Perimeter Area Ratio
MS	Multi Spectral
NDVI	Normalized Difference Vegetation Index
NGO	Non- Governmental Organisation
NIR	Near Infrared
OBIA	Object-Based Image Analysis
OCHA	United Nations Office for the Coordination of Humanitarian Affairs
OFDA	Office of U.S. Foreign Disaster Assistance
OGC	Open Geospatial Consortium
OSM	Open Street Map
PAN	Panchromatic
PDF	Portable Document Format
PDNA	Post Disaster Needs Assessment
RIT	Rochester Institute of Technology
SAFER	Services and Applications for Emergency Response
SAR	Synthetic Aperture Radar

SERTIT	Service Régional de Traitement d'Image et de Télédétection (Regional Service of Image Treatment and Remote Sensing)
SOP	Standardised Operating Sequence
SP	Scale Parameter
TIR	Thermal Infrared
UN	United Nations
UNEP	United Nations Environment Programme
UNITAR	United Nations Institute for Training and Research
UNOOSA	United Nations Office for Outer Space Affairs
UNOSAT	UNITAR'S Operational Satellite Applications Program
UN-SPIDER	Space-based Information for Disaster Management
US	United States of America
USGS	United States Geological Survey
THW	Technisches Hilfswerk (Federal Agency for Technical Relief)
VALgEO	2nd International Workshop On Validation Of Geo-Information Products For Crisis Management
VHSR	Very High Spatial Resolution
WB	World Bank
xml	Extensible Markup Language
Z_GIS	Zentrum für Geoinformatik (Centre for GeoInformatics)
ZKI	Zentrum für Satellitengestützte Kriseninformation (Centre for Satellite Based Crisis Information)

1 Introduction

The global security risk has changed. Recently published studies substantiate a significant increase of extreme natural disasters (e.g. floods in Pakistan 2010, forest fires in Russia 2010) in course of the last decades (STROHMEYER 2010: 1, WORLD BANK 2010). More critical than the frequency of the events is the dimension of the expenses caused by disasters, in particular loss of lives. In absolute numbers, material damage occurs mainly in industrialised countries, whereas fatalities concentrate to more than 90 per cent in developing countries (see Figure 1.2 and Figure 1.1) (WORLD BANK 2010), not least due to settlement structures (EERI 2010: 3).

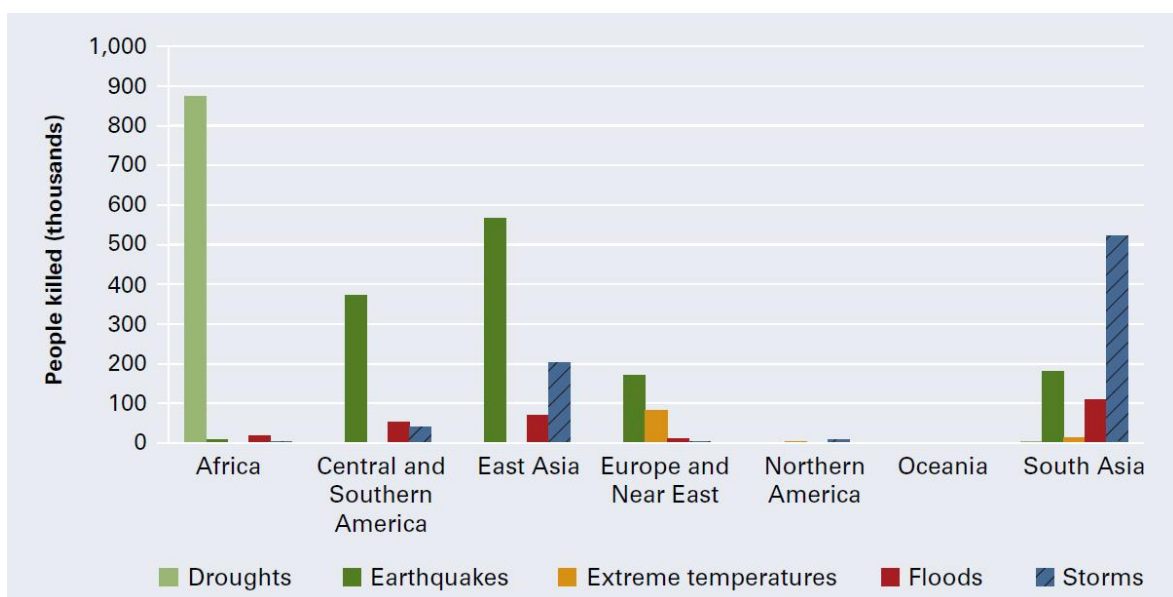


Figure 1.1: Number of fatalities by type of event and by region 1970-2010

Source: WORLD BANK 2010: 29

However, disasters cause considerably more damages in poor countries if measured by the ratio of the expenses and the gross domestic product (GDP) (cf. the earthquake that struck Haiti: 120 per cent, STROHMEYER 2010: 3). Furthermore, technical accidents, such as the oil spills in the Gulf of Mexico in 2010 as well terrorist attacks can cause incalculable damages. The danger of potential attacks on critical infrastructure such as power plants or water supplies brought about a new dimension of civil security.

Due to globalised and urbanised lifestyles throughout the world, there is a high risk of consequential damages apart from direct impacts in the aftermath of the above mentioned disasters (e.g. food shortages resulting from the fires in Russia, rise in prices of resources and limitation of global mobility, LGR/AFP/REUTERS 2010).

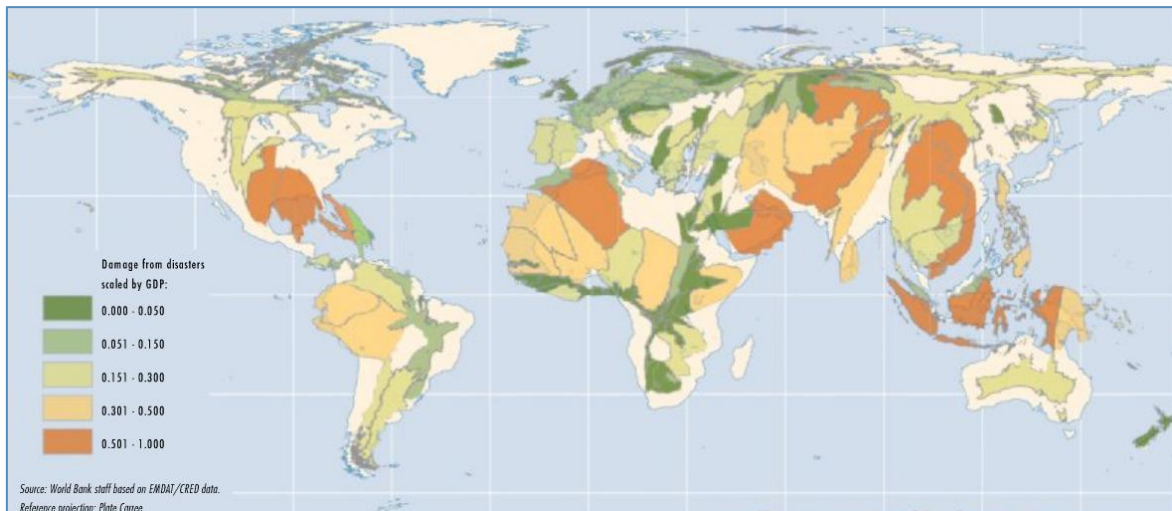


Figure 1.2: Areas reflect cumulative damage from disasters scaled by GDP for 1970 to 2008

Source: *WORLD BANK 2010: 12*

Since global population is rising, human activities are at high risk of increasing rate of natural disaster situations (VOIGT ET AL. 2007: 1520). Prognoses about global changes undoubtedly show an increasing vulnerability of the global population to extreme natural disasters. Rapid urbanisation and development in areas with high exposure to natural disasters lead to far greater harm than experienced in the past (ALTAN 2005: 311). Until 2050, due to rising population and rural exodus, approximately 1.5 billion people – twice as much as today – are going to live in storm and earthquake exposed cities (see Figure 1.3) (WORLD BANK 2010: 20). As a consequence, a high demand for not only preparedness, but, in particular, for the advanced emergency response is given.

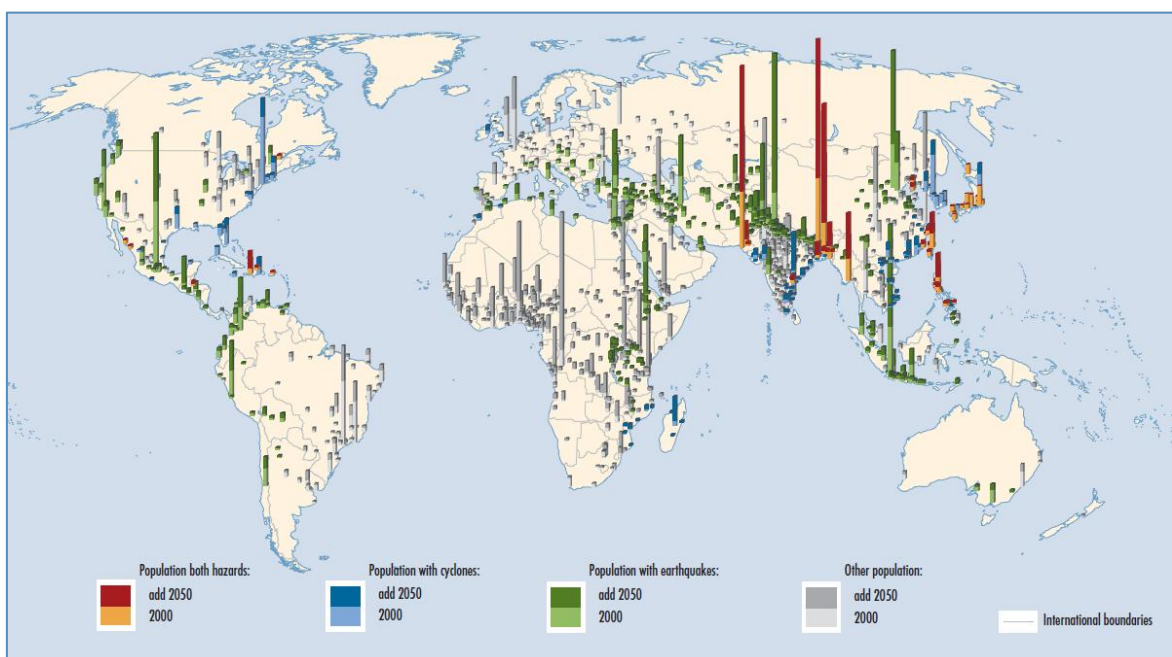


Figure 1.3: Exposure to earthquakes and cyclones may rise from 2000 until 2050

Source: *World Bank 2010: 20*

An example for the delivery of emergency response, in form of rapid mapping products, is the severe earthquake (EQ) that struck Haiti on the 12th of January in 2010. The capital, Port-au-Prince was substantially affected by the main shock. A series of aftershocks followed. The extraordinary event of Haiti is the case study of this thesis. The map below (Figure 1.4) shows estimated damage categories for buildings per 250 metre grid cells, which were derived by visual interpretation of high resolution satellite images. Space-borne imagery, down-linked one day after the EQ, and archive data were deployed as database. The map was produced by the Centre for Satellite Based Crisis Information (ZKI) and is the cooperation partner of the present thesis.

In the context of national and international response to major disasters ZKI is a service of the German Remote Sensing Data Centre (DFD) of the German Aerospace Centre (DLR), consisting of a rapid mapping team with 24/7 availability. Its assignment is the timely provision of processed and analysed satellite imagery made for rapid mapping products in case of natural and environmental disasters, humanitarian relief activities and civil security concerns. The 'on demand' rendered products are available for relief organizations and government agencies and free of charge. The extracted information is provided as map products or digital geo-data and finally utilised in disaster management operations or relief activities (VOIGT ET AL. 2007, STEVENS 2008).

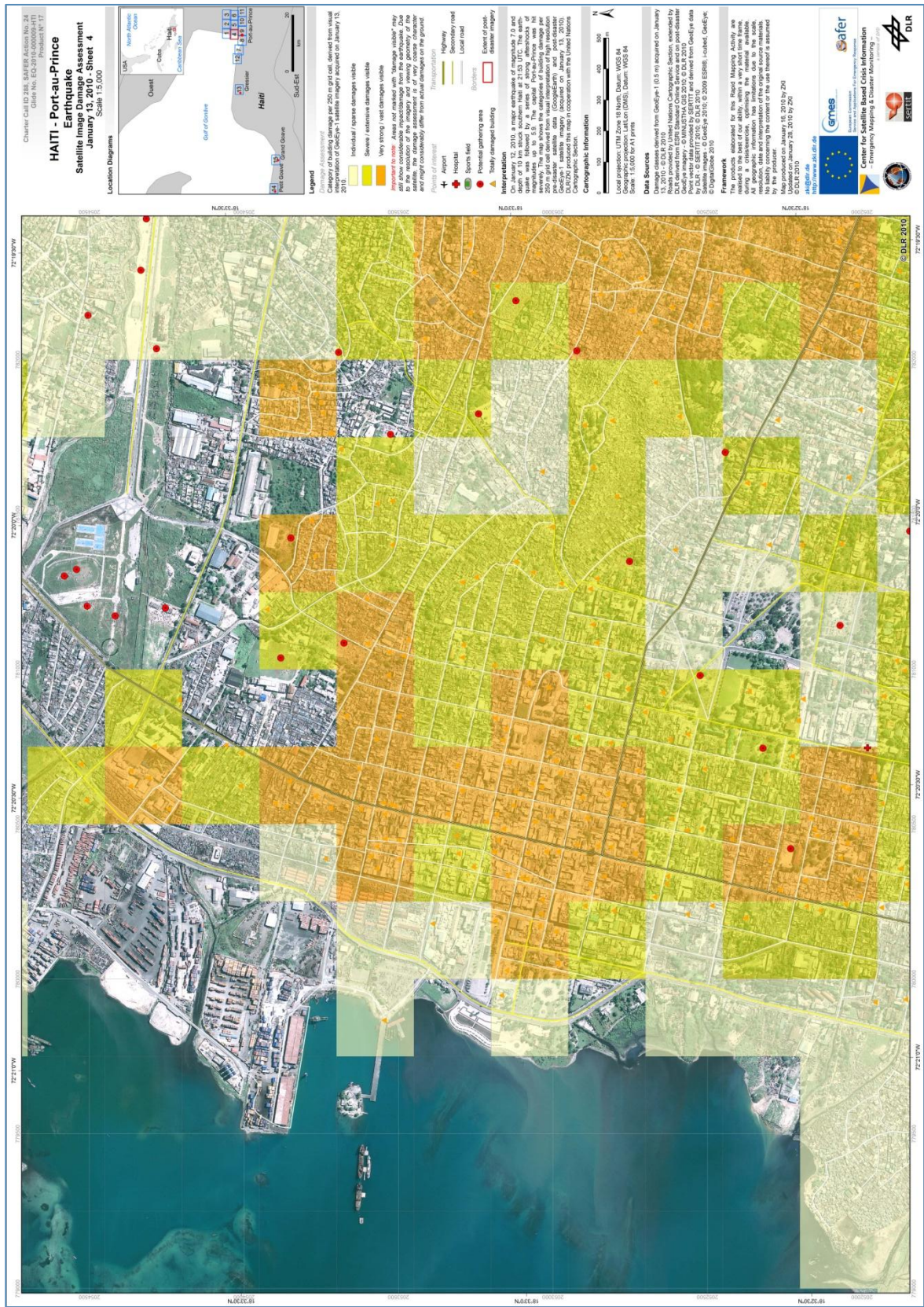


Figure 1.4: Satellite-based damage assessment map of Port-au-Prince, Haiti

Source: DLR 2010

An established source of information in crisis, emergency and natural disaster situations is satellite imagery (VOIGT ET AL. 2005: 520). Especially in the context of rapid mapping activities space borne imagery is capable to provide timely up-to-date and high-quality information. The application of remote sensing and geo-information systems can forward an increase in value. This value adding is obtained by registration, processing, classification and visual interpretation of raw image data (DONNER 2008: 4). Rapid mapping in the aftermath of an EQ consists mainly of data extraction and symbolisation of the extracted features. Thus, the focus of this thesis is on optical sensors because radar imagery is not suited for a visual interpretation. Furthermore, the effects of speckle and double-bounce in radar imagery, especially in urban environments, restrict the application for damage assessment of single buildings.

Concerning visual interpretation there is a wide range of theories how a human interpreter is reaching conclusions. These range from aspects of Aristotle's apprenticeship and cognition research to theories of semiotics (DONNER 2008: 4). The understanding of data mining and evaluation appears to be very difficult. Nevertheless, as a central aspect of visual interpretation it has to be considered.

1.1 The Research Challenge

In the context of the Haiti EQ the aim of this thesis is to develop a team-based method for visual damage assessment of optical very high spatial resolution sensors (VHSR) for the operational use at ZKI.

A central aspect is to explore the possibility to improve the assessment of building damages, which is still carried out by time consuming human interpretation. This task is often performed following disasters, therefore, while on one hand there is a high pressure to deliver a result as quickly as possible, on the other hand it is of highest importance to ensure a high quality of the assessment (CASTOLDI ET AL. 2010: 124). A validation process aims at quantifying the degree of adequacy of a service or product to approved standards and user requirements (VEGA EZQUIETA ET AL. 2010: 54). But in time emergent situations any time, invested in controlling the quality of the product, is time that is not invested in producing information that could be of value for the user. Accordingly, quality control has an impact on rapid mapping. For this reason it is important to invest efforts in in-line quality control, to keep the product inside quality standards for as long as it is produced. The question is how to guarantee quality and reliability for information derived from remote sensing data. The challenges concerning the visualization fall in line. Bearing this to mind, the research challenges are found in the following questions:

- (1) Which thematic accuracy can be achieved in a certain timeframe?
- (2) How can subjective decisions, which are based on qualitative surveys, create a rational and reproducible result?
- (3) How can procedures be designed, that take (1) and (2) into consideration?
- (4) What are the user requirements and how can they be extracted and represented?

To fulfil the research challenges the methodology has to ensure different aspects:

- (1) Follow an easy course
- (2) Optimal working settings, which can be reproduced for different events
- (3) Homogenous teams that deliver comparable results
- (4) Homogenous methodology that leads to rational results
- (5) Meet timelines and quality terms

All the considerations of the thesis will be held under the scenario of a critical situation in which products must be delivered in a timely urgent mode. Therefore it is essential to design an in-line procedure of data extraction and representation. The methodology shall be transferable to different sensor data and also contain an automation of supporting information. It is assigned to optimise the current grievances of visual interpretation. Thus, the challenge is to extract damaged buildings out of randomly provided data and to determine the best data source. The result will be an advanced operating sequence for the rapid damage assessment.

1.2 Objectives

Aim of this thesis is to investigate the conditions of rapid mapping using earth observation data to provide a deeper understanding of the potential of very high resolution optical data for damage derivation. Reflections on this overall goal raise a number of questions. Is the ground resolution of earth observation data of high relevance for the damage assessment? What degree of detail is sufficient to analyse building damages? To figure out the reliability of different sensors, which's imagery is available within the International Charter on Space and Major Disasters, a statistical evaluation has to be conducted.

The increase in quality for damage assessment products is a central aspect in the current discourse of rapid geospatial reporting. A robust, transferable and fast method of data extraction and representation signifies the cutting edge of research. While recent development activities strive to put forward the operational level of such methods in a rapid mapping context, both users and service providers, such as ZKI, are concerned with the trustworthiness of products in general, and under aspects of reliability, timeliness and effectiveness in particular. The demand in supporting time-consuming and work-intensive visual interpretation techniques is undoubtedly rising (cf. LANG ET AL. 2010: 65).

As a consequence, a homogenous visual interpretation scheme that follows an standardised operating procedure (SOP) is crucial. The base for the SOP is the semi-automated extraction of a building mask from satellite data. The intention is to increase accuracy of damage assessment.

For the analysis of disaster extents there is a necessity to work with different teams. When working in teams, qualitative differences of interpretation results are expected. To get an estimate on the variances of visual interpretation a focus group analysis is essential. The results obtained of this statistical evaluation are considered in the development of the SOP.

Currently many service providers apply visualisation techniques that symbolise tendencies of damage distribution in grid cells (see Figure 1.4). Since the current visualisation provides only a small degree of detail for rescue teams, the necessity for developing an advanced data representation is given. With regard to that, a semiotic visualisation that is informative, graphically clear and easy to understand has to be found (ANDRIENKO & ANDRIENKO 2007). In addition, user requirements have to be taken into consideration.

Summing up, a comprehensive, interdisciplinary approach is presented, which aims on raising product quality as far as it is possible within a diploma thesis. This will lead to a sophisticated method, which results in consolidated rapid mapping products with more reliable content.

1.3 Thesis Outline

As was presented, the aim of the thesis is to propose a new approach of a team-based analysis method and to investigate the variations of visual interpretation. Based on the aforementioned research challenges and objectives, the thesis is divided into seven chapters.

Chapter 1 outlines the setting of the thesis within the framework of satellite-based crisis information. Building on this the research challenges and objectives are presented.

Chapter 2 illustrates the fundamentals of methods and techniques applied in the thesis. After an introduction into the study area and the data utilised, the situation in the aftermath of the Haiti earthquake is briefly portrayed. This is followed by the fundamentals of remote sensing and digital classification procedures before a literature review outlines the state-of-the-art in building detection utilising remote sensing methods. Subsequently the processes dealing with visual image interpretation are explained. Continuing with disaster management and its related frameworks concerning earth observation, Chapter 2 closes

with sociological aspects of team-based analysis methods that are of specific interest for image interpretation.

Chapter 3 directs to the background of rapid mapping. The general setting of the damage assessment in the disaster management cycle follows. Subsequently specific user requirements are described. The user needs unconditionally lead to a limitation of available data sources. The restraints which result from the user requirements build the framework for the usability of different sensors, which were analysed and taken into consideration for further analysis and the development of an advanced interpretation method. Followed by the portrayal of damage assessment techniques and their restraints for operational use, the work of ZKI in the Haiti case is depicted. Finally, the potentials and limitations of VHRS optical imagery for damage assessment are further investigated.

Chapter 4 deals with the development of a team-based procedure for visual image interpretation. Initially some basic principles and considerations are discussed, before the development of a semi-automated solution for the generation of supporting information is explained. The supporting information renders assistance during visual interpretation and, consequentially, is the first part of the developed methodology. Afterwards a pre-test study is described, as well as the statistical principles deployed for the evaluation of the results that were obtained from the focus group analyses.

Chapter 5 examines the illustration facilities of damage assessment maps of different service providers. The variety of visualisation techniques is compared and briefly analysed, in order to find an advanced data representation. The optimisation approach occurred with due regard of present inaccuracies. The particular focus was on spatial relations of data representation, which resulted in deliberations for alternative visualisation possibilities.

Chapter 6 demonstrates and discusses the main results of the analyses conducted.

Chapter 7 presents the conclusions derived from key findings of the thesis and briefly outlines implications for further research.

2 Fundamentals and State of the Art

After a short introduction into the study area, Chapter 2 outlines the basic principles and the recent development of commonly applied methods in optical remote sensing. In particular the topics and procedures that are relevant for the thesis are considered. In addition to the methodological background, a thematic context is also portrayed.

2.1 Study Area and Data

Haiti occupies the western part of Hispaniola Island, one of the Greater Antilles islands, situated between Puerto Rico and Cuba. The cities of Carrefour and Port-au-Prince are the area investigated (see Figure 2.1) by this thesis, because they suffered the highest concentration of damages caused by the earthquake in January 2010. In the case of the Haiti earthquake the weather conditions enabled the acquisition of very timely satellite-based optical data, such as WorldView-I and II data (spatial resolution PAN 0.48 m, multispectral 1,84 m – spectral resolution: Red, Green, Blue, NIR1) and GeoEye-1 data (spatial resolution PAN 0.5 m, multispectral 1,65 m in the bands Red, Green, Blue, NIR) (see also Chapter 2.3.1). The images, down-linked on the 13th of January 2010, were used for situation mapping and rapid damage assessment (VOIGT ET AL. IN PRESS) and also for this study. All four available bands were utilised because currently this is the most immediately available information in an emergency situation. An additional street data set, digitised by DLR, was utilised to increase the quality of the machine-based classification (WALTER 2005: 1, cf. VEGA EZQUIETA ET AL. 2010).

During the crisis, data of several other optical and also radar sensors and the corresponding archive scenes were acquired. Most of them were freely available for the disaster mapping community. Even airborne optical imagery such as the joint remote sensing mission of World Bank ImageCat and the Rochester Institute of Technology (WB-ImageCat-RIT) and LIDAR data were made accessible. Furthermore aerial photographs (spatial resolution 0.2 m in the bands Red, Green, Blue) were consulted for statistical evaluation (see Chapter 3.2).

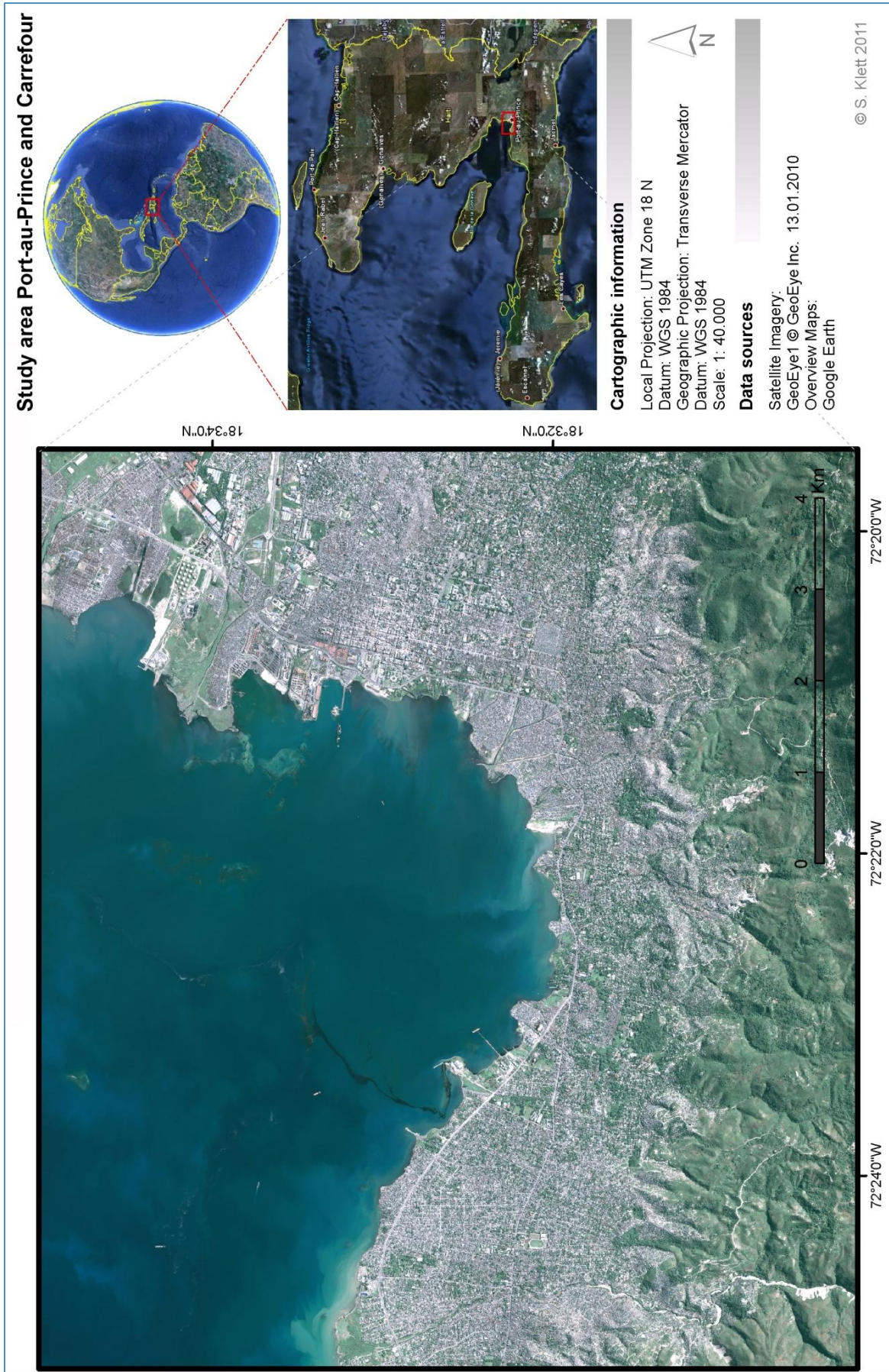


Figure 2.1: Study area Port-au-Prince, Haiti. Source: Own illustration © S. Klett 2011

2.2 The Earthquake Event

2.2.1 Earthquakes

An earthquake is defined as shaking and displacement of the ground due to seismic waves. Seismic waves result in an EQ after a sudden release of stored energy in the earth's crust starting from slip-surfaces (PRESS & SIEVER 2003: 684). They can be released by tectonic or volcanic activities. At the earth's surface seismic waves are felt as a shaking or displacement of the ground. The released energy in the hypocenter can be measured in frequency ranges that define the magnitude of an EQ event (CRED 2009).

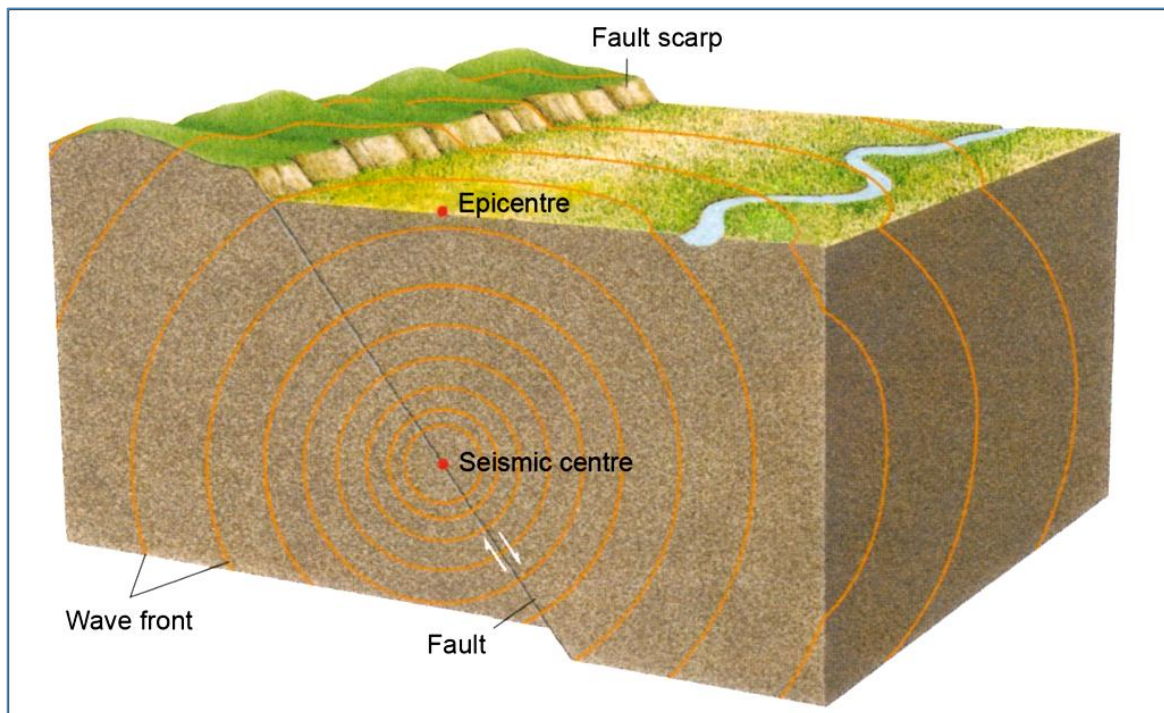


Figure 2.2: Seismic waves spread out into all directions from the seismic centre

Source: PRESS & SIEVER 2003: 482, modified

Due to the eastward movement of the Caribbean plate USGS (2010) reported a small Tsunami with peak-to-trough wave heights of about 12 cm. The earthquake took place in the boundary region of the Caribbean and the North America plate. With a velocity of approximately 20 mm per year the plate boundary is stressed by left-lateral strike-slip motion and compression with respect to the North America plate. The Septentrional fault system in the northern part of the country and the Enriquillo-Plantain Garden fault system in southern Haiti are partitioning the island of Hispaniola, provoking motion between two major east-west trending strike-slip fault systems (see Figure 2.3). The January 12th main shock caused no noteworthy surface displacement of the geomorphologically well-

expressed main-strand of the Enriquillo-Plantain Garden fault system. Nevertheless it has caused several major earthquakes in the last 300 years (USGS 2010).

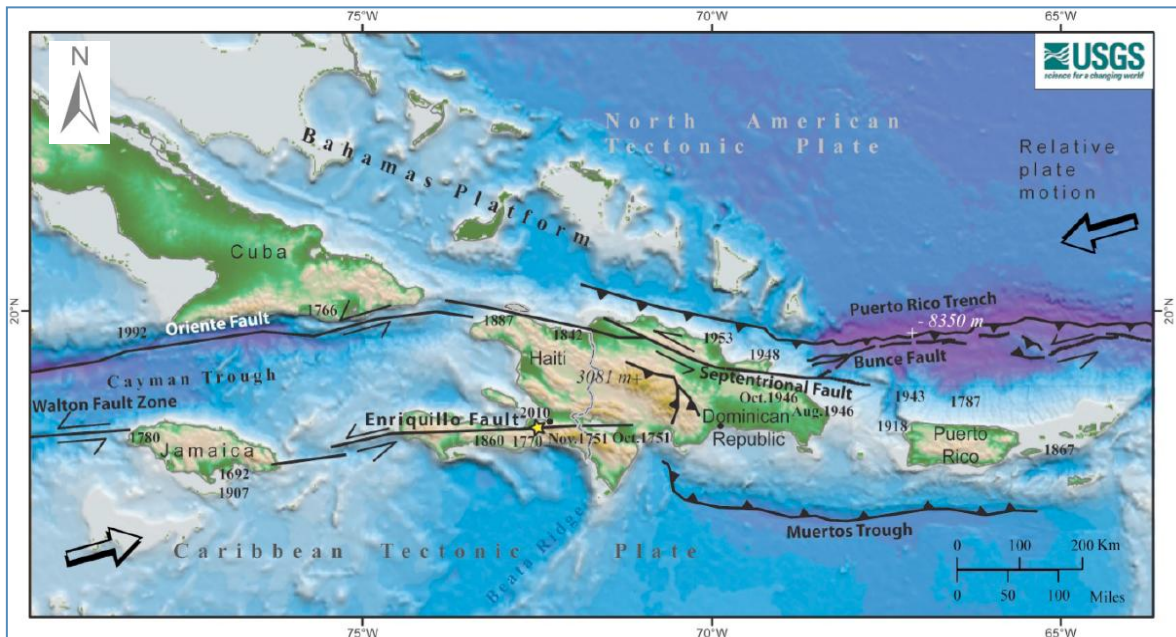


Figure 2.3: Tectonically setting of the Hispaniola Island. Haiti occupies the western third. The star represents the location of the earthquake.

Source: EBERHARD ET AL. 2010: 2, modified

On Tuesday January 12th in 2010 at 21h53 GMT, 16h53 local time, a severe earthquake of magnitude (M) 7.0 on the Richter scale hit Haiti. The main shock's epicentre was located about 15 km to the west of the capital city, Port-au-Prince. The hypocenter at a depth of 13 km was accompanied by 59 aftershocks of M 4.5 or greater. The two largest aftershocks were listed at M 6.0 and 5.9. The severity of this extraordinary incident caused a great number of fatalities and losses. According to official statements in the area of the capital and the southern part of Haiti more than 222,000 people were killed, more than 300,000 were injured, and millions were displaced. The economic losses also took on a dramatic scale. More than 97,000 houses were destroyed and over 188,000 damaged (USGS 2010). Most substantial damage occurred in Port-au-Prince and Carrefour.

The EQ that shocked Haiti caused an activation of the International Charter 'Space and Major Disasters' (see Chapter 2.7) for the provision of satellite data. The event is listed as Charter Call ID 288. The provision of a value adding analysis component was enabled within the framework of the GMES Emergency Response Core Service (ERCS) „Services and Applications for Emergency Response“ (SAFER) activation number 24. The request for information on the disaster occurrence was initiated by the French Civil Protection, the United Nations Stabilisation Mission in Haiti (MINUSTAH), Public Safety of Canada and

the American Earthquake Hazards Programme of USGS and alerted the international humanitarian aid community. To illustrate the importance of the emergency response and the extraordinary severity of the event, the actual situation is briefly portrayed.

2.2.2 Actual Situation

As a consequence of the EQ that struck Haiti, there was an increased vulnerability for significant damages from other hazards or humanitarian crises. These were in this special context tremendous storm damage, violence, exposure to cholera, or political instability to name but a few. Further obstructive problems result from the amount of debris, which exceeded available resources for removal (OCHA 2010, ALERTNET 2011). Heavy machines and other equipment for clearing work of the devastation was very limited (EERI 2010: 1). One year after the event Haiti still is in the transition phase of the disaster management cycle (see Figure 3.2)



Figure 2.4: Complete destruction of a concrete building in Haiti

Source: EERI 2010: 23

All in all the number of affected people was estimated to be about 3.7 million (RELIEFWEB N.D. referring to OFDA/CRED International Disaster Database). Figure 2.5 shows an estimate of the movement of the displaced. These internally displaced persons (IDP) are facing economic as well as societal challenges.

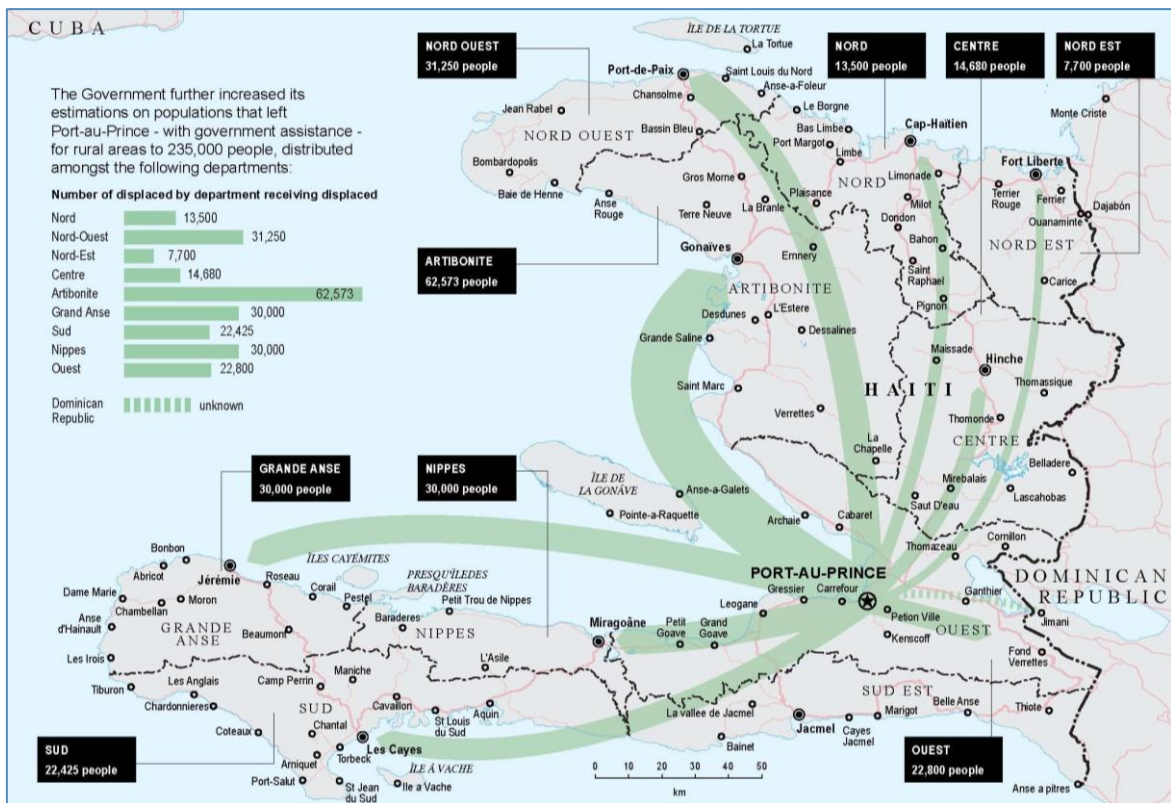


Figure 2.5: Population movement out of Port-au-Prince as of 24 January 2010.

Source: OCHA 2010

The government of Haiti assessed the economic damage, caused by the EQ, at approximately 7.8 billion US Dollar, which exceeds 120 % of Haiti's 2009 GDP (EERI 2010: 1). ALERTNET estimates the damages and losses even higher, up to 14 billion US Dollar (ALERTNET 2011). EERI (2010: 3) sums up the unpleasant state of the affairs: *"The harrowing loss of life during the 2010 earthquake is directly attributable to the exceptional vulnerability of the Haitian building inventory. Large well-engineered structures were largely immune to damage as were single story shacks using indigenous materials. Worse hit were multifamily dwellings formed from concrete. Such vulnerabilities are not unique to Haiti, or even to Hispaniola, but are common in many developing nations."* As a result of the cascading crises, about 150,000 people left the country. Considerably more are still living in tent encampments carving out a miserable existence.



Figure 2.6: IDP camp in Port-au-Prince.

Source: EERI 2010: 9

In July 2010 more than 1.5 million people were still living in 1,200 makeshift shacks and tent camps. Only a fraction of the rubble was removed by then. A main problem was the provision of funds. Even though donors promised 5.3 billion US Dollars the delivery was delayed (OCHA 2010), due to political instability and violent protests (ALERTNET 2011). Therefore the rebuilding process has also been hampered. However, the aid operation saved innumerable lives by the provision of water, shelter, sanitation and food aid. Disregarding all this, criticism came with regard to a the lack of coordination among the plethora of charities (ALERTNET 2011), as well as too many different map products (see Chapter 5), most based on remote sensing data. To overcome extraordinary crisis events like that portrayed above, the application of earth observation (EO) data is crucial for information generation. Remotely sensed imagery is a powerful source to derive timely information for decision support in the aftermath of a disaster (SHANKAR ET AL. 2010: 21). The following section deals with the fundamentals of remote sensing and commonly used sensors for emergency response.

2.3 Fundamentals of Remote Sensing

According to LILLESAND AND KIEFER (2008: 1), remote sensing is defined as the scientific acquisition, storage, processing and interpretation of information about the earth's surface and objects on it without direct physical contact. Air- or space-borne sensors receive and record emitted signals or electromagnetic emission from certain devices involved in an investigation (ALBERTZ 2009: 1f). Fundamentally one has to distinguish between passive and active systems. Optical sensors belong to the passive systems and capture reflected

solar radiance. Active remote sensing systems transmit electromagnetic waves and measure the reflected signal of the illuminated surface. Microwave systems, like radar or laser scanners, belong to these (ALBERTZ 2009: 1f).

With respect to their emitted or received wavelengths, active and passive systems differ. Most optical sensors register a spectrum in the range of visible and near infrared light (0.4-1 μm). There are also specific investigations utilising shortwave infrared and thermal infrared (SWIR: 1-7 μm ; TIR: 7 μm – 1 mm). Wavelength ranges surpassing these are used by microwave systems (up to approximately 1 m) (ALBERTZ 2009: 11). Figure 2.7 illustrates the electromagnetic spectrum and sensor scopes.

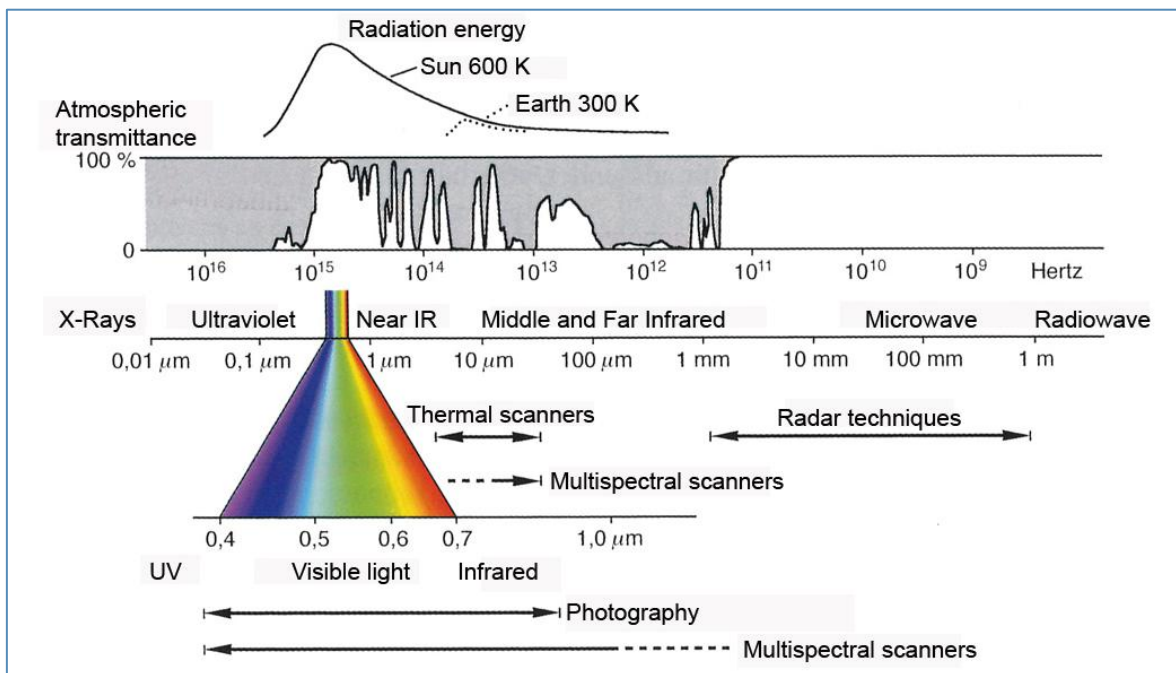


Figure 2.7: Spectral characteristics of energy sources, atmospheric transmittance and common remote sensing systems.

Source: ALBERTZ 2009: 11, modified

Objects studied on the earth's surface, differ from each other in reflectance characteristics. The attributes of different wavelengths of the electromagnetic spectrum of a certain surface are called its spectral reflectance curve (cf. LILLESAND & KIEFER 2008: 13f). The reflection properties depend mainly on physical and chemical characteristics of the respective surface and the existing geometrical relations (ALBERTZ 2009: 17). These differences clarify the demarcation and perception of objects in the various wavelength ranges (LILLESAND & KIEFER 2008: 15).

Single sensors, which are also named bands, are sensitive to a certain wavelength range. The number of bands and the covered wavelength range are called spectral resolution.

Systems that record different spectral ranges at the same time are labelled multispectral (ALBERTZ 2009: 9).

Digital remote sensing data is provided in a raster format and consists, after processing, of quadratic pixels (picture x elements). The edge length of a pixel is the measure for the geometric resolution. It indicates the perceptibility of objects: the smaller the objects, the higher the resolution (LILLESAND & KIEFER 2008: 33, ALBERTZ 2009: 84). At this point the importance of the resolution for the respective analysis must be underlined. Depending on the research interest one has to choose a sensor whose resolution is sufficient to contribute to the analysis of the object of study (see Chapter 3.2.).

The position of a single pixel is fixed in a Cartesian coordinate system. Every single picture element renders one modicum per band. This data is expressed as a grey-scale value, the digital number. Its scale is defined by the bit-depth and depends on the data storage (8-12 bit). Finally, the bit-depth reveals the radiometric resolution (LILLESAND & KIEFER 2008: 31ff., ALBERTZ 2009: 93f).

The temporal resolution is defined as the shortest possible interval within which a space-borne sensor can record the same section of the earth's surface (LÖFFLER ET AL. 2005: 86).

2.3.1 High Resolution Sensors – Principles and State of the Art

This study, as mentioned in the title, is based on VHSR (also called high spatial resolution, HSR, cf. TAUBENBÖCK ET AL. 2010) remote sensing data of the sub-meter domain. In this the highest resolution in the panchromatic band is crucial. For the analysis optical multispectral imagery of the GeoEye-1 and WorldView-I/II satellites were deployed.

The current standard for optical VHSR data is a ground sampling distance (GSD) of 1 m x 1 m or below (cf. NEUBERT 2006: 7), where GSD refers to the size of the pixels expressed in ground units (LILLESAND & KIEFER 2008: 312). The actual highest spatial resolution of space borne systems for non-military use is 0.5 m. Presently the smallest pixel size of 0.46 m x 0.46 m of the WorldView-I sensor is, due to US law, resampled by the operator Digital Globe Corp. to 0.5 m x 0.5 m for commercial use. Table 2.1 shows basic characteristics of selected VHSR sensors of the metric and sub-metric domain primarily used in this study (DIGITAL GLOBE. CORP, n.d.).

Table 2.1: Basic characteristics of most commonly used current VHSR sensors. (GSD = ground sampling distance; ms = multi-spectral; pan = panchromatic; IFOV= instantaneous field of view; # bands = number of bands)

Source: HAGENLOCHER 2010: 24, modified

Sensor	GSD [ms]	GSD [pan]	IFOV [km]	Dynamic range [bits]	# bands [ms]
GeoEye-1	1.65 m	0.41 m	15.2 x 15.2	11 bits per pixel	4 bands
IKONOS	4.0 m	1.0 m	10 x 10	11 bits per pixel	4 bands
Quickbird	2.4 m	0.6 m	16.5 x 16.5	11 bits per pixel	4 bands
Worldview-2	1.84 m	0.46 m	16.4 x 16.4	11 bits per pixel	8 bands

With the tremendous progress of spatial resolution new challenges also arise. Objects, for instance, frequently do not appear homogeneous, because of increased richness of detail. As a result one sees decreased contrast between image objects and spectral confusion as well as shading. Moreover, complex object boundaries lead to misclassifications (NEUBERT 2006: 14f). Figure 2.8 shows examples of the afore mentioned problems.



Figure 2.8: Problems with VHSR satellite data a) Lacking spectral discernment (similarity between roofs and streets), b) spectral variability of a single image object (different degrees of ripeness in a grain field), c) interfering image objects (cars on street).

Source: NEUBERT 2006: 15

Fortunately, this progress was accompanied by methodological advancements such as pan-sharpening (cf. EHLERS & KLONUS 2004). This image fusion technique uses arithmetic operations to transform multi-spectral data onto the same pixel size as the panchromatic band (LÖFFLER ET AL. 2005: 105f, ALBERTZ 2009:120, EHLERS 2010). More processing techniques, that improve the analysis of raw image data, are explained in section 2.3.2.

2.3.2 Digital Image Processing

Before the analysis of earth observation data takes place, preprocessing is necessary (see also Chapter 3). The scope of the preprocessing depends on the geometric and radiometric premises of the respective imagery. By the application of geometric transformations, such as geocoding, datasets are rectified and fitted into a geodetic coordinate system (ALBERTZ 2009: 99). The orthorectification process adjusts distortions caused by missing information on altitude with the aid of an appropriate digital elevation model (DEM). Radiometric corrections, associated with image restoration, encompass atmospheric correction via noise reduction. The image enhancement includes contrast enhancement and is actualised with digital filtering. The afore-mentioned techniques serve primarily to improve visual interpretation (LILLESAND & KIEFER 2008: 499ff.).

In this study, the analyzed data serves as the input for the delineation of building contours. For this purpose the relevant information has to be extracted from the optical imagery through specific interpretation and classification methods. The most common respective procedures are introduced below.

2.4 Digital Classification Procedures

The cutting edge of research are machine-based classifiers. Digital classification algorithms recognize and analyze the image content by machine vision (ALBERTZ 2009: 154). Digital classification methods are based on the statistical comparison of spectral values of single pixels. In this way the „spectral fingerprint“ (LÖFFLER ET AL. 2005: 193) of surface objects can be investigated.

2.4.1 Pixel-based Image Analysis

Various classification algorithms aggregate similar defined pixels into thematic classes. This occurs through multispectral classification in the levels of the spectral bands. In doing so a multidimensional feature space is defined in which the classification of discriminative objects takes place by the aggregation of feature spaces of similar spectral pixels (ALBERTZ 2009: 155f). Consequently, a successful classification is based on correctly measured values, a suitable band combination, the spectral discrimination of each class as well as expert knowledge (LÖFFLER ET AL. 2005: 198). Figure 2.9 shows a theoretical schema of a multidimensional feature space; objects in the scatter diagram usually cross borders (cf. Figure 4.5).

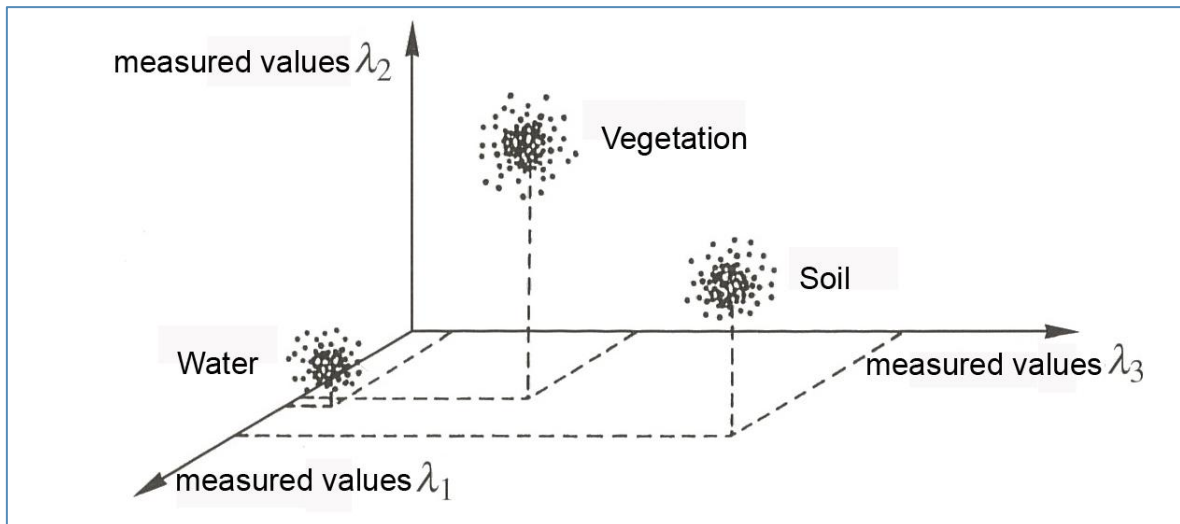


Figure 2.9: Three-dimensional feature space for multi-spectral classification

Source: ALBERTZ 2009: 156, modified.

There are several digital classification techniques which can be applied. Pixel-based procedures consider the spectral characteristics of only one image point. They are differentiated into unsupervised and supervised methods. As a standalone process, unsupervised methods apply statistics such as cluster analysis. In contrast, supervised methods need training sites that have to be provided by the user. Machine-based algorithms combine spectrally similar pixels into a predefined class (LILLESAND & KIEFER 2008: 545 ff.). Further parameters that also support the classification are spectral pattern recognition, texture-based and principal component approaches (TOMOWSKI ET AL. 2010).

In VHSR data one can see „salt-and-pepper-effect“ phenomenon. Especially in heterogeneous regions, such as urbanized areas, there is an enormous spectral diversity on a small scale (cf. Figure 2.8). If one considers an image object, important semiotic information is undocumented, due to the „salt-and-pepper-effect“. This results in error classifications (BAATZ & SCHÄPE 2000: 12ff.). Consequently, this could be considered as the limiting factor of pixel-based procedures and, because of this, extended classification algorithms are increasingly applied. Object based image analysis (OBIA) can be ranked among these (cf. LANG 2008, WURM ET AL. 2009, TAUBENBÖCK ET AL. 2010). In addition to spectral criteria form parameters and topology are considered. The results achieved better approximate human perception.

2.4.2 Object-based Image Analysis

State-of-the-art algorithms for the machine-based interpretation of VHSR images apply OBIA, because pixel-based approaches create artefacts during classification (YANO & YAMAZAKI 2004: 4). Another advantage of OBIA in the pre- and post-disaster image

comparison over conventional pixel-based approaches is the omission of training site determination, which is very time consuming. Recent developments, such as the architect solution guarantee an easy implementation of master rule-sets on different images.

Object-based image analysis usually follows three major procedures. The first step is image segmentation (BAATZ & SCHÄPE 2000). Secondly there is the detection of image objects, which is usually done by a fuzzy classification algorithm (BENZ ET AL. 2004, SUMER & TURKER 2008, CHINI ET AL. 2009, TAUBENBÖCK ET AL. 2010). Lastly the post-processing of the extracted objects follows (LI ET AL. 2005: 642). Thresholds of spectral and relational attributes are common features described in literature to separate objects belonging to different classes. A range of thresholds describes a fuzzy logic, which defines vague borders between different classes. The fuzzy logic based thresholds are determined on screen by the user.

When applying OBIA, first and foremost the image segmentation module is initiated. Neighbouring pixels are aggregated to homogenous segments according to their shape, area and spectral values (BAATZ & SCHÄPE 2000). There are multiple segmentation methods available. Because thresholds in the grey-value histograms are prominent in the generation of object boundaries, multi-resolution segmentation was chosen in this thesis. The image segmentation starts with a region-growing algorithm. The neighbourhood of the seed pixel is investigated. If there is accordance with the predefined homogeneity criteria, unification into a thematic segment is performed. Taking into account different object sizes in the real world, it is advisable to work at different segmentation levels. These levels are iteratively and hierarchically structured (cf. DEFINIENS 2008: 31, TAUBENBÖCK 2008: 39ff.). A lower level contains, for instance, small heterogeneous segments for the classification of building roofs, whereas higher levels are qualified for larger homogenous segments such as forests or water bodies. This procedure is called a bottom-up segmentation concept (TAUBENBÖCK ET AL. 2010: 120)

The classification module results from the following parameters: spectral value, shape, size, texture and neighbourhood (LILLESAND & KIEFER 2008: 581ff., ALBERTZ 2009: 161). The thematic classification of segments follows the principles of a hierarchical object network, which is based on the transmission of the corresponding properties to lower levels (BENZ ET AL. 2004: 240, TAUBENBÖCK 2008: 43f, TAUBENBÖCK 2010: 118f). In this context the classification module is a top-down classification (cf. TAUBENBÖCK ET AL. 2010: 121f). Figure 2.10 displays the bi-modular design of a hierarchical, multi-level, top-down classification approach.

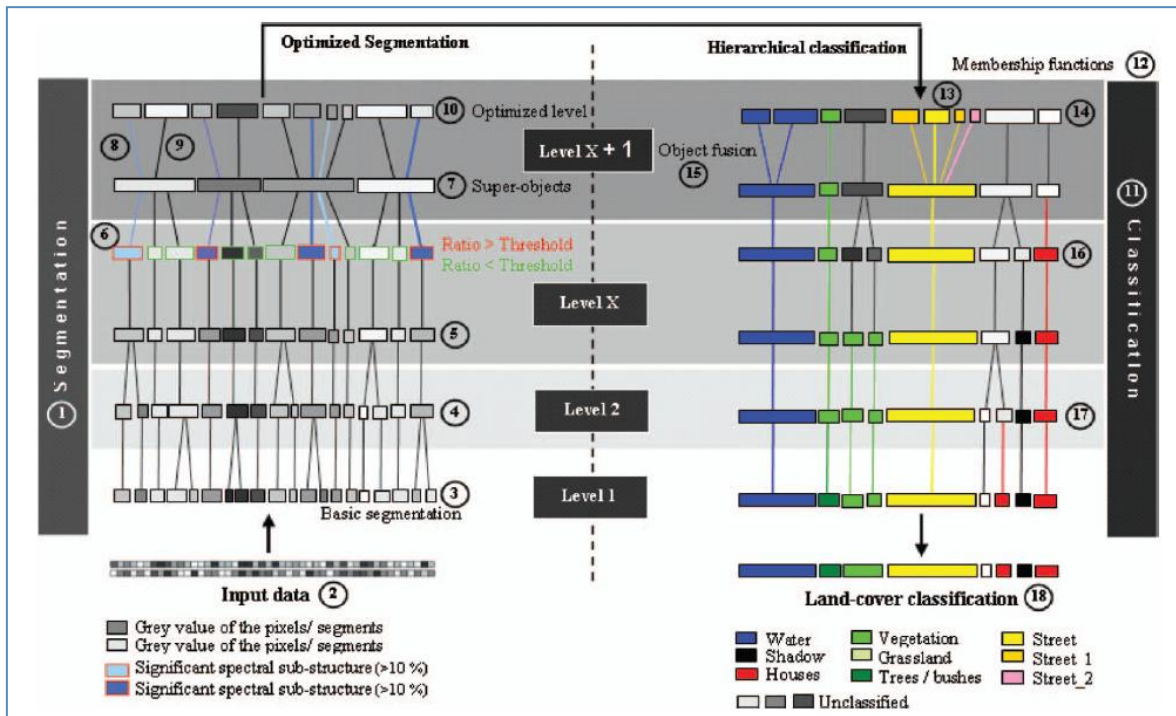


Figure 2.10: Modular framework for an object-oriented urban land-cover classification.

Source: TAUBENBÖCK ET AL. 2010: 121

In contrast to pixel-based classification techniques, the possibility to use fuzzy classification attributes is a major advantage of OBIA. The 'Fuzzy Logic' delineates imprecise class borders that most closely correspond to real objects. Therefore pixels can hold partial degrees of membership in several classes (NAGA JYOTHI ET AL. 2008: 709).

Another possibility to distinguish classes is the use of vegetation indices. They assess whether the object being observed contains live green vegetation or not (ALBERTZ 2009: 221). The ratio of significant bands indicates high reflection of green vegetation as well as its high absorption in the red spectral range. The 'Normalized Difference Vegetation Index' (NDVI) (ROUSE ET AL. 1973) was used for the presented thesis. It is defined by the ratio:

$$NDVI = \frac{NIR - Red}{NIR + Red}$$

The NDVI adopts normalised values in the range from -1 to +1. Higher NDVI values indicate a high density of vital vegetation (HILDEBRANDT 1996: 55).

ALBERTZ (2009), LILLESAND AND KIEFER (2008) and HILDEBRANDT (1996) presented further detailed descriptions of the theoretical principles of remote sensing. OBIA and classification usually result in thematic maps. To make a point about the quality of the classification results, an accuracy assessment has to be performed.

2.4.3 Object-based Accuracy Assessment

LILLESAND AND KIEFER (2008: 568) emphasize that: “[...] a classification is not complete until its accuracy is assessed”. In case of object-based accuracy assessment both thematic and geometrical accuracy is needed (SCHÖPFER ET AL. 2006: 2). The thematic accuracy specifies the correspondence of image objects between the classification and the real world. The geometrical or spatial accuracy describes how well a classified object matches its reference object’s position.

To evaluate thematic accuracy a site specific assessment can be considered. Samples of the classified image are compared with exactly the same locations on the reference data set. The degree of accuracy is defined by the ratio of agreement and all spot tests. Levels of 85 % and more are recognised as the critical benchmark (CONGALTON & GREEN 2009: 55f). The standard method to present the overall accuracy, meaning correctly classified objects, is a confusion matrix. Agreements and misclassifications for each class are recorded in a table. Individual class accuracy is expressed by the producer’s and user’s accuracy. The first is computed by the total number of correctly classified samples divided by the total number of references of the respective category. The latter mirrors the total number of references divided by the total number of classified samples of the corresponding category (LILLESAND & KIEFER 2008: 572f). A further indicator to measure the quality of classification results is the Kappa coefficient (K). The Kappa statistic describes the *“difference between the actual agreement between the reference data and a machine-based classifier and the chance agreement between the reference data and a random classifier”* (LILLESAND & KIEFER 2008: 573f) (see also Chapter 6.2.2).

The spatial accuracy measures the conformity of the boundaries of the classified object and its respective reference object. According to ALBRECHT ET AL. (2010: 2) a lot of uncertainties remain in OBIA. Therefore the spatial accuracy is hard to assess and adequate methodologies are still in the process of development. A mean tolerance value can be set as limited amount of variation. SCHÖPFER ET AL. (2006) presented the Object Fate Analysis. It examines the topological correspondence of the afore-mentioned objects. Since this concept is still in a preliminary state, another possibility could be the analysis based on the mean perimeter area ratio (MPAR) (LANG & BLASCHKE 2007: 246).

$$MPAR = \frac{Perimeter}{Area}$$

The MPAR of randomly selected objects could be compared with manually digitised objects (ESCH ET AL. 2008: 466). These are considered to be true, even if there remains uncertainty in the production of the reference objects (LANG ET AL. 2010: 67). The difference between the reference objects and the ones delineated is a measure of the

quality. The higher the difference, the lower the spatial accuracy. For earthquake damage assessment, a statement on the geometric accuracy could be made concerning contours of buildings. An overview of established methods for building detection in satellite imagery is given below.

2.5 Building Detection using Remote Sensing Methods

As a result of the Haiti EQ thousands of houses were destroyed or damaged. The key task of damage assessment in the aftermath of an EQ is to determine the number of damaged houses. Thus, a high demand for the detection of single buildings is given.

Urban landscapes, especially emerging megacities in developing countries, are facing rapid spatial and socio-demographic changes (THIEL & ESCH 2008). If there are data sets available at all, they are often generalized or outdated (MEINEL ET AL. 2001, ALBERTZ 2007, VOIGT ET AL. 2007, TAUBENBÖCK 2008). Hence, the extraction of desired information is the main task in the application of EO data (LI ET AL. 2005: 641).

Multisensoral Remote Sensing is a valuable tool for building detection, which has proven to be a reliable information source (KAMPOURAKI & WOOD 2006, MEINEL ET AL. 2007, NETZBAND ET AL. 2007, SUMER & TURKER 2008, BRUNNER ET AL. 2010, TAUBENBÖCK ET AL. 2010). In addition to spectral analysis of different parts of the electromagnetic spectrum, such as VIS/NIR or TIR (VOIGT ET AL. 2007) and the microwave spectrum (THIEL ET AL. 2008, BRUNNER ET AL. 2010, GAMBA ET AL. 2010, STRAMONDO ET AL. 2010), there are many methodological approaches such as texture analysis (TOMOWSKI ET AL. 2010) as well as object-oriented classification approaches (ZHOU ET AL. 2009, TAUBENBÖCK ET AL. 2010). Land use and land cover classification are established methods, as well as the determination of building density and statistical derivations (MEINEL & HEROLD 2006). But also small-scale information on settlement structures and environmental conditions can be gained from remote sensing data. Furthermore there is the possibility to derive risk maps (MITCHELL 1999, MEINEL ET AL. 2007, TAUBENBÖCK 2008). The analysis of remote sensing data and derived GIS data is able to provide valuable planning basics and information technology for disaster management, mainly in terms of decision support.

Small-scale information on settlement structures and environmental conditions can be gained from remote sensed data. Determination of site density from satellite imagery alone is an established procedure. In a next step, statistical data such as population density, can be linked to the location of built up areas and the distribution of residents can be estimated (MEINEL 2007: 1f). This information complements the global population distribution dataset of LandScan™. Since the resolution of this data is too coarse (1 x 1 km) the need for a more detailed estimation is given. It is concluded that VHRS

satellite imagery is most qualified to close this gap. Meanwhile, the surface roughness and the building height can be derived from microwave data. With the automatic building detection, settlement structural indices can be deduced (MEINEL & HEROLD 2007). As it can be seen in the upper right section of the satellite image shown in Figure 2.1, bigger buildings indicate industrial areas, whereas smaller buildings represent residential areas. Also the buildings geometry, size, hierarchical relationships and their neighbourhoods can be taken into consideration (PILZ & STROBL 2002, MEINEL & HEROLD 2007) for EQ damage assessment, e.g. debris around collapsed houses.

For the detection of houses affected by EQ it is necessary to utilize pan-sharpened VHSR data like GeoEye-1, WorldView, Quickbird or at least IKONOS imagery (LI ET AL. 2005: 642, KERLE & WIDARTONO 2008: 15, JOYCE ET AL: 2009: 201). TAUBENBÖCK ET AL. (2010: 119) stated, that: *“reliable detection of objects representing small individual buildings requires a spatial resolution of less than the dimension of the object itself. This data quality can only be provided by HSR sensors [...] with a spatial resolution higher than 1 m”*.

Techniques for object recognition affected by EQ differ in the literature. The most common ones are outlined below. OK (2008) applied a mean-shift segmentation algorithm for the detection of buildings. Features, which do not belong to a building class, were removed. This follows a vector-valued canny edge detection of the segmented colour image. Unconnected edges were bridged by using morphological operators and converted to vector polygons via a boundary tracing algorithm. For the derivation of building regions LI ET AL. (2005: 647) also use an edge detection algorithm. The analysis was made in the urban residential area of Toronto, Ontario, with very structured and also isolated houses. Even in this ‘ideal’ case scenario there were a lot of corrupted objects. The filtering in the post-processing brought about easily recognisable building outlines, but the shape of the final objects does not match the original contours, which is indispensable for a pre-/post-disaster comparison. GAMBA ET AL. (2007) also used an edge detection algorithm for the extraction of object boundaries in the segmentation process.

SUMER AND TURKER (2008) introduced an adaptive fuzzy genetic approach for the extraction of buildings from high resolution satellite data. The aim is to improve the feature extraction routine. This is done by a coding of image processing operators into genes. A predetermined number of genes is outlined as a chromosome – a set of image processors. The authors collected sample data for building and non-building areas which were categorized by the Fisher Linear Discriminant module, a classification algorithm. In doing so the training data is sorted by an optimal discriminating hyper-plane between the different image objects. The implementation of a mutation operation allows superseding

single genes randomly until the best-fitting chromosome is found. The mutation is thought of as an adaptive fuzzy component. With approximately 91 per cent, the building detection rate of this methodology is among the highest, but very time-consuming and elaborate and therefore not suitable for rapid mapping.

The major research deficit might be found within the operational delineation of single building damages resulting from earthquakes, since thus far the analyses were concentrated mostly on single case studies (TURKER & SAN 2004, GAMBÀ ET AL. 2007, OK 2008, SUMER & TURKER 2008, CHINI ET AL. 2009). Other studies use additional GIS-data (GAMBÀ ET AL. 2007, AYDÖNER ET AL. 2009) or LIDAR data (HOMMEL 2009), which is often not available in a devastating emergency like the Haiti event. TIEDE ET AL. (2010a) use shadow indices but this machine-based technique still has a high error-proneness (VOIGT ET AL. IN PRESS, LANG ET AL. 2010). Further limitations in machine-based analysis for supporting information in the rapid damage assessment will be outlined in Section 3.3.2. Thus, there is a demand for a transferable and universal methodology in the sense of practicability for different VHSR datasets. As it was shown, automated processes are whether time consuming or rather unreliable. Accordingly, the key-task is to render assistance to the manual interpretation. As discussed in Chapter 3, the visual interpretation of EO data is still the most reliable method for damage assessment, due to high complexity of disaster situations.

2.6 Visual Interpretation of Remote Sensing Data

Visual interpretation, often also called manual interpretation, of remote sensing data can be defined by the sense perception of raw data or image content and by inference from logical processes (DONNER 2008: 4, ALBERTZ 2009: 123). Deduction and conclusion signify the most important component in a problem solving procedure that is guided by assignment rules. In the interpretation of image features as an object of importance these rules are labelled as interpretation schemes (DONNER 2008: 4ff.). During the inspection of images the interpreter recognises content-related and functional nexus. These nexus are then linked to relevant data or sensory perception. Finally, the interpretation itself construes functional relations between relevant objects. The aim of the interpretation is the description and declaration of spatial differentiation through the aid of single elements and their relationships among themselves (DONNER 2008: 125ff., ALBERTZ 2009: 133).

Foreknowledge is a central aspect of the visual interpretation (DONNER 2008: 127, ALBERTZ 2009: 133). Human vision utilises experiences from real life for the interpretation of images. In this regard two levels need to be distinguished. The first level relates to the recognition of objects, the second one to the interpretation that is based on the afore

mentioned experiences (ALBERTZ 2009: 123). ALBERTZ underlines the importance of foreknowledge for answering the question „what is existing where?“. The answer implies conclusions that develop from a deliberate thought process. An indispensable premise of this process is foreknowledge and experience, that increases with recognition and interpretation during iteration (ALBERTZ 2009: 133). Figure 2.11 provides a simplified sequence of the iteration process for visual interpretation.

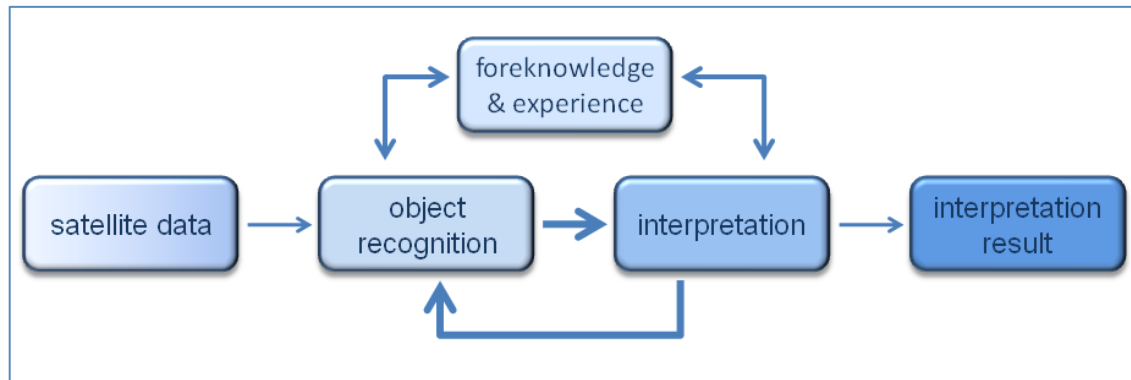


Figure 2.11: Iteration process of visual interpretations

Source: ALBERTZ 2009: 133, modified

Ambiguity is the foremost complication relating to visual interpretation of remote sensing data. In the context of earthquake damage assessment, the difficulty is to distinguish between construction sites, real building damages, partially damaged buildings and still intact ones. NIESYTO (2006: 272) stated that context-dependent knowledge influences the image interpretation in a substantial manner. Accordingly, the analysis results from different interpreters may vary to a certain degree. Intentions and reflections of interpreters can be influenced by instructions and standardized procedures (NIESYTO 2006: 274, COLLIER 2010: 54). The result will be a more reliable and consistent, when recognising that selection and interpretation patterns follow impact-based reflections (NIESYTO 2006: 274). According to BELL (2010: 21) “*reliability refers to the degree of consistency shown by one or more coders in classifying content according to defined values on specific variables. Reliability can be demonstrated by assessing the correlation between judgments of the same sample of relevant items made by different coders [...]*“. One can conclude that consistency in an visual interpretation is an indicator for quality of the achieved results.

In an optimal setting the interpreters are highly qualified to apply data evaluation techniques in a systematic and reflected manner (NIESYTO 2006: 279). This speeds up the analysis due to important contextual knowledge (COLLIER 2010: 57). However, coherence compulsion can lead to over-interpretation.

A more detailed and specific description of processes related to visual image interpretation is provided in Chapter 4.

2.7 Earth Observation and Disaster Management

This section highlights selected aspects related to EO and disaster management, that are of specific interest for data provision and value adding. However, the complex relations and hierarchies are not subject of the thesis and thus cannot be presented in detail.

As presented in section 2.3.1 remote sensed imagery and image analysis techniques have improved substantially. Since ground resolution has reached the sub-meter domain, space borne data is a powerful tool to support disaster and crisis management (LI ET AL. 2005: 641), particularly rapid mapping damage assessment (VOIGT ET AL. 2007: 1520). With the International Charter on Space and Major Disasters a network was established which focuses on the international satellite-based disaster response. Communication, inter-operability and cooperation bring synergy effects for data provision and product delivery in an adequate spatiotemporal manner (THE INTERNATIONAL CHARTER 2007). This is realised by a consolidation of different satellite systems that enables data sharing.

In 1999, the Charter was established at the UNISPACE III conference which was organized by the United Nations (UN) and took place in Vienna. The principal agreements signed by the European Space Agency (ESA) and the Centre National d'Études Spatiales (CNES) of France were regarding space data acquisition and delivery to those affected by natural or man-made disasters through authorized users (STEVENS 2008: 64).

An increase in accessible space-based data, especially for developing countries, for the support of emergency situations arose lately. This is a result in part from the foundation of the Charter for improving the availability of space-based technologies for disaster management. Along with the initiation of the Charter, of which the United Nations Office for Outer Space Affairs (UNOOSA) is the cooperative body, the awareness of the needs of developing countries rose. Hence the Committee on the Peaceful Uses of Outer Space (COPUOS) launched the United Nations Platform for Space-based Information for Disaster Management (UN-SPIDER). This program established a global coordinating platform that supports a rising number of international initiatives operating in the humanitarian community. The main goal is the incorporation of geospatial solutions in their daily work (STEVENS 2008: 57f).

At the World Conference on Disaster Reduction, which took place in January 2005 in Kobe/Japan, the potential of space technology to support disaster preparedness was admitted. To pursue the strategy of promoting the use, the application and affordability of recent disaster related information until 2015, the so-called Hyogo framework was

developed. The Secretariat of the International Strategy for Disaster Reduction (ISDR) is therefore in charge of dissemination of relevant information and communications among different users (STEVENS 2008: 59).

„*To what extent image-based information can aid in an emergency situation depends primarily on the disaster type*“ (KERLE & WIDARTONO 2008: 16). Being aware of this, UNOOSA organized a series of workshops for improving capacity and advancing knowledge. In addition, further issues such as data access, availability and information extraction as well as national, regional and global coordination were addressed. At the national level governmental institutions are responsible, whereas at the regional level different interested parties need to work together (STEVENS 2008: 60). At the European regional level the European Commission and ESA designed the Global Monitoring for Environment and Security (GMES) initiative (STEVENS 2008: 66). At the global level a coordinating entity, the UN-SPIDER program, was established. Its main task is the “*one-stop shop for knowledge and information sharing (best practices) and also [...] a platform for fostering alliances*” (STEVENS 2008: 60f) in the humanitarian community. In order to improve the access to maps, satellite imagery and geographical information, the so-called RESPOND alliance, which consists of international organisations, was founded (RESPOND 2008). Between 2004 and 2010, their work focussed on all phases of the disaster cycle (see Figure 3.2). To ensure high quality products, training and support services were organised (STEVENS 2008: 68).

A further step to professionalising and harmonising the international humanitarian aid community was the implementation of the SAFER project. It is reinforcing the European capacity to respond to disasters like the Haiti EQ in the framework of the GMES ERCS. The main goal of SAFER is the provision of rapid mapping capacities in response to emergency situations. Since 2008 a full scale delivery service was established. The service covers response to real events as well as to simulated events during specific exercises. The prompt response time is the preeminent performance criterion (cf. Chapter 3). In addition to UN agencies there is also an international network of civil protection authorities in the SAFER consortium as well as scientific partners and service providers.

With the establishment of a full range end-to-end service EO data is finally made available for emergency relief teams (STEVENS 2008: 68). In the context of national and international response to major disasters the ZKI embodies a service of the German Remote Sensing Data Centre (DFD) of DLR. It is assigned the task of providing contemporary processed and analyzed satellite imagery necessary for specific rapid mapping products in the case of natural and environmental disasters, humanitarian relief activities and civil security concerns. The ‘on demand’ rendered products are available for

relief organizations and government agencies alike free of charge (STEVENS 2008: 68; ZKI 2010). The extracted information is appropriated in terms of maps or digital geo-data and finally utilised in disaster management operations or relief activities (VOIGT ET AL. 2007: 1521, STEVENS 2008: 68, ZKI 2010). In remote sensing, data extraction is the operation that allows the generation of value added information from the interpretation and analysis of satellite images (VEGA EZQUIETA ET AL. 2010: 55). The role of the value adding entities like ZKI is shown in Figure 2.12.

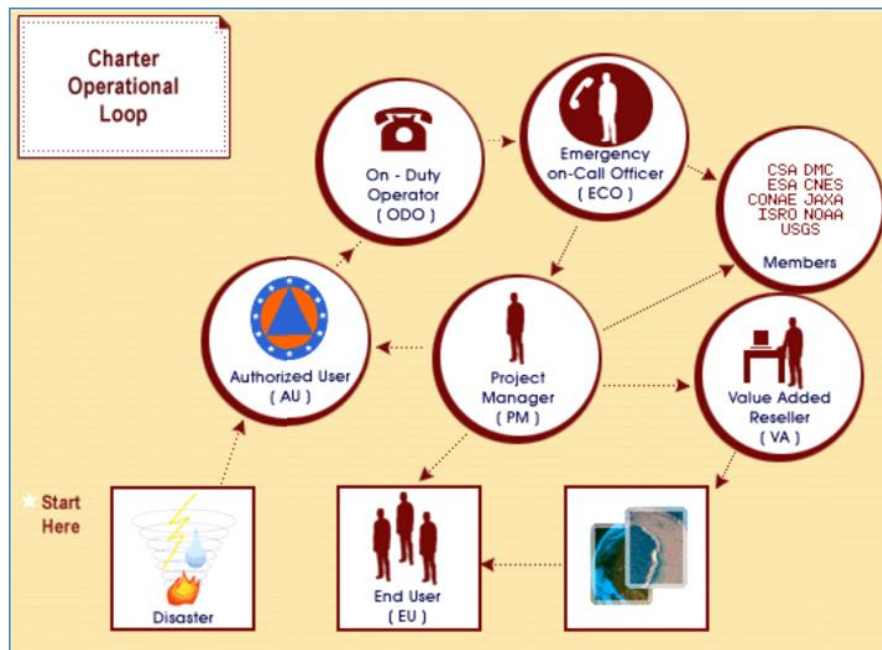


Figure 2.12: Operational loop of the International Charter on Major Disasters

Source: *DISASTERSCHARTER.ORG (N.D)*

Another tool for decision support to a wide variety of users is the Global Earth Observation System of Systems (GEOSS). Among other issues, it is a global and flexible network of content providers that focuses on developing new systems where gaps currently exist, e.g. promote common technical standards for combining different data sources into coherent data sets. By making it possible to integrate different types of disaster-related data and information from diverse sources, GEOSS aims to strengthen analysis and decision making for disaster response and risk reduction. A component of GEOSS is the Group on Earth Observations (GEO). It proposes to coordinate service providers and product developers. The aim is to establish a service permitting disaster-response teams to benefit from all available space-based observations through maps of affected areas. The maps are accessible via the Disaster Management Clearinghouse the delivery portal of GEO.

As a consequence of the aforementioned developments, such as distribution and data exchange networks, the focus within the Charter has changed. The present discourse is dominated by the increase of quality of value added products and its respective validation (see also Chapter 4). In this, as a value adding entity, ZKI is researching for methods that increase product quality and, in particular, reliability. In the context of visual interpretation it is assumed, that team-based analysis has got certain advantages over conventional analysis. Hereafter some basic aspects are presented.

2.8 Fundamentals of Team-based Methods

Team-based analysis methods can handle large data sets, complex protocols and compressed timelines, because they profit from multiple players (MACQUEEN & GUEST 2008: 3). An integrated team-based analysis avoids dividing tasks and fitting them into a hole in the end. The increase in perceptions, approaches as well as mutual learning of analytical strategies can lead to synergetic effects, that result in higher reliability of the achieved output (ibid.). This effects are intensified by the common purpose and the mutual accountability of team members, that build on each other's strengths. Spontaneous conversations broaden the range of perceptivity, whereas smaller teams reduce vocal domination (MACQUEEN & GUEST 2008: 5f).

Since a certain degree of subjectivity is unavoidable in an interpretation process it should become an integrated component (NIESYTO 2006: 274) that is always considered in the developed methodology (see Chapter 4). As outlined in Chapter 2.6 context dependent knowledge influences the image interpretation in a substantial manner (NIESYTO 2006: 272). It is believed that gauging and training (NIESYTO 2006: 274) in an understandable and credible manner (CAREY & GELAUE 2008: 228) will guide the analytic work and considerations of interpreters (NIESYTO 2006: 274). Hence, to limit variations in the image interpretation, instruction and standardized procedures are proven techniques to assure a more reliable and consistent outcome, because selection- and interpretation patterns follow impact-based reflections (NIESYTO 2006: 274).

Due to subjectivity documentation is useful. This emphasises the understanding of the interpreter (NIESYTO 2006: 274, COLLIER 2010: 59). The transmitted knowledge remains fresh and the translation onto the picture and the interpretation is direct (COLLIER 2010: 59).

An interpretation scheme or a guideline compels the interpreter to consequent and systematic actions. The reduction of misinterpretations supports this fact. Hence, a given example scheme lets the interpreter recognise conformities, that influence the quality of the result (LÖFFLER ET AL. 2005: 133). Regarding the process of development during

iterations (see Chapter 2.6) teams run through a cycle of forming, norming and performing.

In the context of EQ damage assessment the application of team-based analysis methods is thought to assist the rapid mapping at ZKI. Accordingly, Chapter 3 deals with the analysis of EO data and focuses mainly on the rapid mapping process and damage assessment products.

3 Rapid Mapping

The demand for timely and accurate information in emergency situations is rising (LANG ET AL. 2010: 65). The increase in the number of natural disasters and emergency situations (see Figure 3.1) requires more precise and contemporary geo-information (VOIGT ET AL. 2007: 1520).

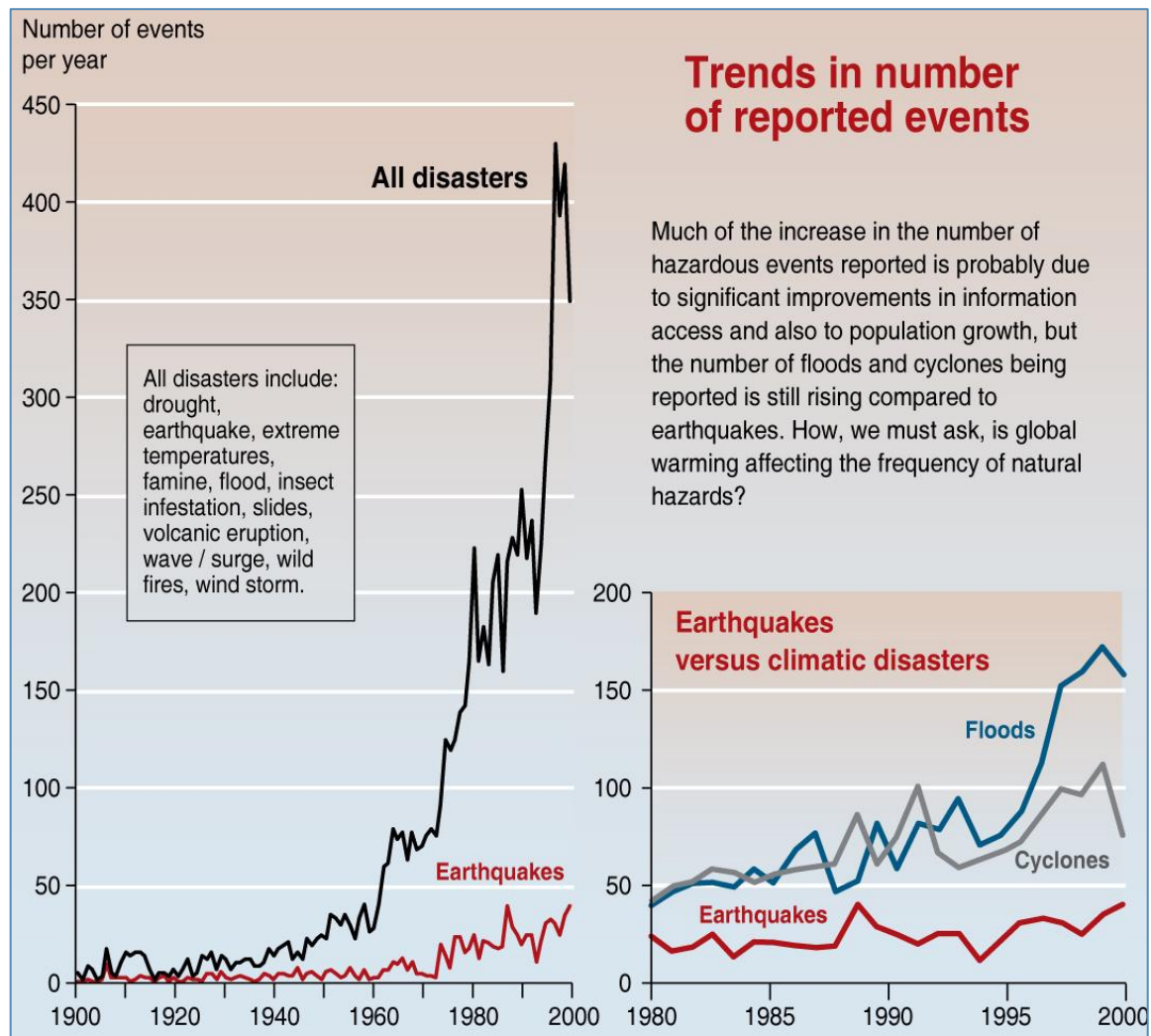


Figure 3.1: Trends in number of reported events

Source: UNEP / GRID 2005

The number of reported crisis events is still rising. Population growth, increasing economic value and improved information technologies (UNEP/GRID 2005) increase the need for and, at the same time, ease the access to disaster relevant data. Timely high-quality data and information are necessary for decision making in disaster management. In the given context it is a matter of spatial data and geo-information (KOEHLER 2005: 171). Therefore rapid mapping and damage assessment are crucial imperatives especially in situations where lives are to be saved and losses are to be minimized. For the provision of rapid

mapping products, all kinds of EO data is considered for the extraction of relevant crisis information (ZKI n.d.). The available data and its respective image content directly influence the quality of rapid mapping products. Information extraction from the provided data and its representation are the main tasks in the emergency response. Within the SAFER framework, reference mapping is made available to users within just six hours after an emergency situation occurs. Assessment maps of the disaster are available within eight hours after data reception (GMES n.d.).

The following citation underlines the essential need of EO-data for timely decision support, especially for earthquake events: „Given the magnitude and complexity of transportation networks, near-real time field-based assessment is not an option considering the critical 48 hour period that urban search and rescue teams have to locate survivors, accessibility must be quickly and accurately determined in order to reroute response teams and avoid life threatening delays“ (EGUCHI ET AL. 2010: 304). Therefore it is of great importance that space technology and geo-information is provided in an easily useable and readily accessible form to the relief community (VOIGT ET AL. 2005: 531). To assure an operational workflow, throughout all phases of an disaster, the disaster management cycle was developed (see Figure 3.2).

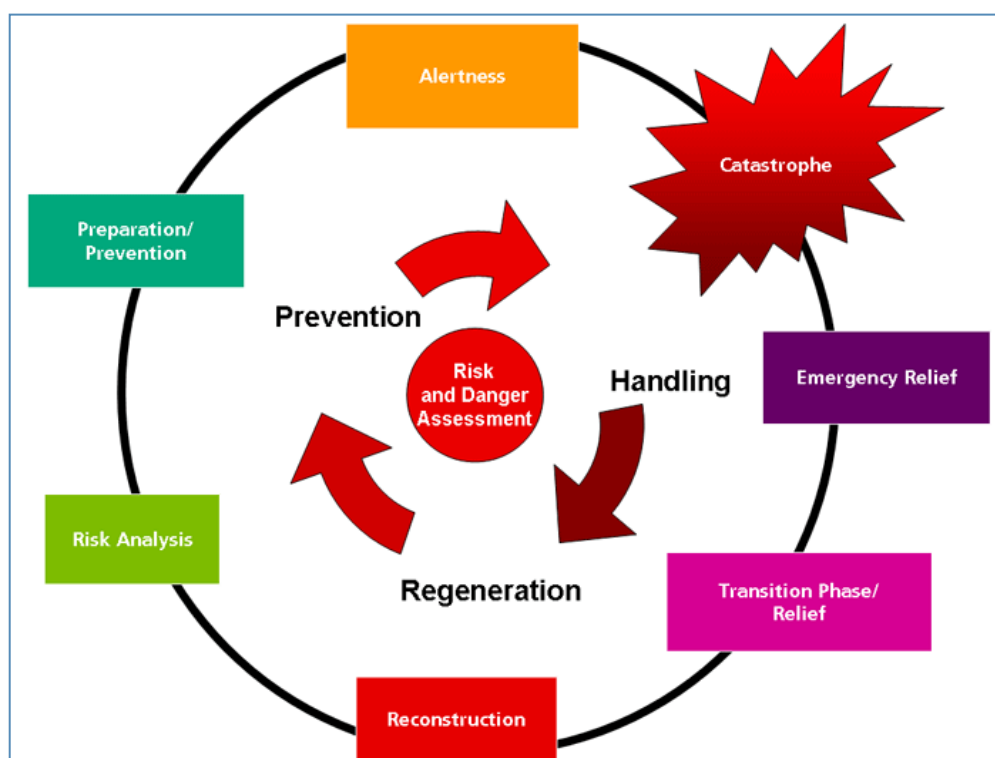


Figure 3.2: Disaster Management Cycle

Source: ZKI (n.d.)

Maps rendered after a disaster pursue various goals. Reference maps provide a first overview of the affected area and are most important for areas that are not regularly mapped or where maps are not accessible. Auxiliary maps are mostly made up of thematic information. Disaster extent maps depict disaster related aspects such as building damage or the like. Maps that are used as planning basis show information such as possible shelter locations (KERLE & WIDARTONO 2008: 16). Any information product, such as a reference maps or a damage assessment maps, can support decision making during all phases of the cycle (VOIGT ET AL. 2007: 1521). The disaster management cycle covers all phases after a crisis event. Each stage needs different information products. Service providers like ZKI make valuable contributions especially during the emergency relief phase. In terms of rapid mapping the provision of relevant and up-to date cartographic products derived from satellite imagery, an operational data flow from satellite operators and distribution networks (as outlined in Chapter 2.7, cf. BUEHLER & KELLENBERGER 2007) is the base for a fast information sharing between decision makers and relief workers (VOIGT ET AL. 2005: 520). The use of GIS for analysing the derived data during the initial response provides important visual and spatial information (EGUCHI ET AL. 2010: 296), and *“can support decision making and situation awareness during all phases of the disaster and crisis cycle”* (VOIGT ET AL. 2007: 1521). This is the case especially in a large disaster area (OGAWA ET AL. 2000: 1), such as the Haiti EQ.

For the rapid mapping of such events it is advisable to use quality management to assure a consistent output. Standardised procedures guarantee a hitch-free course of analysis. Figure 3.3 shows the generic rapid mapping workflow of ZKI during crisis situations. Immediately after the event mobilization is initiated. Satellite tasking as well as the archive search then proceed. Relief organizations and governmental agencies receive first information products based on archive images regarding the crisis event during the first six hours after the activation.

The post-disaster images are used to delineate the affected areas and estimate the damages caused by the disaster (ZKI n.d.). Preprocessing usually is limited due to time constraints. Time consuming processes like atmospheric correction are applied only if essential for (machine-based) analysis, because, for EQ damage assessment, the focus is mainly on visual interpretation. Other preprocessing tasks are e.g. projection to a coordinate system, data fusion or image enhancement, as described in Section 2.3.2. In the analysis phase state-of-the-art processing chains and algorithms support visual interpretation for the requested information extraction (VOIGT ET AL. 2007: 1521ff., ZKI, n.d.). Finally, the results are transferred into the map products, for example damage assessment maps.

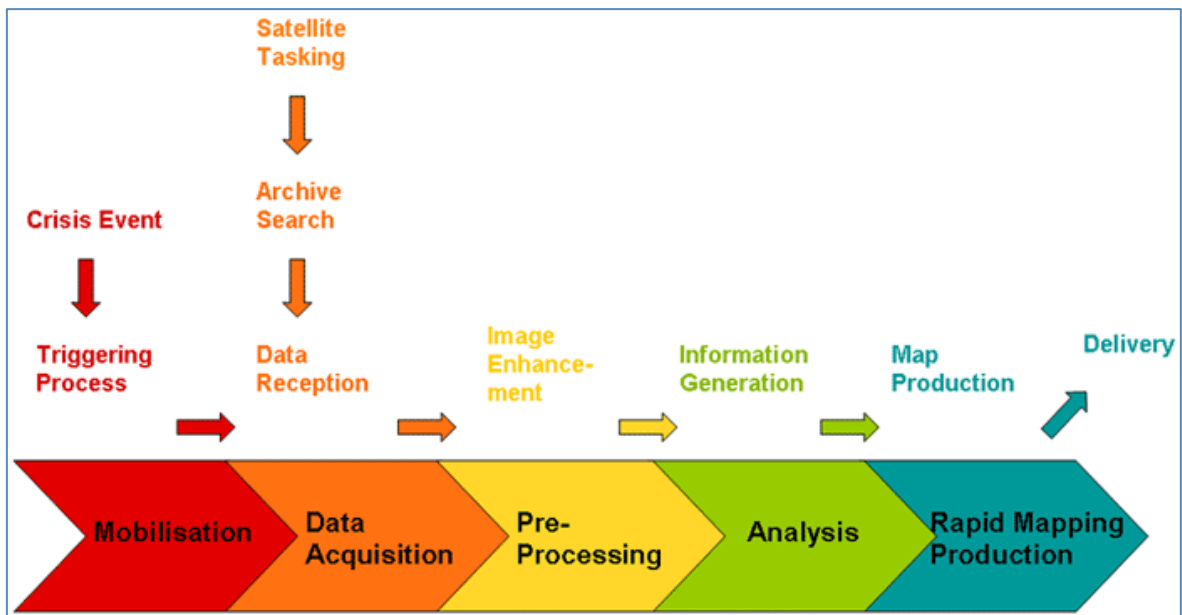


Figure 3.3: Rapid Mapping workflow of ZKI

Source: ZKI (n.d.)

The information is spread in the internet via Reliefweb, AlertNet, the USGS Hazard Data Distribution System or the GEO Portal of GEOSS and the website of ZKI, where all products are freely available. These platforms are effective tools for making disaster relevant information available. On personal request of certain entities data is also distributed via e-mail or ftp-servers. The most significant constraint in the chain is the link to the user. Only if map products suit the need of the user, are timely, accurate, and can be readily accessed, there is potential aid in the emergency response (KERLE & WIDARTONO 2008: 16). The information products have to reflect the individual and variable needs of the users, which are presented hereafter in detail.

3.1 User Requirements for Map Products

Training and consulting of decision makers and relief workers, NGO's and relief agencies is a crucial task for efficient flow of information, since understanding of space-based information products can support fast and direct mission planning and decision making (VOIGT ET AL. 2005: 530). In addition, compliance with flexible but clear standards helps to face disaster situations well prepared. KERLE AND WIDARTONO (2008: 21f) report from the Indonesia Earthquake in 2008 that there were only one-fits-all damage maps available. They regret while there were great efforts and good intentions, user needs were neglected. As a result the utility of the maps was below value. A good communication with the users is an advantage and avoids „map disasters“ (cf. Chapter 5). The current discourse tends to a standardised but flexible product portfolio. This is thought of keeping

products resource effective. The main disadvantage is, that there will be a greater choice of maps and simultaneously leads to higher expenses.

Coordination of time-critical decision needs is based on availability of relevant data. To guarantee hitch-free support of processes and workflows, user requirements have to be considered (KOEHLER 2005: 176f) Therefore the fulfilment of their needs is a crucial task. It is a key factor that determines and ensures a well-addressed and tailored product and therefore a good usability (VEGA EZQUIETA ET AL. 2010: 57).

The implementation of services providing disaster relevant data and information enables unified information flows. A chain of effective consequential actions requires optimal availability and usability of spatial data, unification of data and information management, as well as the development of application-oriented prototypes and standards. These are for example the analysis of working processes and the specific user requirements such as digital maps or print versions (KOEHLER 2005: 177).

The products of the value adders within SAFER are utilised by a large group of registered users. The Public User Board of SAFER, as a part of the entire user group, prepared a document in which user requirements are listed in detail. According to this there are two types of map products needed in the emergency response in the aftermath of an EQ: overview maps and detailed maps. The maps should contain the disaster extent, affected areas, the condition of the infrastructure, the population, gathering areas and distribution points for food aid or the like (Safer 2010: 1). Further demands elaborated by the Project User Board are shown in Table 3.1. The table provides an overview of specific products as well as their respective content and delivery time.

Table 3.1: User requirements for earthquake emergency response within the SAFER framework

Source: SAFER 2010: 3

Product	Content	Delivery Time	Scale	Frequency
Potentially affected populated places	Identify potentially affected populated places	8 hours	Detailed: 1:5,000 – 1:25,000	Daily updates in emerging priority areas
Potentially overall affected area	Accessibility analysis	8 – 24 hours		
Damage Assessment	Affected infrastructures, damaged buildings, population living in the area	24 – 48 hours	Overview: 1:25,000 – 1:500,000	
Monitoring	Emerging new affected areas	8 – 24 hours		

The time window of a few hours for information delivery restrains the eligible sensors. However, for the production of detailed maps not all EO data is suitable. To figure out which sensors and resolutions are most qualified for a damage assessment a survey was conducted (see Chapter 3.2). The following statistical evaluation was carried out to focus on the most valuable sensors and limit the variety in order to assure accuracy/reliability.

3.2 Usability of Different Sensors and Resolutions for EQ Emergency Response/ damage assessment

KERLE AND WIDARTONO (2008: 22) hold the opinion that limitations of rapid mapping in the aftermath of an EQ are shown in a detailed house-by-house assessment. As a logical consequence the richness of detail in the EO data has to be very high. Otherwise it is impossible to detect small variances. In the context of EQ emergency response these variances could be possible damages. Damaged or collapsed houses show, in comparison to intact buildings, different characteristics. Among others these are very small-scaled shadow areas, debris and fuzzy contours. Hence, the buildings are not crisply separated from their surroundings or are slightly distorted. In conformity with VOIGT ET AL. (IN PRESS: 8) the structure and the contours show major changes. Figure 3.4 shows the mentioned phenomena.



Figure 3.4: Pre- and post-disaster comparison of a collapsed building in Carrefour

Source: Own illustration. Data: Digital Globe Corp. (World View II 13.12.2009/03.02.2010)

To appraise the dependency of sensor resolution and damage recognition, a statistical evaluation, regarding the sensors available within the Charter, was carried out. For this study a visual comparison and analysis of pan-sharpened pre- and post-disaster data was performed. Since there was no ground truth data available, the post disaster needs assessment (PDNA) from UNOSAT/WB/JRC was taken for validation.

The number of visually detected houses of the categories 'severe damage' and 'collapsed' in the focus area was recorded. Additionally, houses categorised by UNOSAT/WB/JRC of the same categories were also counted (see Chapter 3.3) and subsequently set in relation. The investigation was conducted on a central part of Port-au-Prince for the aerial and GeoEye-1 imagery, without any time limit. Due to cloud cover in the WorldView scene another subset, located in Carrefour, was chosen. The lower percentage of recognition of the WorldView-Imagery results probably from the lower ground resolution, especially in the multispectral bands (see Table 2.1). For QuickBird data (Pan 0.61 m, MS 2.4 m) a further decline in recognition is expected, but analysis is possible (JOYCE ET AL. 2009: 201). For this evaluation also Spot-5 and RapidEye imagery was consulted. Nevertheless their ground resolution is barely sufficient for the assessment of single house damages and is therefore not further considered in this study. At this point it is important to note that DLR provided rapid damage assessment within eight hours, based on GeoEye-1 data. Whereas UNOSAT/WB/JRC made the PDNA in a timeframe of four weeks based on ImageCat-RIT data. Table 3.2 summarises both investigated subsets. The columns 'Buildings (all)' and 'Damaged' belong to UNOSAT/WB/JRC reference data of the chosen subset. The last column, 'Percentage of recognition' shows the result of the visual interpretation. Although there is no comparability, given the damage assessment of ZKI was evaluated. The count of DLR in this Table shows collapsed buildings only and is seen as a benchmark for rapid damage assessment and further analysis (see Chapter 4.2).

Table 3.2: Sensor dependent damage recognition in comparison to UNOSAT/WB/JRC

Source: Own survey

Sensor	Buildings (all)	Damaged	Percentage of recognition
ImageCat-RIT	2066	538	95.4 %
GeoEye-1	2066	538	87.7 %
WorldView	1883	259	72.6 %
DLR (GeoEye-1)	2066	538	10.2 %

To consider the results of Table 3.2, it is stated that the better the spatial resolution of the data source, the higher the percentage of recognition. Thus, the percentage of damage recognition logically depends on the ground resolution of the data. As was shown aerial photographs are most qualified for a high detection rate of damaged buildings. This result is confirmed, for example, by LEMOINE (2010: 33). Since airborne photography is rarely available immediately after the event, the high potential of the investigated space borne

sensors for the damage assessment should not be underestimated. Based on the results obtained from this evaluation, the developed methodology (see Chapter 4) considers the sensors GeoEye-1 and WorldView-II.

3.3 Damage Assessment

Damage assessment is a central aspect of the emergency response to evaluate the efforts needed and to mitigate the effects of a disaster. As outlined above the interpretation of remote sensed imagery can be an effective tool for the detection of spatial distribution of damage in a EQ disaster situation (OGAWA ET AL. 2000: 1). The European Macroseismic Scale (EMS) is a well established scheme for the classification of EQ damages (GRÜNTAL 1998: 15ff.). Figure 3.5 shows the recommendation of the EMS for categorising damages into five classes. Due to general limitations of satellite imagery it is not possible to fulfil requirements for this classification scheme (see Chapter 3.3.2). Time constraints also limit the possibilities to distinguish between the grades 1 to 3 (see also Chapter 4). Therefore it is advisable to redefine the classes into damaged vs. undamaged, notwithstanding an extra category for total collapse. For example OGAWA ET AL. (2000: 2ff.) categorised into 3 classes: collapsed, fallen roof tiles and no damage.





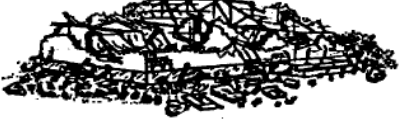
	<p>Grade 1: Negligible to slight damage (no structural damage, slight non-structural damage) Hair-line cracks in very few walls. Fall of small pieces of plaster only. Fall of loose stones from upper parts of buildings in very few cases.</p>
	<p>Grade 2: Moderate damage (slight structural damage, moderate non-structural damage) Cracks in many walls. Fall of fairly large pieces of plaster. Partial collapse of chimneys.</p>
	<p>Grade 3: Substantial to heavy damage (moderate structural damage, heavy non-structural damage) Large and extensive cracks in most walls. Roof tiles detach. Chimneys fracture at the roof line; failure of individual non-structural elements (partitions, gable walls).</p>
	<p>Grade 4: Very heavy damage (heavy structural damage, very heavy non-structural damage) Serious failure of walls; partial structural failure of roofs and floors.</p>
	<p>Grade 5: Destruction (very heavy structural damage) Total or near total collapse.</p>

Figure 3.5: Classification of damage to masonry buildings according to the EMS

Source: GRÜNTAL 1998: 15

Damage assessment pursues different goals. The key task is to determine the locations for prioritised relief efforts. Damage assessment maps that are provided in a rapid manner are usually of rather coarse character due to time constraints and available data. However, continuous updates are made to show latest information and refined damage assessments (VOIGT ET AL. IN PRESS: 6).

To derive information from EO data, in a first step preprocessing is performed. (ZKI N.D.). This is followed by the archive search as well as the production and analysis of auxiliary data, such as street data and supporting information. After the production of reference maps the manual interpretation proceeds. The generation of damage assessment maps during a disaster situation follows two major characteristics. On one hand they are directly derived from remote sensing data, on the other hand by multi-temporal comparison of

post-crisis and archive information (if the respective archive data is available). In a first step the focus is on the damage type, its extent and the situation-related restraints of key infrastructures like transportation networks (GMES 2010). The following analysis focuses on the estimation of affected people and more detailed damage assessment. Damages to buildings and infrastructure are then of specific interest in urban environments (EGUCHI ET AL. 2010). The final result of the operating sequence (as shown in Figure 3.6) is a thematic cartographic product, that finally is delivered to public authorities or rescue teams such as the Technisches Hilfswerk (THW) (THW n.d.).

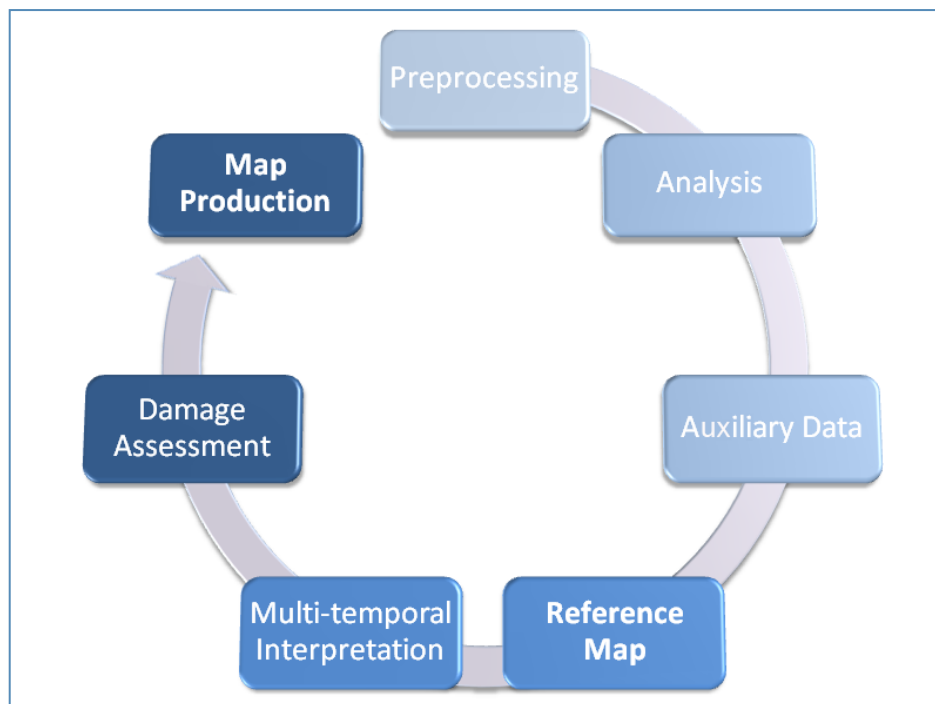


Figure 3.6: Damage assessment workflow referring to VOIGT ET AL. IN PRESS: 11

Source: Own illustration © S. Klett

In respect to emergency response, advanced technologies such as remote sensing and GIS have an advantage over conventional ground-based techniques (EGUCHI ET AL. 2010) as outlined above. As a result of the great variety of unstructured information the damage assessment entails a lot of effort in terms of time and manpower (ALTAN 2005: 312). Most studies delving into earthquake damage assessment use pre- and post-disaster imagery. Common problems are, for example, the documentation, visualisation and analysing of the building damage. Furthermore the documentation of damage effects is mostly sketchy and can only be carried out focused on a limited area of the disaster (ALTAN 2005: 312). Most research describes case studies for extracting single house damage. Others are only interested in general damage areas and use medium resolution imagery (CHINI ET AL. 2009, EGUCHI ET AL. 2010).

Damage assessment techniques for the extraction of single house damages after an earthquake differ in the literature. Some authors use manual digitizing (TURKER & SAN 2004), other studies tend to apply machine-based solutions (TURKER & CETINKAYA 2005, YAMAZAKI & KOUCH 2006, TURKER & SUMER 2008, TIEDE ET AL. 2010a). Mostly auxiliary data such as LIDAR (HOMMEL 2009) or GIS data (GAMBA ET AL. 2007, AYDÖNER & MAKTAV 2009) is used. Furthermore there are many change detection approaches based on synthetic aperture radar (SAR). Most of them lack archive information with the same acquisition parameters as the post event images, especially for the high resolution modes (VOIGT ET AL. IN PRESS: 7). Since the present thesis deals with optical data, further descriptions of SAR-based techniques were reviewed but not further considered here (cf. MATSUOKA & YAMAZAKI 2004, STRAMONDO ET AL. 2006, GAMBA ET AL. 2007, AYDÖNER AND MAKTAV 2009, TAHAYT ET AL. 2009, BRUNNER ET AL. 2010). Hereafter some methods used for damage detection, based on optical data, are listed and structured into applied indices groups.

A wide spread method for assessing damaged houses is a change detection of pre- and post-disaster imagery. Shadow edges are identified and linked in the two images. The main indicator for damage is the absence of a corresponding shadow in the post-event image (VU ET AL. 2003, TURKER & SAN 2004, AL-KHUDHAIRY 2005, TURKER & SUMER 2008, TIEDE ET AL. 2010a). The main problem of these methodologies is the high degree of uncertainty of the results. Calling the available EO data to mind, shadow formation is unreliable in respect to differences in seasonal, sensor and solar conditions at acquisition times. This can cause false signals or overlap real changes. Hence, there is a high probability of geometric shifts of shadow objects in an emergency situation. Shadow-based damage assessments could be used as supporting information, if computing is fast enough. Finally one has to note that tendencies are shown, but no absolute values of detected damages (TIEDE ET AL. 2010a: 4) (see also Chapter 4).

To assess damages with a change detection method, some authors used image matching and subtracting (GUO ET AL. 2009: 3303, VOIGT ET AL. 2007: 1525). The main disadvantage is the need for a precise radiometric correction and accurate geometric registration of the image sets, which are very time consuming. Furthermore, the output allows no intuitive reading, since results appear abstractly (VOIGT ET AL. 2007: 1525). In case of an emergency the respective archive scenes may not be available, which results in limited operational usability. Due to varying looking angles of the sensors the matching and subtracting method is likely to cause biases (AL-KHUDHAIRY ET AL. 2005: 834), especially if there is a long time-span between the two acquisitions (VOIGT ET AL. IN PRESS: 7).

The consideration of elevation data promises a high detection rate of partially damaged and collapsed buildings. The most precise results might be achieved with LIDAR datasets (HOMMEL 2009). Unfortunately they are very expensive and there are no area-covering archives. After an EQ these kind of data are rarely available. The same problems pertain to other change detection procedures based on elevation data, for example stereoscopic photo interpretation or three-dimensional modelling (SHINOZUKA 2000). By interpreting aerial photographs OGAWA ET AL. (2000) identified severely damaged and collapsed buildings. When comparing single photo and stereoscopic photo interpretations, the second technique resulted in higher accuracy. In common with matching and subtracting, the methods for damage assessment based on object elevation face two problems: either the archive data is not available or computing efforts are very time consuming. As one can see the methods lack practical suitability in the emergency response.

Another approach is machine-based debris detection, based on high reflection values of the post-disaster image (YANO & YAMAZAKI 2004: 5). As shown in Figure 3.4 and Figure 3.5 houses affected by an EQ produce debris in their direct neighbourhood. However, errors are found for segments of which the grey values and shape look like, but actually are not debris.

The above portrayed standard change detection methods are not always suitable for VHSR data. For example, even in 'optimal' case scenarios there are a lot of corrupted objects. Filtering in the post-processing brought about easy to understand building outlines, but the shape of the final objects do not match the original contours (LI ET AL. 2005: 647). This procedures are therefore not suitable for the depicted approach because of the multi-temporal analysis. In addition, the elaborated processing requires a long time. Since machine-based solutions are still not yet fully developed for rapid emergency response (LANG ET AL. 2010: 65), in that they provide reliable results only in single case studies, the ZKI currently is working with a visual interpretation technique for damage estimation. It is currently the most practicable method for the emergency response (AL-KHUDHAIRY ET AL. 2005: 836, VOIGT ET AL. 2007: 1525, VOIGT ET AL. IN PRESS: 8), and was also used for the Haiti event.

3.3.1 The Case of Haiti

This particular disaster was unusual insofar as a large number of multisource data became quickly available (LEMOINE 2010: 33). Although the Charter was activated and damage maps were produced from different entities, knowledge from the field was scarcely incorporated in the process. Nevertheless the crisis mapping service of ZKI created maps that contain specific information (e.g. affected houses).

Data reception, selection and preprocessing of the satellite imagery and aerial images (VOIGT ET AL. IN PRESS: 10) provided by the International Charter were time consuming, but in the end resulted in valuable accuracy despite the limitations of purely image-based damage maps (see Section 3.3.2). The analysis of the affected areas in Haiti encompassed, in cooperation with SERTIT, a building damage assessment, logistical information, critical infrastructure, gathering areas, population density, land cover and land use and water resources (VOIGT ET AL. IN PRESS: 11).

After an initial survey of the emergency, a multi-temporal visual building damage assessment was initiated, followed by a more detailed one (VOIGT ET AL. IN PRESS: 12). DLR produced initial damage assessment maps based on 250 m grids (see Figure 3.7).

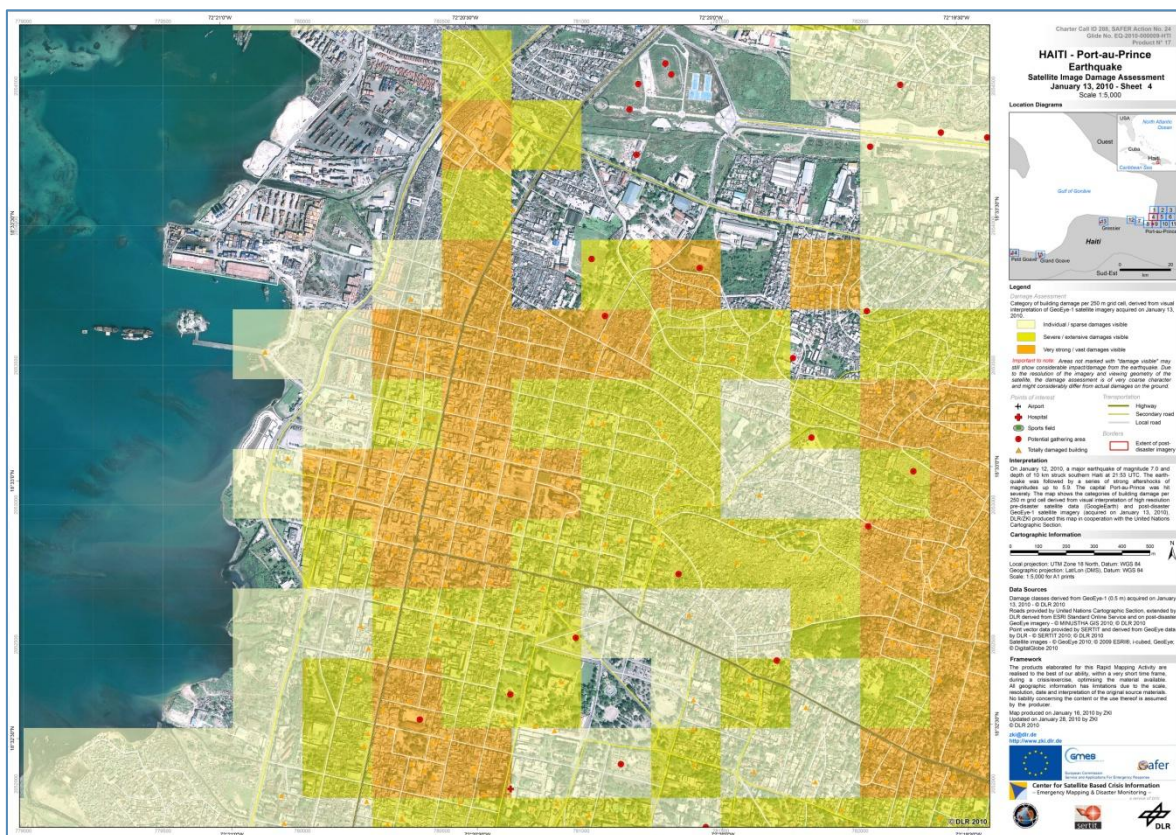


Figure 3.7: Detailed damage assessment map of Port-au-Prince.

Source: DLR (2010)

The editing on a layer file in a multi-user GIS environment occurred by 25 interpreters (oral communication: DR. TOBIAS SCHNEIDERHAN, 2010). In these grids an average damage level was estimated during the analysis (ibid.). As one can clearly see there was no house by house damage assessment. Consequently also no absolute numbers were provided, only tendencies of the damage grade of the respective grid cell. The damage classes, as presented in Figure 3.5, were redefined (no damage, sparse damage, severe damage, vast damage), „in order to account for general limitations of satellite information

content“ (VOIGT ET AL. IN PRESS: 12). Totally destroyed buildings were marked separately. The main advantages of such qualitative damage categories are the better interpretability, the higher reliability and the shorter time period needed for the analysis (VOIGT ET AL. IN PRESS: 13). However, biases occur when the number of damages is set in relation to the built up area. If a grid cell contains only one single building that is collapsed, it is assigned to the same damage level as a grid cell containing 50 buildings, of which all are collapsed (ibid). As a result many service providers confided that deviations from ground-based assessment are possible (see also Chapter 5). Also KERLE AND WIDARTONO (2008: 22) stated as far back as 2008, that significant damage might not be shown. This could be observed de novo in the case of Haiti (cf. Chapter 3.2). In an extraordinary situation like the Haiti EQ, fatigue is the consequence of the stress situation and continuous load. The lack of concentration intensifies existing limitations of remote sensing which are mentioned below.

3.3.2 Limitations of Remote Sensing for EQ Damage Assessment

As outlined in section 2.3.1 there are several limitation problems with VHSR satellite data (see also Figure 6.3). A closer look at the more specific problems for the damage assessment is presented here. KERLE AND WIDARTONO (2008:14) point out that the damage mapping which is initiated after a Charter activation „[...] *is carried out on a best-effort basis, typically without feedback from the field, constrained by the available or affordable data, [...] and with very limited time. Therefore, focus on especially affected areas at the expense of comprehensive coverage is frequent*“. This generalized statement needs to be more specifically detailed.

The value adding entity usually produces maps in foreign countries far away from the disaster spot. Typically there is no feedback from the field. Yet, the information content of satellite imagery is limited. „*By purpose the provided maps show no absolute values of detected damages but only tendencies. Absolute figures are very much depending on the resolution of the available imagery, and even on aerial images not all damages are visible from the bird's eye view*“ (TIEDE ET AL. 2010a: 4). Minor cracks or damage in walls are indistinguishable from undamaged states by reason of the (near-) nadir view of the sensor (OGAWA ET AL. 2000: 1, EGUCHI ET AL. 2010: 304, LEMOINE 2010: 33) (see Figure 3.9). Completely crushed houses are also hard to identify, if the roof remains undamaged (VOIGT ET AL. IN PRESS: 13). Furthermore it is difficult to identify damage, if a single storey of a multi-storey building has collapsed (OGAWA ET AL. 2000: 6), because the contours of the building do not alter and it therefore appears undamaged to the interpreter. The detection rate of partially damaged houses is below forty per cent (OGAWA ET AL. 2000: 7). See Figure 3.9 and Figure 3.10 as illustrative examples. Also dense urban areas cause

difficulties. The differences in height create occluded areas in the shadow of trees or multi-storey buildings hiding potentially damaged houses (AL-KHUDHAIRY ET AL. 2005: 829).

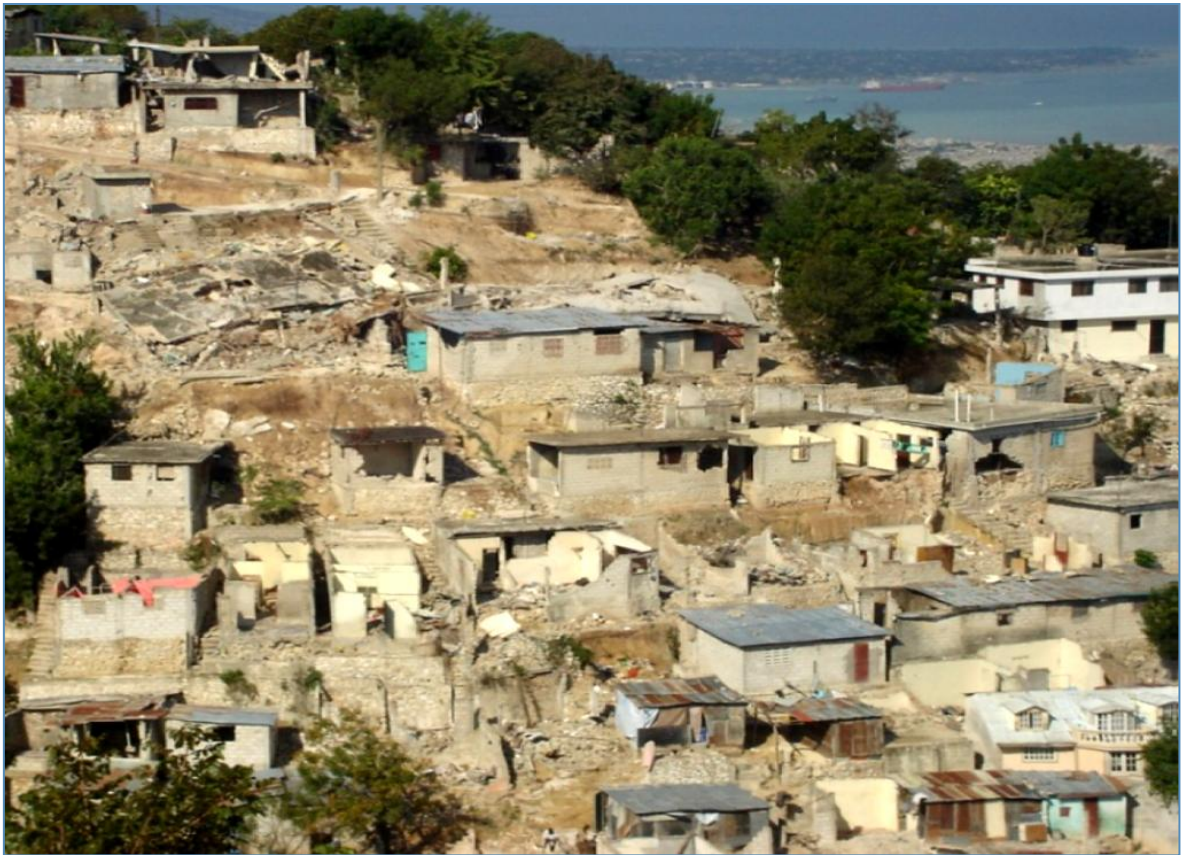


Figure 3.8: Still intact roofs of a settlement in Port-au-prince hide crushed sidewalls from the interpreter

Source: GRÜNEWALD ET AL. 2010: 1

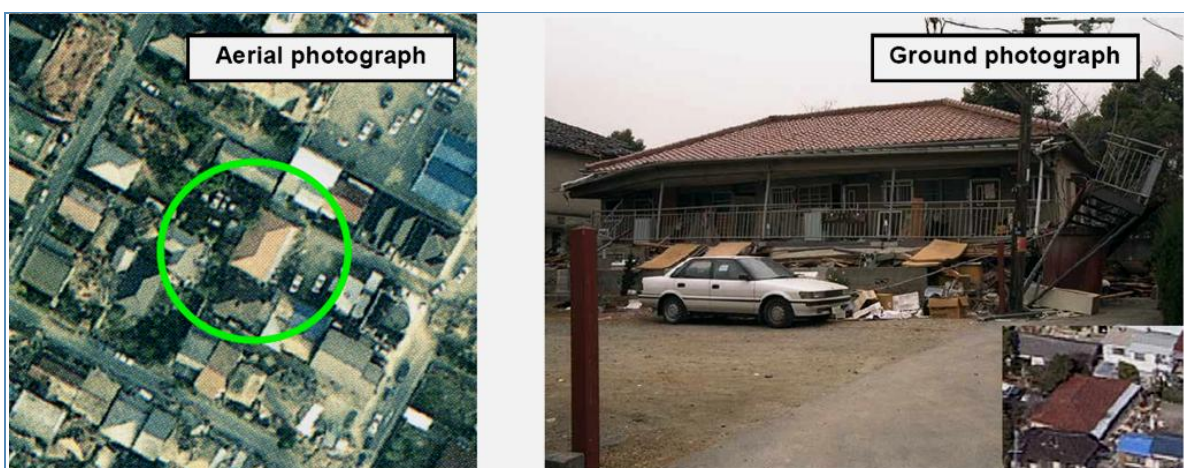


Figure 3.9: Comparison of an aerial photograph and a ground photograph of the EQ in Kobe/Japan in 1995 (this building was not identified to be “collapsed” by the interpreters although the first storey was completely crushed)

Source: OGAWA ET AL. 2000: 6

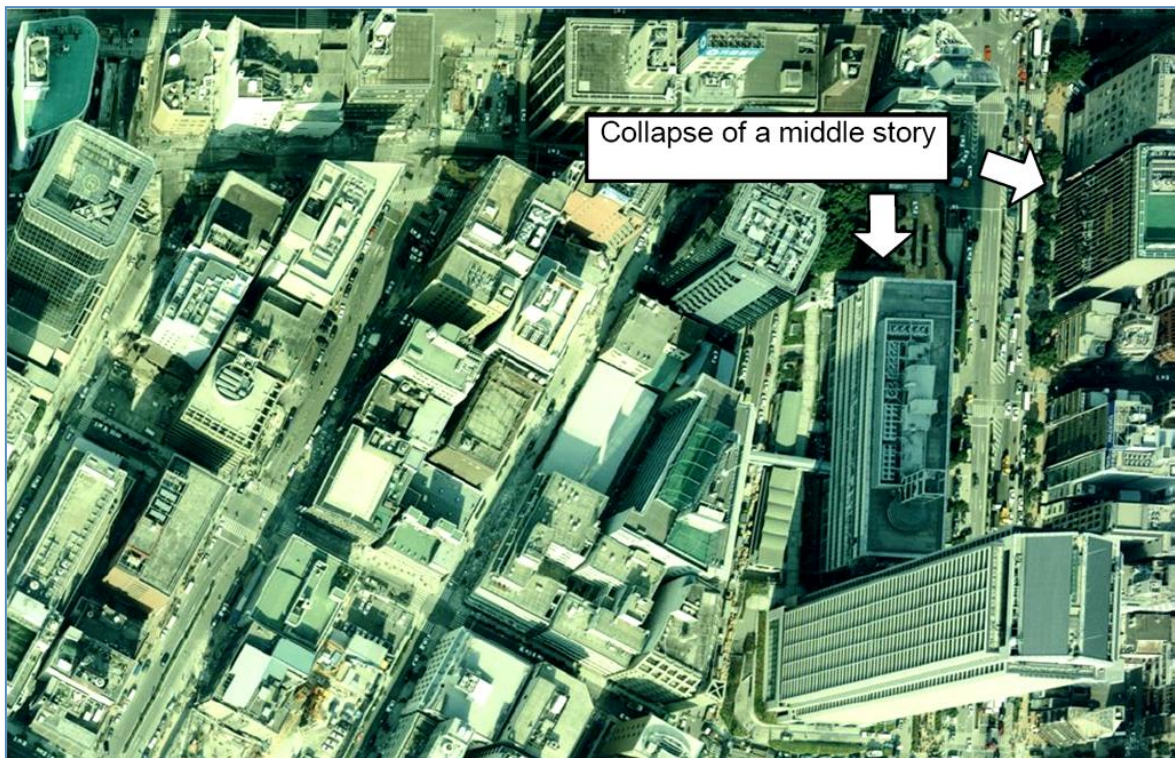


Figure 3.10: Examples of middle storey collapse resulting from the EQ in Kobe/Japan in 1995

Source: OGAWA ET AL. 2000: 7

Concerning data availability there are other challenges. On one hand, crisis management has to rely on whatever geo-information is available (VOIGT ET AL. 2007: 152f). On the other hand, due to the rising availability of EO data, the humanitarian action community receives an immense overflow of disaster relevant data, more than it can possibly handle (EGUCHI ET AL. 2010: 314). Data sighting takes a lot of time, therefore the focus should be only on VHSR sensors (see Chapter 3.2). Also if timely VHSR data is available, a long time-span between the acquisition of the images complicates the damage detection. New buildings might have constructed (VOIGT ET AL. IN PRESS: 8) or old ones been demolished. Also buildings under construction can lead to misinterpretation (OK 2008: 5, VEGA EZQUIETA ET AL. 2010: 60). That is because, among other reasons, the spectral resolution with only four image bands of the presently used sensors is comparably limited (TAUBENBÖCK ET AL. 2010a: 119). The WorldView-II sensor, for instance, has got 8 bands, but only four are delivered in case of emergencies.

Another substantial limitation is the available time. As described by VOIGT ET AL. (IN PRESS) the qualitative representation is well suited for a timely damage assessment. Many service providers produced initial maps based on grids. Consequently, a comprehensive house by house analysis is neglected and significant damage not detected. This leads to the question how useful maps can be, which are produced in a very short time, whereby the reliability cannot be rated (KERLE & WIDARTONO 2008: 22).

Fundamentally, a damage assessment under previously unpredictable conditions is difficult. The chapters ahead clearly demonstrate the need for an optimised and standardised method for rapid damage assessment. Being aware of not knowing the specific sensor for data provision in advance, a robust and transferable procedure is advisable. As a result one can note the need for the development of a methodologically sound damage extraction process.

4 A Team-based Method for Damage Assessment

As discussed in Chapter 3 there are many different approaches for satellite based EQ damage assessment. Since the machine based interpretation is considered as an objective analysis approach there may be advantages over subjective visual interpretation. But, as Figure 4.1 shows, there still remains a high degree of uncertainty.

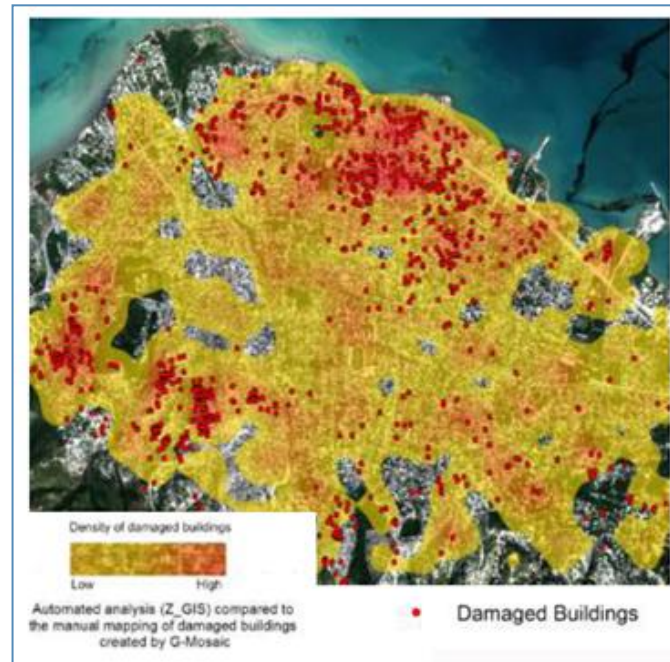


Figure 4.1: Comparison of machine-based and manual interpretation

Source: TIEDE ET AL. 2010a

This specific map was produced with a machine-based damage assessment. The authors call this kind of representation „*damage indicator map*“ (TIEDE ET. AL. 2010a: 3), because it is based on shadow indices and there are only tendencies of the distribution shown (in this case by purpose). At length, working with the machine-based approach is still regarded with a high uncertainty due to the dependence on shadow indices only. As TIEDE ET AL. (2010a) stated, the machine-based vision is incapable to distinguish between the shadow of houses and those of construction works, what causes false-alarms. Another limit is seen in the hampered differentiation of shadows casted by vegetation and buildings, if the NIR information is not provided, as it was in this case. Also seasonal variations of the vegetation can cause false-alarms. The most weighty factor for limitation of automated multi-temporal interpretation, though, results from the different viewing angles in the pre- and post-disaster images.

Accordingly, the machine-based analysis is under the given conditions relatively unreliable. “*It has to be stated, that the aim of such a machine-based approach is not to replace the manual interpretation. It rather helps users and manual interpreters to get a*

faster impression of the spatial distribution of damages in emergency situations” (TIEDE ET AL. 2010a: 4). This statement is reinforced by LANG ET AL. (2010: 63) and also other studies, not dealing with EQ damage assessment (e.g. KRANZ ET AL. 2010: 189). Because of this reason most rapid mapping providers use visual interpretation for damage assessment even in the frame of crisis situations. Unfortunately, each individual has specific knowledge and experiences that influence the interpretation results (see Chapter 2.6). Additionally there are case specific influences of environmental conditions and human interactions.

Aim of this chapter is to propose the new approach for a team-based analysis method based on an investigation of the variations of visual interpretation. To get an impression of the variations a guideline for team-based damage detection was developed and tested with a supervised group of students. An additional group of experts, performing a single interpreter analysis, was analysed to get insights of the variations of educated personnel. A statistical analysis was carried out using the same subset of the GeoEye-1 image as the survey conducted in Section 3.2. The analysis (see Chapters 4.2 and 6.2.3) considered more than one geographic location to avoid convenience sampling (CAREY & GELAUE 2008: 228).

In the case of emergencies, at ZKI data handling and processing currently follow the guidelines of a SOP. Therefore the actual core business of value adding in the emergency response context, (1) damage assessment or data extraction and (2) map production or data representation, should follow basic rules, too. The question is, how to guarantee quality and reliability for information derived from remote sensing data (CASTOLDI 2010: 124). Regarding the second point, the challenges concerning the visualisation fall in line (see Chapter 5). The product design encompasses both parts. However, these are two different aspects that can be rated. For data extraction it is the quality of the information, for the representation it is the usability (cf. VEGA EZQUIETA ET AL. 2010: 53). This chapter will cover the extraction process, whereas Chapter 5 deals with representation of the data. Having in mind the close relation of data extraction and representation for the in-line production, some intersecting considerations are mentioned here.

A recommendation for information generation that was presented at the 2nd International Workshop On Validation Of Geo-Information Products For Crisis Management (VALgEO) calls for a quality index on the maps. The *„reliability or assumed range of accuracy should be explicitly stated on the product“* (LANG ET AL. 2010: 72). VOIGT ET AL. (IN PRESS: 19) claim even interpretation keys and legends should be standardized, also for manual extracted information content. The benefit would be a higher comparability and compatibility at a global scale. Moreover there would be a high potential for rating quality

and reliability in a fast and transparent manner. But: in timely urgent situations there is almost no chance to evaluate both reliability and accuracy. The common quantitative external validation is not suitable as a quality control (VEGA EZQUIETA ET AL. 2010: 55). To assure the quality of the product an alternative warranty must be applied. As a result the right balance between the amount of extracted information, its reliability and time required has to be found. Quality control usually consumes a lot of time, but for all that, the emphasis is on the information generation (ibid). *„This means that, any time invested in controlling the quality of the product is a time that is not invested in producing something more that could be useful for the user. This means that any quality control has an impact on rush production. For this reason it is important to invest efforts in in-line quality control, an assessment of the design of the product, to keep the product inside quality standards for as long as it is produced“* (VEGA EZQUIETA ET AL. 2010: 53). Presently, at ZKI the information generation consumes about 80 per cent of the available time and the quality control about 20 per cent, and follows an standardised operating sequence. The SOP is a predefined process that ensures quality in the information extraction. Before the data is delivered a product quality control considering a checklist is applied.

Having this in mind, the development of a specific extraction procedure is a very sophisticated process. The product design has a strong influence on the final quality of the product regarding usability and accuracy (VEGA EZQUIETA ET AL. 2010: 55). One has to know in advance which outputs are desired and which techniques are best to apply for preserving proper results. Furthermore the medium capabilities should be considered (cf. VEGA EZQUIETA ET AL. 2010: 53), otherwise it would not be a sound methodology. The proposed method will establish a minimum set of standards for information delineation from satellite data. Consequently it is designed in a manner that ascertains a higher reliability through the implementation of increased quality. This leads to an improved usability of the product, if representation follows close upon. The final user of the proposed method (ZKI) expects a process fast enough to quickly cover large areas, and at the same time, enough detail to provide useful information and reliable enough to take decisions based on it (cf. VEGA EZQUIETA ET AL. 2010: 55).

Presently ZKI is working with a visual interpretation for the damage assessment as outlined in Chapter 3 (cf. VOIGT ET AL. 2010 IN PRESS). As was described, the most reliable results are achieved with this method of image content analysis. *„In visual interpretation, cognitive processes run simultaneously and only if we are not sure about the identification of features, we start reflecting on the single components of object recognition“* (LANG ET AL. 2010: 66). In case of an EQ there are a lot of unstructured features and components that underline the high demand on supporting information (cf. LANG ET AL. 2010: 65). This

is why the author assumes that the delineation of building outlines from the pre-disaster image will provide a visual assistance for object recognition, that improves more rapid interpretation. The process of developing a new team-based method for visual interpretation, based on ZKI operational standard, is introduced below. The method will make use of additional supporting information.

4.1 Supporting Information

The supporting information renders assistance to the visual interpretation to quicken the process. Since it makes use of archive data it can be generated immediately, once the affected area is determined. For use at ZKI it needs to be operational, robust and transferable. Only a basic technical knowledge of eCognition is necessary for the handling. For that reason the eCognition architect solution was chosen. To support the team-based analysis of the EO data for damage assessment (described in Section 4.2) a building footprint has to be derived.

For the initial generation of the supporting information different tasks were performed according to the operating sequence (see Figure 3.6). The preprocessing of all datasets consisted of rectification, pan-sharpening, filtering and contrast enhancement (cf. VOIGT ET AL. 2007). Pan-sharpening was made in the ERDAS Imagine 2010 environment using the resolution merge tool for creating contrast-rich, good-looking outputs. When using this tool there is some loss of spectral fidelity, but it is not necessary for emergent visual interpretation. This was followed by a look-up-table stretch to reduce the effects of outshining. The (co-) registration in the ArcGIS environment was applied to the pre- and post-disaster images (for the multi-temporal analysis) and to the street data. The additional thematic layer (auxiliary data), the road network, was used to improve the accuracy of the classification results. The extraction of the road network in case of a disaster is a standard procedure at ZKI for the generation of overview maps, therefore the data basis is available in every activation. In most cases the dataset is aligned with that of Open Street Map (OSM), depending on the coverage, consistency and accuracy of the OSM data set. Before the analysis in the remote sensing environment, a buffering in ArcGIS 9.3 was carried out, in accordance with the road types and its functionality. A dissolve operation followed. The main advantage is the better discrimination between objects belonging to the road class and the building class respectively, since the spectral diversity of image objects belonging to these classes is too similar.

In case of an earthquake disaster the specific satellite sensor is not known in advance, therefore transferability broadens the range of application. Presently there are only a few studies dealing with transferability of rule-sets onto other images. But in order to assure

an operational support it is essential (LANG ET AL. 2010: 67). The eCognition architect solution assures the fast adjustment to other images and localities as well as an easy intelligibility for varying users. According to the results obtained in Chapter 3.2, the ready-to-use solution was tested on two different VHSR-sensors of the sub-meter domain (GeoEye-1 and WorldView-II) at representative subsets.

By using the eCognition architect module different tasks such as object detection, classification or exporting results can be configured as actions. A set of actions is transferred into a ready-to-use solution for performing image analysis tasks. Rule-sets, that are prepared in the manner described, are called action libraries (DEFINIENS 2009: 200). In action libraries, there exists the possibility to create dynamic variables that are interactively controlled by the user and communicate with the rule-set. This happens through the implementation of widgets. Widgets are user interface components to adjust action parameters (DEFINIENS 2009: 200). A schematic depiction is given in Figure 4.2.

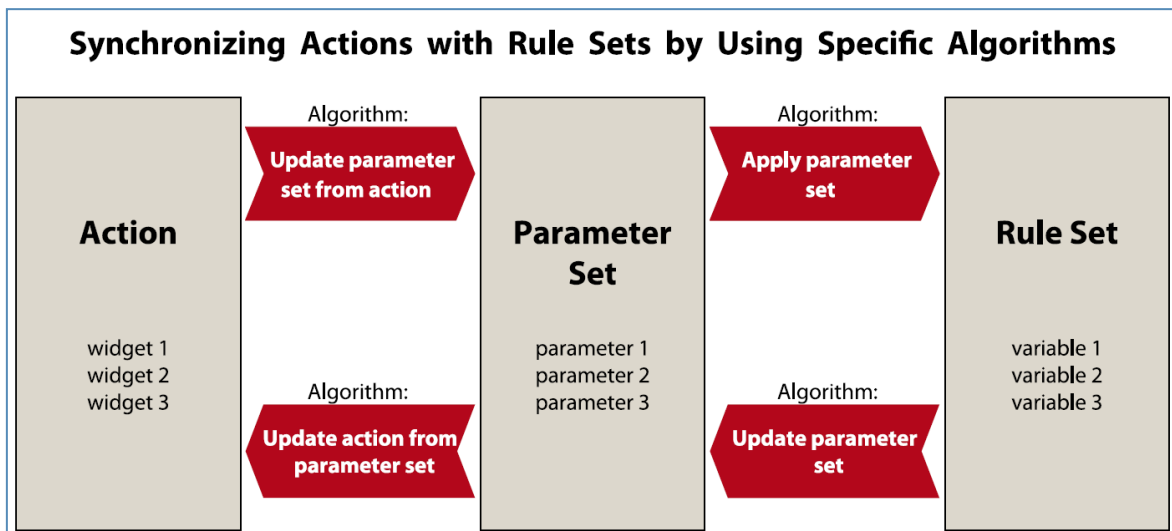


Figure 4.2: Communication between action and rule-set.

Source: DEFINIENS 2009: 200

In the eCognition architect environment standard fuzzy classifications are not suitable for transferrable master rule-sets. The fixed thresholds implemented in fuzzy master rule-sets are not adjustable. Therefore root-variables were generated, that access on the widgets through implemented sliders. In that way the specific thresholds are defined, according to the input data. The interactive adaption onto the particular satellite image preserves the master rule-set while the thresholds are adjusted. This enables a similar high classification accuracy for both tested sensors, if the thresholds are defined properly. The thresholds, that were determined in the present data are shown in Appendix 2. In a further step additional variables were generated that use arithmetic expressions to create dependencies to the root-variables. Thus, ranges in the spectral values of single classes

are implemented, whereby a fuzzy classification is simulated. Furthermore text-variables have been created that access the Extensible Markup Language (xml) codes of eCognition. These variables enable the interactive generation of new projects, definition of desired export formats as well as output-path and output-names. Finally icons were produced that symbolize the specific process of the respective action in the graphical user interface (GUI) of the architect solution (see Figure 4.3).

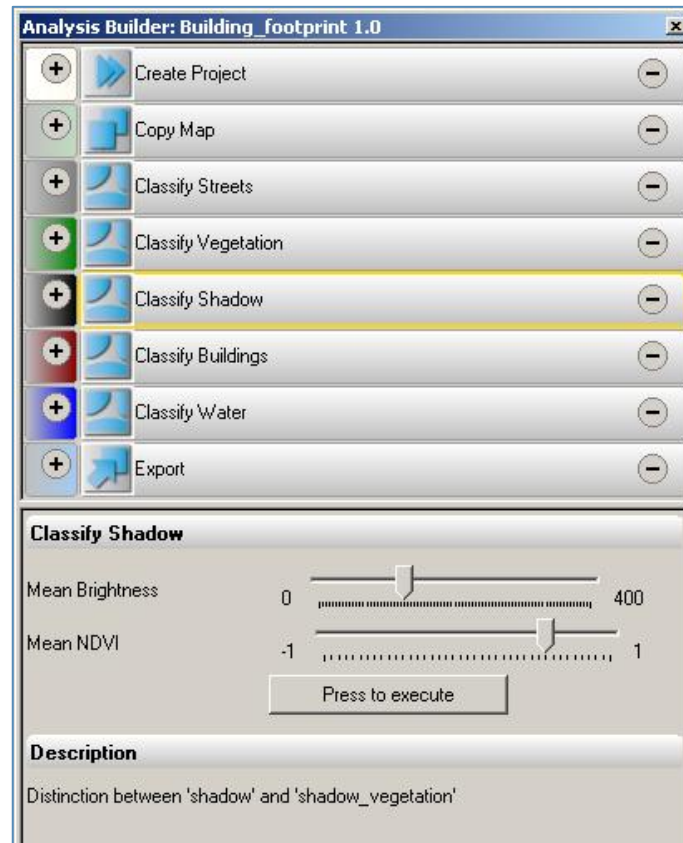


Figure 4.3: GUI of the eCognition architect action library

Source: Own illustration © S. Klett

Based on an object-oriented hierarchical classification approach with different segmentation levels (cf. TAUBENBÖCK ET AL. 2010a) a master rule-set was developed, which enables an easy and fast transfer to other areas (cf. TIEDE ET AL. 2010b). The best results for the delineation of a building footprint were obtained by applying a combination of a hierarchical multi-resolution (TAUBENBÖCK ET AL. 2010) and spectral-difference segmentation (ESCH ET AL. 2008). On three levels (see Figure 4.4) the satellite data is differentiated into areas covering vegetation, shadow, sealed ground, streets, water bodies and built-up areas from VHSR optical data (in particular WorldView-II and GeoEye-1). The class 'sealed ground' serves the situation of camps. The shadow class is divided into 'shadow' and 'shadow_vegetation'. The former could provide additional information in large areas of destruction, e.g. the number of collapsed houses via counting the

respective shadows. The number of classes is comparatively low, in respect to the faster performance of the automated process (AL-KHUDHAIRY ET AL. 2005: 6). This is thought to be more practicable, because the high complexity of analysis tasks „in a complex situation such as an earthquake with virtually all kinds of destroyed man-made or natural features is (still) too high to fully grasp the potential set of target classes automatically” (LANG ET AL. 2010: 65). The classification of streets follows on a separated map. The utilisation of the thematic layer created artefacts, because of the hierarchy, so that the ‘copy map’ algorithm became necessary. In a later step of the process tree, the results are unified.

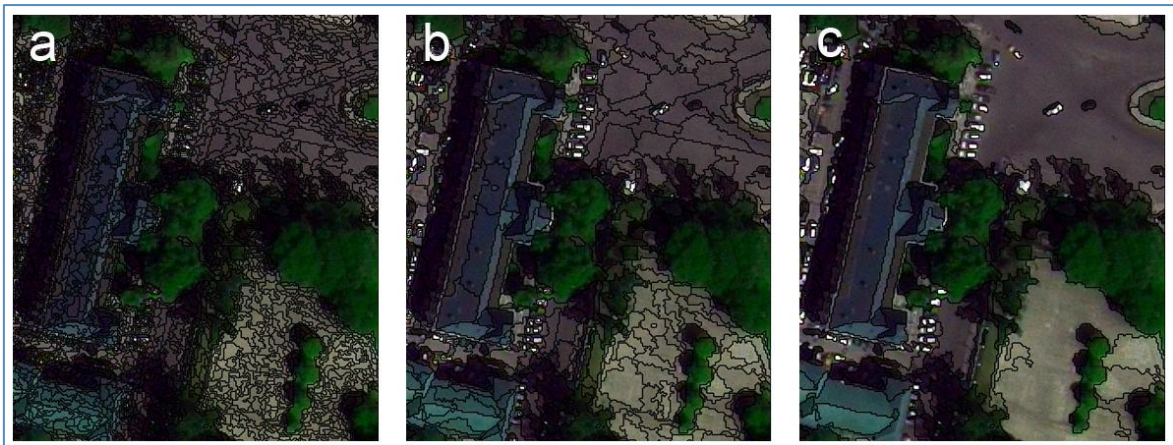


Figure 4.4: Scale parameters (SP) used for hierarchical classification of image objects on a subset of the GeoEye-1 image. Figure a) shows the segmentation level vegetation, SP: 10; b) shows the level shadow, SP: 20; c) shows the level built-up areas, SP: 80

Source: Own illustration

All derived objects of the compact master rule-set are based on five fuzzy spectral values, determined with the feature space plot (see Figure 4.5). The respective values for each class can easily be adapted to different sensors by visual on screen inspection of spectral thresholds (TIEDE ET AL. 2010b: 3). However, the main focus was on relational attributes, such as length/width ratios, geometrical features or neighbourhoods and texture attributes, to assure fast transferability (cf. LANG ET AL. 2010: 67). A subset showing the result of the object based image analysis can be seen in Figure 6.2.

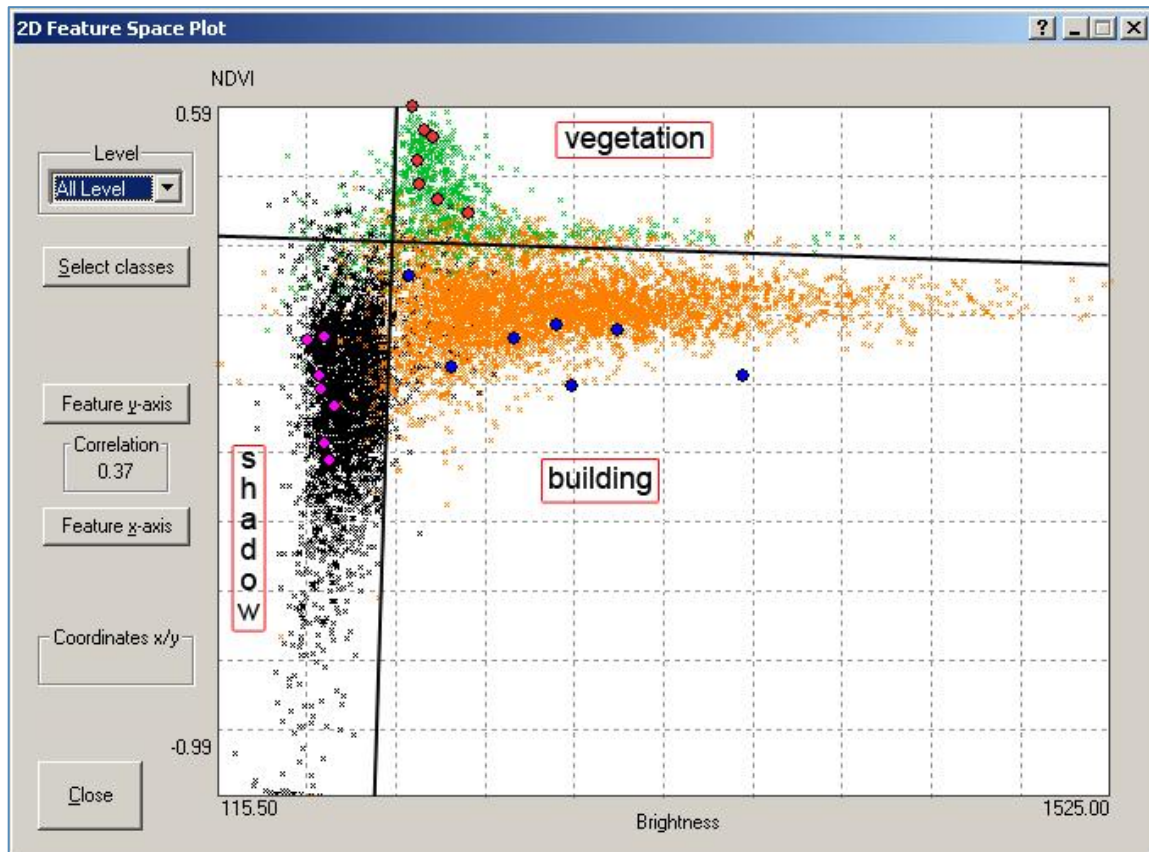


Figure 4.5: Spectral thresholds of selected classes in the modified GUI of the eCognition feature space plot showing the parameters mean Brightness and NDVI. Dots show samples used for the determination of optimal feature space class distinction.

Source: Own illustration

The intention of using the supporting information, the extracted building footprint, is to render assistance to the experts performing the visual damage assessment in an on-screen GIS-environment (see Chapter 4.2). The advantage of the proposed methodology is to recognize shifted buildings, and beyond that, a more accurate number of collapsed houses. The application of the supporting information is described below.

4.2 Developing a Team-based Method

Concerning visual interpretation the team-based analysis has a high potential to improve analysis, because of “*the ability for multiple views of precisely the same phenomena*” (COLLIER 2010: 54). The different readings of various interpreters can be compared and linked. Through the implementation of a mapping guideline, team analysis has a high competency to speed up the analysis of large quantities of images (ibid.). Team-based analysis is also expected to produce more reliable outputs and ensuring the quality of data, or in this specific context, damage extraction.

The development of the team-based method is based on the results of the investigation of variances in visual interpretation. OGAWA ET AL. (2000: 2ff.) evaluated visual interpretation

differences in the damage assessment accuracy based on aerial photographs of the Kobe earthquake in 1995. The difference was evaluated through ground survey data. The investigated interpreters were six civil engineers, but in this small group the rate of damage detection varied from 40-70 per cent, containing a great deal of individual deviance. The most accordance in the interpretation results was found in the class collapsed (see also Chapter 3.3).

To reassess this study within a team-based survey a cross-sectional research design for qualitative methods was developed. This signifies a primary data collection method (CAREY & GELAUE 2008: 227f) with an experimental project design (MACQUEEN ET AL. 1998: 232). The survey consists of a statistical content analysis approach, because this kind of analysis is seen as efficient and reliable (NAMEY ET AL. 2008: 138). Two focal groups were selected in respect to the maximum variations method. This entails a wide range in perspectives and selection of persons (CAREY & GELAUE 2008: 233). The design of the data collection instrument focused on a group guideline for two reasons: (1) enabling the evaluation with multivariate statistics, (2) performing a pre-test. For the developed method the author preferred guidelines instead of standards. The main advantage is that a guideline consists of more flexible recommendations than of absolute rules. These recommendations may be modified in the development process of the teams, on condition that needed. Essential ideas or insights related to the specific situation can be expressed by the teams. The preliminary guideline (see Appendix 1), or training manual, contained an intents list as well as example pictures that acted as interpretation guides to ensure understanding of the instructions (CAREY & GELAUE 2008: 235ff.) and promote a structured analysis (COLLIER 2010: 54). In regard to on-screen visual interpretation, the team size has to be limited (MACQUEEN & GUEST 2008: 5f) to two persons. Accordingly, groups of two share two screens for digitizing building damages. The intention is to analyse the area under investigation twice in a short time with the assistance of the aforementioned building footprint (Chapter 4.1). Short breaks with moderated discussions ensure consistency, because possible questions and concerns can be expressed (see also VEGA EZQUIETA ET AL. 2010). Hence, edits agreed upon can be made by the teams, if needed (CAREY & GELAUE 2008: 253). Since the interpretation will be consistent among different interpreters, no further quality control is required (cf. VEGA EZQUIETA ET AL. 2010: 55f). The damage assessment was achieved by assigning one point per damaged building identified, instead of giving an overall qualitative degree of damage level per grid based on the analyst's interpretation, which is rather unreliable.

For the study, the focus was on the quantitative aspect (how much will be recognized), and not on an qualitative (which class does the building belong to). For consistency

assurance the focus groups received gauging via an instruction and a training manual. A grid divided the focus area, a subset of the satellite image, into 100 m x 100 m cells, that helped facilitate the interior orientation and avoided redundant editing. The teams were given one hour time to analyse a central part of Port-au-Prince. The study area covered an area of one square kilometre. Under normal conditions it would take considerably more time to analyse a region of that size in detail, but to simulate an realistic stressful situation time was limited. To get familiar with the task, visual examples of each damage class were distributed to all image interpreters. Afterwards the teams had to write down their own comments on how to recognise damaged buildings by means of predefined examples in the study area. This was done in the Google Earth environment, using aerial photography. Afterwards the symbology of the provided data was visually adjusted and hierarchically ordered, in order to perform a multi-temporal damage assessment in the ArcGIS environment. By using the swipe tool the interpreters could compare the pre- and post-disaster images ad-hoc. The interpretation started in the upper left grid cell, continuing sequentially. For each recognised damage a point was set. In the case of uncertainty, whether damage existed or not, the layer 'building_footprint' was activated. This helped to identify changes in the former outlines of the respective house. The analysis was carried out on a scale of 1:1,000. During the editing there were expected diverging ratings inside each team, therefore differences were documented. The final result of the interpretation was then delivered to the author.

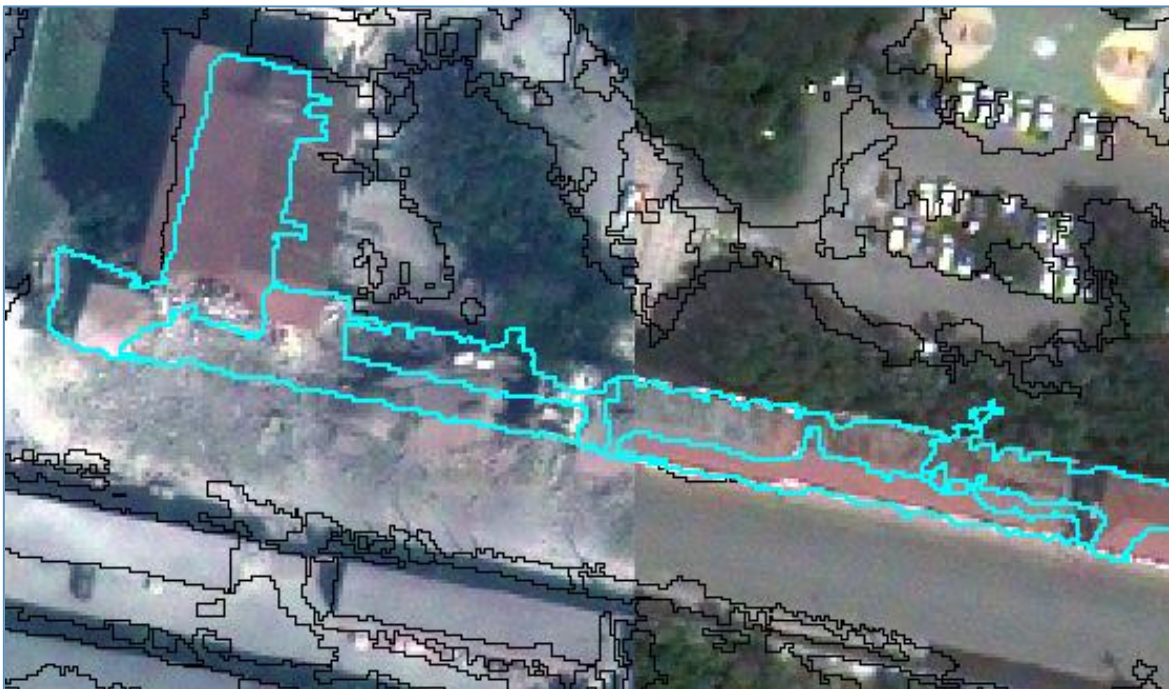


Figure 4.6: Multi-temporal analysis using the swipe tool: on the left the post-disaster image is shown, on the right the pre-disaster image

Source: Own illustration

To get an estimate of the advantages of team-based analysis an identical survey was carried out with another focus group, consisting of ten individual interpreters. The results of both groups, the ten teams of two interpreters and the ten single interpreters, were then compared.

The transformation into a raster surface became necessary because the edited point features were scattering within the contours of a building identified to be damaged. For the presentation of the reference group analysis a density tool of the ArcGIS environment was used. It distributes a measured quantity of an input point layer throughout the area under investigation to produce a continuous surface. Density surfaces show where point features are concentrated. In this context the surface indicates graphically the accordance of recognized damage buildings in a raster of ten meters. The Kernel Density Estimation (KDE) „calculates a magnitude per unit area from point or polyline features using a kernel function to fit a smoothly tapered surface to each point“ (ESRI 2009). In other words, KDE is a procedure that smoothly fits a curved surface over each point. The value is highest at the location of the point and diminishes with increasing distance, reaching zero at the search radius distance from the point. Only a circular neighbourhood is possible. The volume under the surface equals the input field value for the point. The density of each output raster cell is calculated by adding the values of all kernel surfaces where they overlay the raster cell centre. Accordingly, the KDE shows the density of point features in each output raster cell.

In statistics it is common sense that statistical occurrences have a certain probability (P). P is considered to be explained by samples. In the thesis the samples are spot-tests, presented by the interpretation results. For the analysis of the results a T-distribution was chosen, because it is especially suited for random samplings with number smaller than 30 [$(n) < 30$]. For a plurality of degrees of freedom the T-distribution approximates the normal distribution (BAHRENBURG ET AL. 2010: 118ff.). For the representation in a graph the probability density function was deployed. It is used as a tool to calculate P of a continuous random variable to be between two real numbers a and b. It is seen as a measure of theoretical distribution (BAHRENBURG ET AL. 2010: 133). To make a statement on the normal distribution in the continuous case of damage estimation the probability density function was utilised. With the aid of this function it is possible to state the probability of a random variable although there are infinite possibilities in the integral of a and b (BAHRENBURG ET AL. 2010: 94). a is then 0 and b the total number of damages.

The expected value ($E[\bar{x}]$) of the survey is the observed modal value of the ascertained spot tests. The variance (σ^2) of the random variable \bar{x} measures the scatter of all values

relative to the expected value. In the process the squares of the deviation are weighted according to their probability (P) (BAHRENBURG ET AL. 2010: 118ff.). For the transformation of the spatial distribution into a chart a trend interpolator was used. The trend surface method is an approximate and global interpolator. Its procedure minimizes the difference between the interpolated value of a data point and its original value. As a type of regression model it approximates a mathematically defined surface through all data points (HEYWOOD ET AL. 2006: 198). The second order polynomial, which was used for representation of the trend surface in Figure 6.7, fits the greatest trend of variation in the data.

The study produced quantitative data with a qualitative assertion. This can be seen in the evaluation (Chapter 6.2.3) as well as in the result variation. The results were analysed and evaluated for further development of the team-based method.

In real emergencies, unlike the pre-test study, the extracted data or the interpreted image content has to be visualised. This is the interface between the producers and the users of the value added products. Hereafter the representation in maps is the centre of attention.

5 Visualisation of Damaged Buildings

Following Chapter 4 the semiotic representation of the extracted data is the next step in the damage assessment workflow. Thereby, as presented in Chapter 3, it is of great importance that space technology and geo-information is provided in a easy to use and ready to access information solution to the relief community (VOIGT ET AL. 2005: 531). For the representation of information in emergency situations it is necessary to take the specific constraints into consideration which consist primarily of time pressure and stress factor (ANDRIENKO & ANDRIENKO 2007: 890). Furthermore, at a global scale, harmonization of data representation needs cultural sensitivity (COLLIER 2010: 54f).

Depending on their information content, the maps are needed by different users and at different times. Ideally they are produced with a specific user group in mind. Especially maps prepared in the first few days after an event, however, are typically prepared far away from, and without a direct communication link to, the disaster area. This leads to the risk that maps are prepared without awareness of the specific information needs of the users in the affected country (KERLE & WIDARTONO 2008: 16f).

The Haiti EQ was unusual insofar as a large number of multisource data became quickly available (VOIGT ET AL. IN PRESS). Thereby, the humanitarian action community faced an immense overflow of satellite images and corresponding maps. Although the International Charter on Space and Major Disasters was activated and damage maps were produced, knowledge from the field was scarcely incorporated in this process as the situation in the field is complex and the crisis teams in the field are fully concentrated on the urgent rescue work. The different service providers applied various methods for the visualisation of damage assessment maps. According to VOIGT ET AL. (IN PRESS: 15f), in the case of the Haiti EQ this resulted in a „*mapping disaster*“, as a high diversity in the representation of the similar features was observed. As a consequence, the variance in representation of information delayed relief efforts (cf. SHANKAR ET AL. 2010: 21) (see Section 5.1).

To pick upon the statement of KERLE AND WIDARTONO (2008: 16f) (see Section 3.3.2) the next step from best effort practice to a more structured and standardized basis is necessary (VOIGT ET AL. IN PRESS: 18). In the international discourse presently there is a debate about the need of harmonising the analysis and visualisation approaches in order to reduce the variability of information representation and increase accuracy as well as ease interpretation by users (cf. VOIGT ET AL. IN PRESS: 15ff.). As mentioned in Chapter 4 recent recommendations comprise quality indices on the maps, interpretation keys and

legends. The main advantages would not only be higher comparability but also better rating quality and reliability in a fast and transparent manner.

To achieve homogeneity in map design many aspects have to be considered, for example the data represented, scale, symbology and the further. The product usability and the end-user skills are of paramount importance in the design (VEGA EZQUIETA ET AL. 2010: 56). However, the design starts with the extraction of data (cf. Chapter 4). Different add-on methods of its representation lead to different perceptions of the final map content (VEGA EZQUIETA ET AL. 2010: 56). To counteract this problem ANDRIENKO AND ANDRIENKO (2007: 893) propose a generic knowledge base containing map specifications about how to represent the desired features. The meta-information could contain statements on the quality and reliability of information (ANDRIENKO & ANDRIENKO 2007: 896), in the manner described by LANG ET AL. (2010: 72).

LANG ET AL. (2010: 73) rated the map shown in Figure 5.2a with medium quality and reliability, because its content is derived from satellite imagery alone. Certainly, the input data is of high quality (GeoEye-1, pan-sharpened) and well registration (range of Google Earth or better), nevertheless there is no validation against other independent products. Also no field based accuracy or user feedback is incorporated. *"This approach could give a quick indication for the usability of a mapping product, when decisions are due"* (LANG ET AL. 2010: 73). According to this quality level system in the emergency response there is little chance to produce assessment maps that surpass medium quality and reliability, since possibilities for validation are limited (see also Chapter 4). The rating and validation of rapid mapping products is an emerging field that deserves attention. However, it is not subject of this thesis, thus it is not covered.

In the given context the visualisation of damaged houses has to be semiotically easy to grasp, to ensure a fast and correct recognition of the meaning conveyed by the information (ANDRIENKO & ANDRIENKO 2007: 989f). To *"give everybody the right information at the right time and in the right way"* (ANDRIENKO & ANDRIENKO 2007: 890) the information load on the recipient should be reduced. Relevant data should be adequately aggregated and generalised, irrelevant information excluded. The final map product is more *„effective if a smaller number of graphical objects is used“* (ANDRIENKO & ANDRIENKO 2007: 892). DONNER (2008: 131f) refers to visual variables, which allow to make numerical proportions sensually perceivable. This means, that numerical data is made intuitive perceptible. Out of this reason the representation should look familiar to the user to ease understanding and utilisation (ANDRIENKO & ANDRIENKO 2007: 893). Furthermore the perception of the different users would be less different. An appropriate level of detail, that

could also be obtained by aggregation (ANDRIENKO & ANDRIENKO 2007: 897), can support the hitch-free utilisation of rapid mapping products.

Since the data extraction and its visualisation are inextricably linked with each other the proposed method (Chapter 4) also requires an adequate visualisation. Below there are shown selected illustration facilities of the Haiti EQ. These were taken as an inspiration because of simple standards that are already manifested.

5.1 Illustration Facilities

Following the Haiti EQ on January 12th 2010, a large number of maps was produced by different entities. Most of them were derived from Remote Sensing data, due to difficult social and political conditions (SHANKAR ET AL. 2010: 21). RELIEFWEB (n.d.) lists some 600 maps for the Haiti event, SHANKAR ET AL. (2010: 21) put the number of maps at even more than 2000. Many of them were produced in the first few days after the EQ as an act of emergency response (see Figure 5.1).

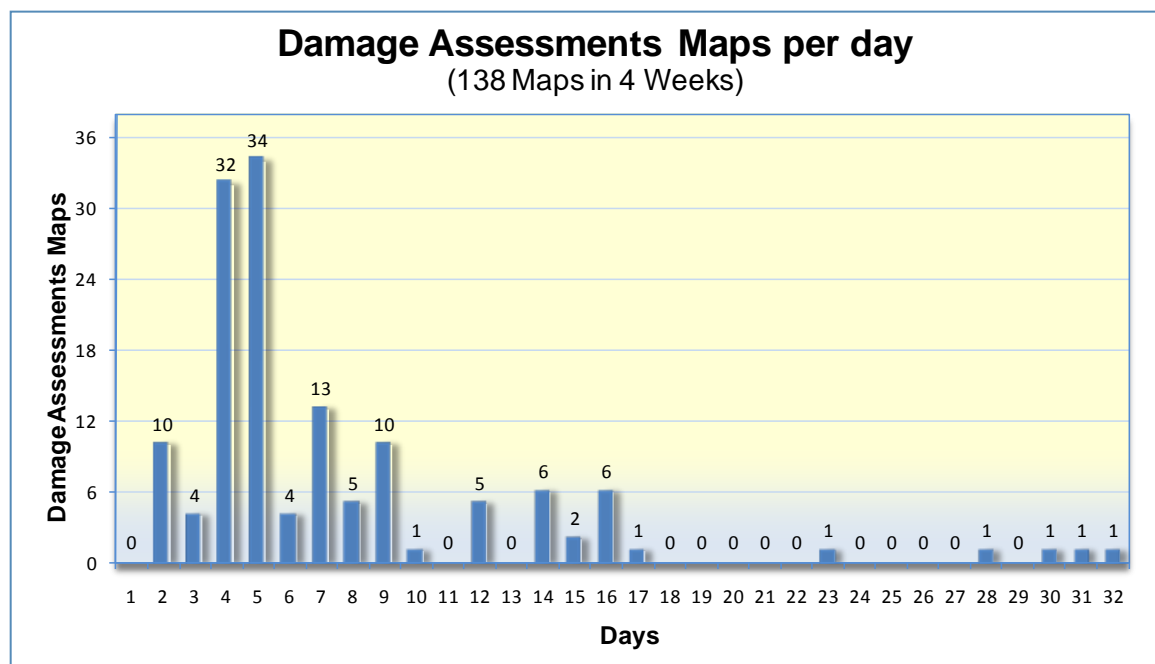


Figure 5.1: Timeline of damage assessment maps in response to the Haiti EQ

Source: Own illustration; Database: RELIEFWEB n.d.

As mentioned in Chapter 3.3.1 the qualitative representation of damage products causes biases. Therefore damage assessment products of selected service providers were analysed and compared. The intention was to find an adequate measure that presents the density of collapsed houses (see also Chapter 5.2). The great heterogeneity of the illustration methods hampered map interpretation by the users. The investigated damage assessment representations were produced by e-geos, JRC, MapAction, SERTIT,

UNOSAT and Z_GIS. The service providers used different presentation methods on scales ranging from 1:7,500 up to 1:55,000. Almost all maps are of high cartographic standard, optimized for large scale printing (DIN-A3). They reflect an overall increasing specialisation of different response organisations, each providing assistance according to its specific expertise and (satellite) resources, generating map products related to specific aspects of the disaster. Below selected damage assessment maps are shown (Figure 5.2, for larger copies see Appendix 3). To pick up the statement from ANDRIENKO AND ANDRIENKO (2007: 890) that „*information should be presented in a way that promotes its rapid perception, proper understanding, and effective use*“ the potentials (strengths and weaknesses) of the maps are discussed, with respect to data representation.

Among other organisations, Z_GIS used a kernel density estimator (KDE) for the representation of the automated analysis of the spatial distribution of damages (Figure 5.2a). The scale of this map is 1:20,000. The KDE is a very complex presentation method that is not easy to grasp. The main disadvantage of the kernel density visualisation is that areas, marked as damage areas, do not feature damages. This is due to border effects of the calculation. Examples can be seen in the stadium area (centre) or in the forestland (see also Figure 4.1). The map provides a good overview of the tendencies, where damages might have occurred.

Another illustration facility is the interpolated building damage surface deployed by UNOSAT. The data is produced by visual interpretation of single house damages, based on aerial photos (Figure 5.2f). The scale of 1:10,500 is adequate for the representation of single houses and the representation of damages is semiotically easy to understand. Yet, the interpolation process caused biases, as can clearly be seen, for instance, in the harbour area. Since the map is no rapid mapping product, this is recognised to be the main reason of the advanced visualisation.

Another map, published by SERTIT, used a building damage density surface visualisation, too (Figure 5.2d). The scale is 1:7,500. A bias is caused by the interpolation, which can be seen around the stadium and harbour areas. On one hand it provides a good estimate of the spatial distribution of the damages for the user. On the other hand it is a very complex visualisation, based on 100 meter radius circles, which represents the tendencies of damage occurrences.

JRC chose a grid-based presentation of the visual interpretation results (Figure 5.2b). The scale is 1:55,000 and therefore an overview map. The quantitative assertion, in grids of 200 m x 200 m, is based on a house-to-house analysis. Since only necessary information is presented, the visualisation seems to be of rather coarse character, however, as a

consequence it is easy to grasp. Nevertheless there remains a high level of inadequacy in grid based data representation (see Chapter 3.3.1).

The map provided by DLR (see Figure 3.7) also applied grid-based representation for the detailed damage assessment with a scale of 1:5,000. The grid symbolises artificial boundaries, that do not allow an intuitive reading of the delivered information. The qualitative presentation of categories such as 'moderate damage' or 'sparse damage' correspond an subjective estimation, which is relatively unreliable since it cannot be reproduced. Moreover, this kind of categories is hard to rate in order to make assertions about the reliability of the maps.

Another means of illustrating the damage analysis is the generalised representation in city blocks (Figure 5.2g), as deployed by e-geos. A combined optical and interferometric analysis was performed for the information extraction. The scale of the map is 1:25,000. An interferometric coherence, derived from a radar image, serves as map background. This complex illustration is difficult to interpret for users not common with radar imagery, thus not advisable. The damage assessment was made on city block basis. The blocks are represented as squares that are hard to understand. The map is obviously overloaded, especially in the city centre, because also blocks with no visible damage are symbolised. Finally the blocks delineated out of optical imagery, do not have any quality measure.

MapAction represented visual interpretation results in a block-based damage assessment (Figure 5.2h). The scale is 1:35,000. Due to internal quality checks the map was not published until 25th of January, which means a long delay. The relative block-based representation caused biases in interpretation, for example around the Presidential Palace and the harbour area. The red colour indicates extensive damages, whereas the total number is not pointed out. In total, the damages do not exceed a dozen, in the harbour area it is only one single damage. Nevertheless, the easy perception is supported by the block borders, that are related to the street network.

SERTIT used a combination of block-based and single damage visualisation (Figure 5.2c). The scale of the map is 1:7,500. Although this representation is very detailed the relative damage is expressed on the basis of damages per square kilometre. This is a very complex assertion. At a first glance half of the city seems to be damaged. For this reason it is difficult to recognise where the major damages are located. Also non visible damages are highlighted, for instance around the cemetery and the stadium in the lower centre. This conveys the impression of an overloaded map.

UNOSAT produced a comprehensive building damage assessment map based on visual interpretation of single houses (Figure 5.2e). The scale of this map is 1:25,000. The comprehensive damage assessment is a very time consuming analysis, and consequently no rapid mapping product. Despite all this, the advantage of this representation is the richness of detail and high comprehensibility.

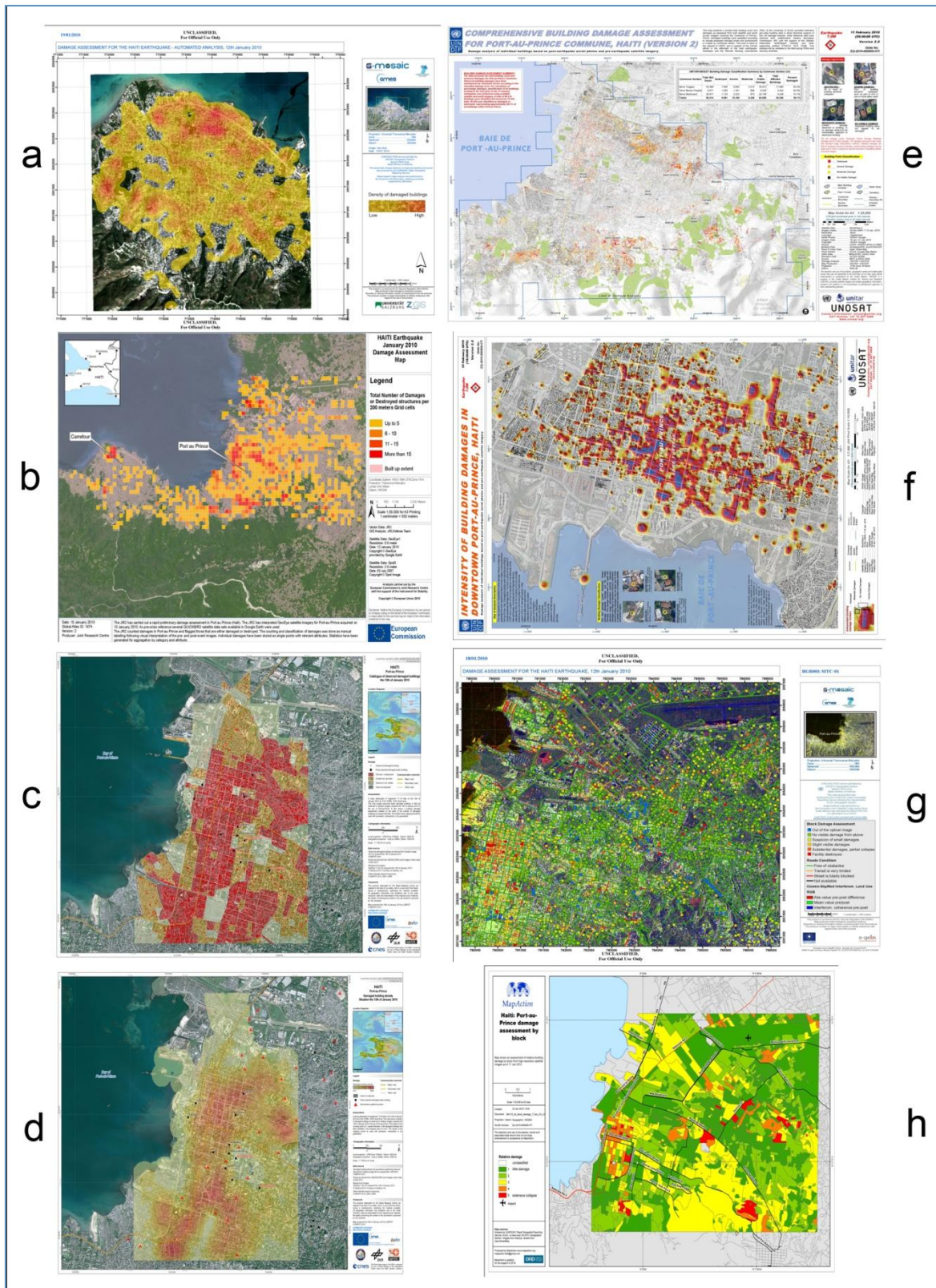


Figure 5.2: Damage assessment maps of Port-au-Prince/Carrefour produced by different service providers (see appendix 3 for larger copies): a) KDE of damages / Z_GIS, b) Grid-based damage assessment / JRC, c) Combined block-based and single building damage / SERTIT, d) Damage density surface / SERTIT, e) Single building damages / UNOSAT, f) Interpolated building damage surface / UNOSAT, g) Block-based damage assessment / e-geos, h) Block-based damage assessment / MapAction

Source: Own illustration Maps: GMES n.d. (map a), RELIEFWEB n.d. (maps b - h)

5.2 Spatial Relations of Data Representation

The qualitative information in the representation of damages and their spatial relations create biases. The spatial representation of point data (here: building damage) is mostly done with an estimator, such as interpolation or density methods. Yet, the interpolation process estimates values at unsampled sites in between areas of existing observations (HEYWOOD ET AL. 2006: 194). The interpretation of the real damage distribution by the user is hampered, since the qualitative representation is not able to map absolute numbers. Accordingly, the main problem of interpolated representations is the uncertainty for the users caused by distortions in the approximation process.



Figure 5.3: Distorted data representation caused by interpolation (here: KDE): red and yellow dots are damaged buildings, green points represent undamaged buildings. This effect is additionally enforced in densely populated areas

Source: Own illustration inspired by ZKI

The distortion depends mainly on the chosen type of representation and the used method of generalisation. Hence, the relation of the total area and damaged buildings depends mainly on the type of area that is chosen. In the calculation of zonal statistics the output raster size has a direct impact on the final qualitative representation if it is used in relation to damages. Consequently, the beholder will conclude differently where high damage areas are located and how high the real damage is (VEGA EZQUIETA ET AL. 2010: 57). The perception, therefore, varies in dependency to the representation (see Figure 5.4). For spatial aggregation the damage pattern is not represented adequately and the highly affected areas are not appropriately delimited (Figure 5.4 – Figure 2). For spatial interpolation an overestimation of damages occurs, due to spatial influence onto the neighbourhood. Areas without damage occurrence are labelled incorrectly because of their spatial proximity (Figure 5.4 - Figure 3). If the feature, which is used for interpolation,

diversifies on small-scale, the opposed values (here: conditions (1) no damage and (2) damaged in juxtaposition with each other) are extenuated, because they are not constant (cf. HEYWOOD ET AL. 2006: 194). An exact or an abrupt interpolation method is better suited because values do not alter and the appearance is of a stepped character (HEYWOOD ET AL. 2006: 194 ff.). Furthermore the question is, whether there is a spatial cohesion of damages (dependency to the basic structure of a building) and, consequently, whether the interpolation is an appropriate method to represent the occurrence of single building damages.

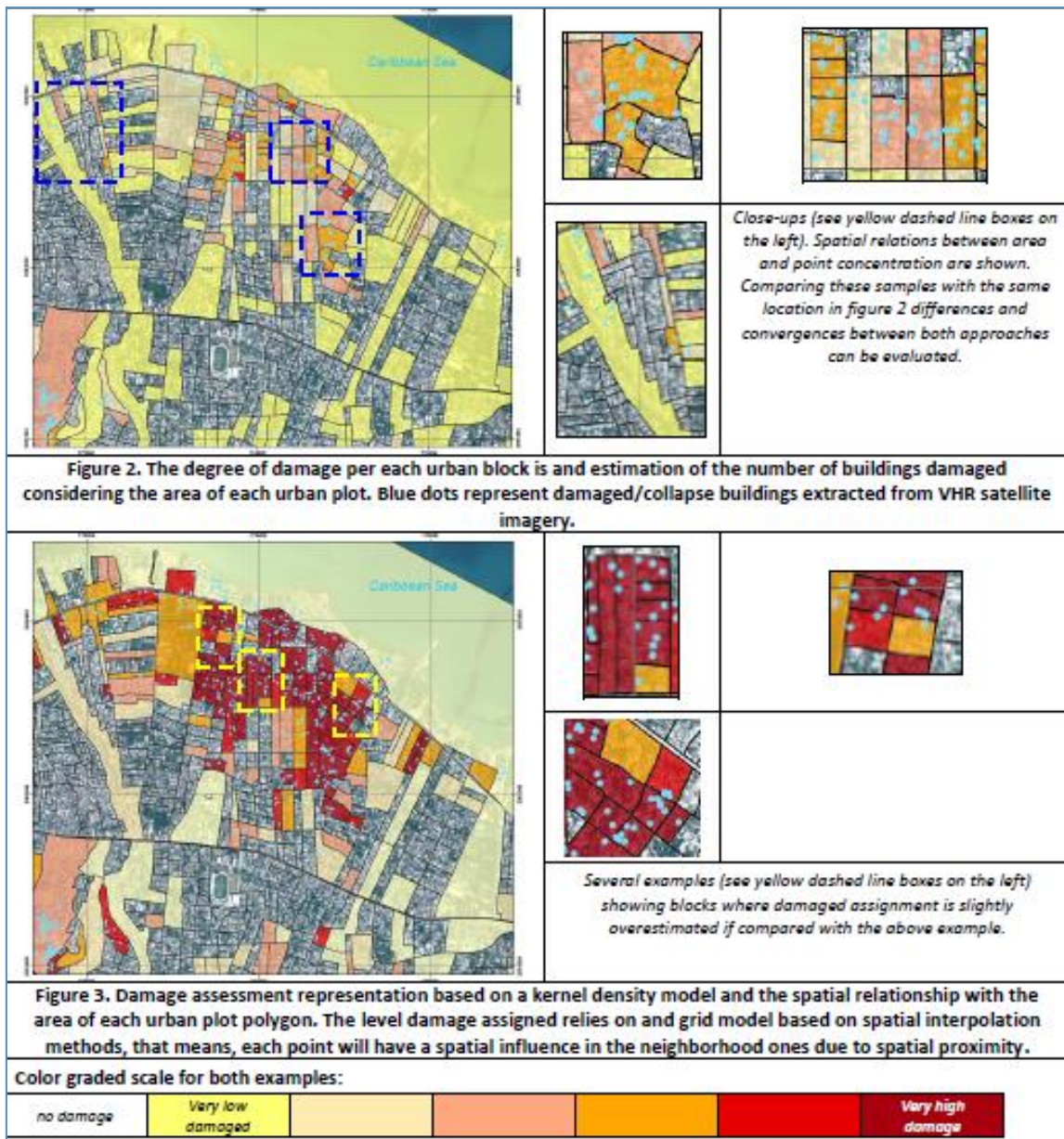


Figure 5.4: Illustration facilities and comparison of block-based damage estimation for the same data source

Source: VEGA EZQUIETA ET AL. 2010: 58

In contrast to the qualitative representation, a quantitative measure is reproducing a result closer to reality. VOIGT ET AL. (IN PRESS: 14) propose to introduce a measure that represents the total number of damaged buildings within a grid square. The author assumes the block-based damage representation to be closer to reality, and, moreover, to support a apposite understanding (see Figure 6.10). As mentioned above, in case of a disaster the street network is digitised by DLR. The network and the city blocks structure the area under investigation into smaller units (TAUBENBÖCK ET AL. 2010b: 87) and therefore build a reference level for the spatial distribution of damages. Accordingly, semiotically easy to understand borders would be readily accessible, regarding the building block as a meaningful unit of representation (cf. VEGA EZQUIETA ET AL. 56).

Since detail maps contain specific information on points of interest an interactive portable document file (PDF) could be an advanced medium for delivery (see Figure 6.9). This solution enables the user pointed request for information. The interactive PDF contains layers, for example single damages and block based representations, that can be individually switched on and off, as liked. Measuring tools, map coordinates and also attributes to single features can be interrogated. The printing, as a consequence, is focused easily on the actual needed information. Hence, an overload of the product is avoided, but at the same time the detail richness preserved. The Adobe Reader is an open standard for document exchange, that is freely available, but on most computers already installed. Currently map products at ZKI are distributed via download on the website, just the same could be done for the PDF. The export size of the file depends on the delivered attributes, that can be specified by the producer, and is done in ArcGIS.

To seize the idea of VOIGT ET AL. (IN PRESS) and to provide a realistic representation a new block-based visualisation approach was carried out. By using a choropleth map the qualitative assertion still remained. If this representation is extended into the third dimension the quantitative aspect is also considered. A point in polygon analysis transferred the attributes of the visual interpretation results (point features for damaged houses) into the attribute table of the building blocks. Under consideration of the total damage number as the 'z' value the blocks were extruded. The technical implementation ensued in the ArcScene environment. By using the Animation Manager a new track was created. The animation of the scene was rendered with 30 frames per second and gives a panoramic view of Port-au-Prince.

6 Results and Discussion

Aim of the thesis was the development of a team-based method for visual damage assessment. This chapter presents the result of the analyses conducted in this study. According to the structure of the thesis they are subdivided with respect to the thematic affiliation. The first section shows the results for the rapid mapping. The subsequent one portrays the findings for the team-based damage assessment. The last section describes the results of the illustration facilities. Brief discussions and recommendations reflect the results obtained and show potentials and shortages of the applied methods, which were developed in particular for the operational use at the ZKI.

6.1 Rapid Mapping

The short timeframe restrains data acquisition, sophisticated preprocessing and extraction methods (both manual and automated interpretation). In case of EQ disasters a rapid mapping product could still be of high importance to relief agencies even with a lower absolute accuracy. The fulfillment of the user needs, as a consequence, has highest priority and is the first step to support decision making in emergency relief. Elaborating on user requirements is a key factor that determines and ensures a well-addressed and tailored product and therefore a good usability. The questionnaire, that was developed to get deeper insights into user requirements, unfortunately, remained unanswered. The tremendous EQ event that stroke Japan in 2011 hampered answering, because those polled (THW) were busy in field operations for emergency relief. However, the requirements prepared by the User Board are a framework of high expertise, which needs to be incorporated in the product design by all means.

Due to general limitations of EO data it is not possible to identify the de facto number of damages. For the information extraction in case of disasters it is advisable to use data of highest resolution. The present study results have shown a significant approximation of recognised damages on the real damage count the higher the resolution of the utilised sensor. The high potential of VHRS optical satellite imagery for damage assessment is not yet exhausted, if advanced analysis methods are applied and further developed.

The differentiation of three damage classes for single buildings is the most reasonable and practicable possibility. In conclusion it is not possible to separate the different levels of partial damage of the EMS in a short time. Therefore the classes 'no damage', 'damaged' and 'collapsed' should be implemented. The transfer of this distinction to other localities creates new challenges, due to varying settlement structures all over the world.

To name an example, it is hard to delimitate a single house, e.g. ribbon building in Munich, Berlin or other metropolitan areas.

The spectral resolution with only four image bands of the presently used sensors is comparably limited. This equally applies to the spatial resolution. Cutting edge sensors are to close the gap in the rapid damage assessment. The higher spatial resolution of future satellite missions such as GeoEye-2 (Pan 0.25 m) is almost as high as those of aerial images used in the thesis. This will lead to an increased detail richness, and therefore to a higher number of damage detection, as was shown in the analyses. Additionally, hyper-spectral missions are expected to deliver better results for building damage detection. Small scale changes in the materials will be better distinguishable, since the electromagnetic spectrum is detected continuously. Unfortunately, the present spatial resolutions (5 m) of these systems are not suitable for damage assessments. If these considerations are thought ahead, the use of sensor merging techniques could improve the analysis task. By using the advantages of different systems the development of computationally efficient algorithms and procedures could enhance final quality of the extracted information. Consequently, the products of the value adders will be more reliable (even if a certain degree of uncertainty remains). Therefore reliability or the assumed range of accuracy should be explicitly stated on the product to ease usability and interpretation by the users.

Under the given conditions, which were presented in the thesis, satellite based damage assessment of EQ damages remains difficult. The spatial resolution is still too coarse to assess the total extent of damaged buildings, in particular in shantytowns. Further research for solutions to face such difficulties is needed. Therefore, improved and faster procedures for the quantitative EQ damage assessment from EO data need to be developed. The plurality of urban structures, especially in developing and transition countries, causes further problems. In all probability, planned urban spaces are expected to receive higher damage recognition rates because of their regular housing structures and standardised roofing characteristics. Also the better availability of thematic data such as road or LIDAR datasets and archive images is widespread and can, as a result, ease the analysis. Recent developments in the international emergency response promise a more structured and coordinated way of collaboration of rapid space-based mapping and assessment of extreme disaster events.

6.2 Team-based Method

From a remote sensing point of view the Haiti region is a difficult context, especially the urban morphology. The spectral homogeneity of the image objects is considered as the

main limitation both for the machine based analysis (supporting information) and the manual interpretation. As was presented the visual interpretation is still the most reliable source for the delineation of desired crisis relevant information. The combination of visual interpretation and supporting information resulted in a higher degree of damage recognition.

6.2.1 Classification

The main advantages of OBIA classification over pixel-based approaches are (1) the elimination of artefacts that result from the high spatial resolution and (2) the results achieved are more adequate to human perception. Both aspects are essential for the support of visual interpretation.

The object-based classification method for the extraction of a building footprint evolved in this study was realised in the eCognition Developer 8 environment. The aim was a delineation of a building footprint for the operational use. By developing a robust master rule-set the transferability on different sensors was ensured.

To support the damage assessment the exact and actual land cover mapping of urban areas is essential (see Figure 6.1). The presented methodology allows different applications in terms of rapid mapping like the determination of open spaces for camps. The registration of settlement structures according to form-parameters and building density enabled the definition of population density to some extent and additionally sign out the focal areas for disaster response activities.



Figure 6.1: OBIA classification of Carrefour using the architect solution

Source: Own illustration

©S. Klett

The eCognition architect solution is an easy applicable and adjustable method for the operational use in case of disasters. The ready-to-use solution assures the fast adjustment to other images and localities. Besides that, an easy applicability for varying users is provided. Since it uses archive information the processing can be launched immediately. After the production of overview maps, when the actual damage assessment starts, the supporting information is available. To speed up the process a server processing is recommended. The main disadvantage of the developed architect solution is that an initial step is left out. Before applying the solution, a subset has to be segmented with the purpose of on-screen determination of adequate thresholds.

The rather few classes do not restrict the usability of the supporting information. Due to a great variety in building forms and spectral ranges, in some areas it was impossible to extract single buildings and retain fast processing at the same time. The aggregation of buildings, back yards and also some street elements was necessary. However, in the analysis the human perception is able to grasp object boundaries easily and associates them with real objects. Instead of increasing the number of classes further effort should concentrate on a segmentation optimisation, to avoid over-segmentation. This can be seen in Figure 6.2. Since there are a lot of noise objects in the classification of optical imagery a post-processing could be of advantage, e.g. a simple generalization of building outlines.



Figure 6.2: Classification example of a GeoEye-1 subset in Carrefour, Haiti (blue: streets; green: vegetation; light-blue: sealed soil; orange: built up areas). The house in the centre of the image shows an example of over-segmentation

Source: Own illustration

Table 6.1 shows selected thresholds that were used for the generation of the supporting information with the architect solution. Since the scenes were too large for the processing on a single computer the tiling and stitching algorithm was applied for a server processing. Although the master rule-set was developed for the operational use with relatively slim algorithms, a small scale parameter was needed. For the separation of objects belonging to vegetation and other features this SP was essential. This results in a high computational cost because the number of created image objects is very high. The recommended solution is the computation on a multi-core blade server.

Table 6.1: Selected thresholds used for object-based classification

Source: Own compilation

Class	Feature	GeoEye-1	WorldView-II
Street	Street data	thematic layer	thematic layer
Vegetation	NDVI	0.6	0.25
Shadow	Brightness (mean)	125	220
	NDVI	0.55	0.25
	Area	≤ 650	≤ 650
	rel. Border to shadow	≥ 0.25	≥ 0.25
Built-up	Brightness (mean)	685	705
	NDVI	0.55	0.25
	rel. Border to shadow	≥ 0.009	≥ 0.009
Water	NDVI	≤ -0.2	≤ -0.2
	Area	≥ 1000 Pxl	≥ 1000 Pxl
sealed ground	Area	> 800 Pxl	> 800 Pxl

In some areas, in which spectral contrast between houses and ground is very low, the object boundaries are floating. Even if there is still a slight under-segmentation for areas in between backyards and dusty roofs according to spectral similarity to bare ground, the advantages are the high degree of automation, the more detailed damage assessment and the saving of time. Areas with complex building geometries, especially patch-work roofs, and high spectral differences tend to over-segmentation. The distinction between roofs and streets is a prominent problem. This was solved to the greatest possible extent by using the street data as a thematic layer. The most common problems that occurred while analysing the images are shown in Figure 6.3.



Figure 6.3: Illustrative examples of common problems for OBIA in the Haiti case: a) similar spectral values of roofs belonging to different houses b) shading of roof-parts belonging to the same dwelling c) low differences in spectral reflectance between buildings and streets d) spectral similarity of roofs and backyards

Source: Own illustration

A further step in the analysis could be the segmentation optimisation. Because of the logically related attributes the method was made transferable to a large extent, since building geometries and construction standards differ worldwide. Further investigations are needed to estimate the degree of correctness in other parts of the world. Nevertheless, the extracted features within the supporting information method resulted for both sensors in an almost equal high degree of accuracy, as presented below.

6.2.2 Accuracy Assessment

For the accuracy assessment of OBIA the thematic and the spatial accuracy were investigated. The validation of the classification results, based on the architect solution, occurred in a region of Port-au-Prince. The thematic accuracy assessment of the classification results was carried out by a visual inspection of 200 randomly distributed sample pixels (at least 20 samples per class). The overall accuracy, obtained by applying an error matrix, was 84.3 per cent for the GeoEye-1 image and 82.7 per cent for the WorldView-II data (see Table 6.2 and Table 6.3). These values were regarded as sufficient for the support of the team-based analysis.

Table 6.2: Thematic accuracy of GeoEye-1 data classification*Source: Own compilation*

Class	Producers accuracy	Users accuracy	Kappa Index	Overall accuracy
Street	98.25 %	98.13 %	0.9623	84.32 %
Vegetation	92.13 %	94.76 %	0.9161	
Shadow	75.67 %	100 %	1	
Built-up	100 %	50.3 %	0.5024	
Sealed ground	89.42 %	81.80 %	0.7973	
Water	95 %	92.56 %	0.934	

Table 6.3: Thematic accuracy of WorldView-II data classification*Source: Own compilation*

Class	Producers accuracy	Users accuracy	Kappa Index	Overall accuracy
Street	100 %	97.83 %	0.9623	82.73 %
Vegetation	94,72 %	95.63 %	0.9165	
Shadow	81,86 %	92.46 %	0.901	
Built-up	92.34 %	63.21 %	0.6102	
Sealed ground	77.81 %	80.50 %	0.7831	
Water	97.53 %	95.17	0.9247	

The best results were achieved for the classes street and vegetation. This can be ascribed to the utilisation of the street dataset for the street class. For the vegetation class the usage of the NDVI assured a high accuracy. A slight but constant over-segmentation of the satellite images was observed for the delineation of the 'built-up' class. This over-segmentation was found, in particular, in the fragmentation of roofs due to spectral

reflectance variability. The most common reasons were sun facing and shaded gable roofs (see Figure 6.3) as well as patch-work roofs (see Figure 6.4). Also roof-top terraces and chimneys were a frequent cause.



Figure 6.4: Over-segmentation due to patch-work roofs and chimneys

Source: Own illustration

To face this problem the usage of advanced segmentation algorithms could be used. Examples of those algorithms were developed by DRAGUT ET AL. (2010) and TAUBENBÖCK ET AL. (2010a). The latter was tested but considered to be not useful for the emergency response, due to a processing time of several hours for one satellite scene.

The spatial accuracy considered the size and shape of the classified features. The reference objects, which were manually digitised, were considered to be true, although a certain degree of uncertainty remains in the production of reference objects. Accordingly, the spatial accuracy remains hard to measure. For the accuracy assessment the same objects as for the thematic accuracy were analysed. The water class was excluded due to the size of the Caribbean sea in the image. The merge algorithm produced a single, large-sized object. Further uncertainties in the OBIA remained, as can be seen in Figure 6.5. The MPAR value of the classified objects was constantly higher than the value of the reference objects, due to pixel-based fuzzy contours. The generalisation of the manual digitised reference objects eliminated this effect. The shown object has got an MPAR difference of 0.2 and was recognised as well fitting. Therefore the mean tolerance of 0.2 as limited amount of variation was set.



Figure 6.5: Comparison of MPAR values. The green polygon represents the classified object (MPAR 0.56), the red polygon the reference data (MPAR 0.36).

Source: Own illustration

Based on the presumption, that the classification represented image objects close to reality, the MPAR was considered to judge accuracy. The classes 'street' and 'vegetation' were well represented because the thematic layer and the NDVI created well matching borders of the objects. The class 'built-up' was represented rather poorly because of high differences in the texture (grey value transition probability) and constant over-segmentation. The class 'shadow' showed constant high MPAR values, that almost all exceeded the mean tolerance, although they were properly fitting the reference objects. Further investigations have shown that the uncertainty increases, because the MPAR value varies with the size of the object. If the shape was hold constant, an increase in the object caused a decrease in the MPAR. This explained the constant high values for the shadow class. As a result, the MPAR is not suited to make an assertion on the spatial conformity of classified and reference objects, because the MPAR does not explain the spatial fit of classified and reference objects to each other. Thus, no result of the assessment on the spatial accuracy was provided.

According to the findings portrayed above, the transferability limited the accuracy. The developed method still has a potential for the support of visual image analysis, although it could be optimised.

6.2.3 Developing a Team-based Method

As it was shown the specific individual experience and prior knowledge could increase the ability to recognise a high number of (partial) damages. The application of team-based methods focused on increasing this effect. The possibility to swap ideas on potential damage and the twofold covering of the area under investigation did not only quicken the

damage assessment, but also delivered more precise results as the following evaluation demonstrates.

The evaluation of variances resulting from visual interpretation were analysed by a focus group survey as was presented in Chapter 4.2. Most single interpreters were not able to complete the analysis of the given subset, in contrast to the teams, that covered almost the entire area. The author had a great foreknowledge of the image content because of the comprehensive work on the images, such as classification and sensor evaluation (Chapter 3.2). Accordingly, the damage detection of the author was well above average, wherefore his analysis was not taken into consideration. The results of the focus groups are shown in Figure 6.6.

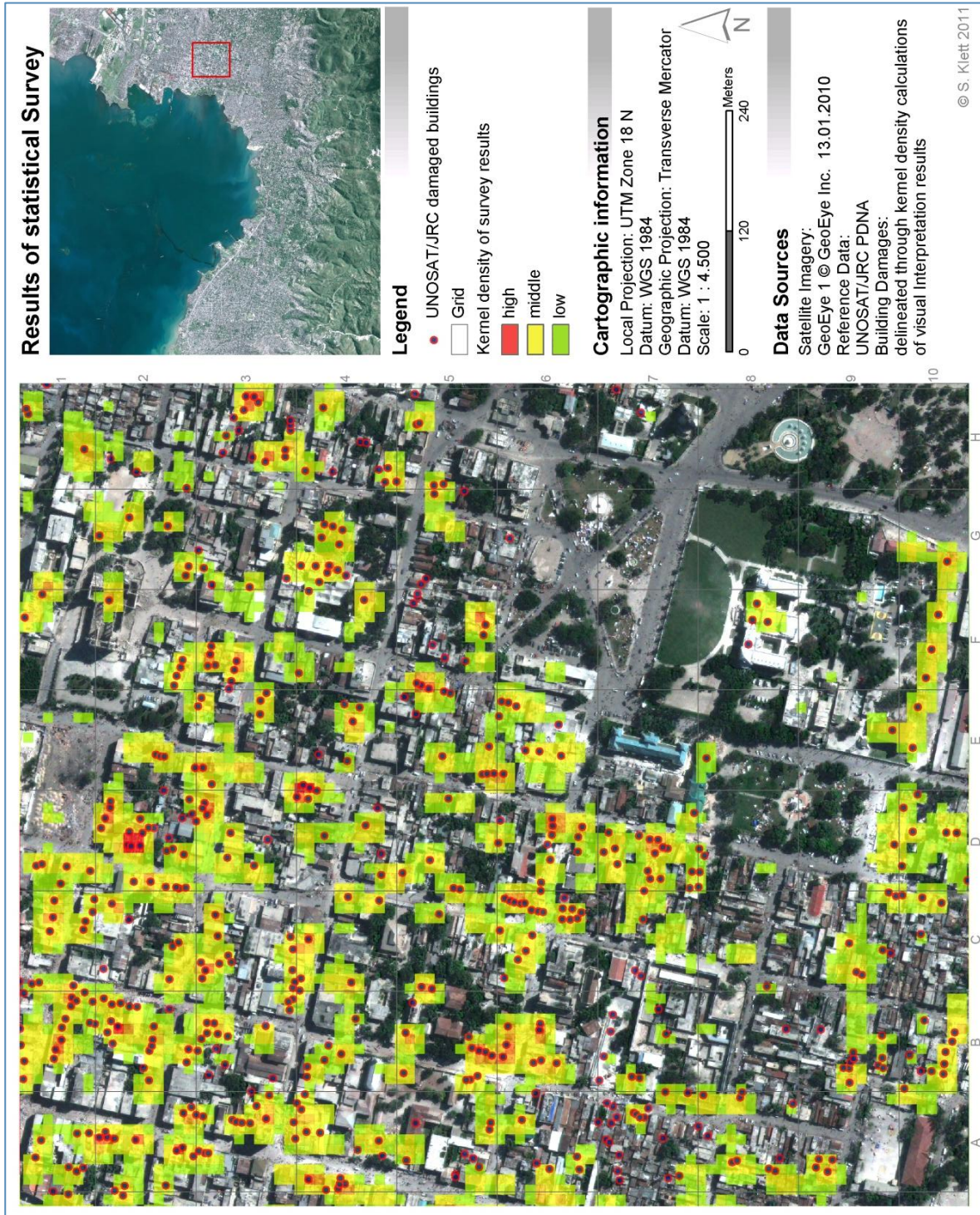


Figure 6.6: Kernel density of interpretation results. Points show reference data.

Source: Own illustration

© S. Klett

The output raster cell size of KDE is 10 m x 10 m. The maximum count in the red square (D 2) is 36 hits. During the analysis of the interpreters a frequently mentioned question was: what is a single house? This can be seen, for instance, in cell F 8. The evaluation of the focus group results revealed some other general problems. In particular densely built up areas cause a high misinterpretation (A 7 and H 3/4). This results mainly from the limits of spatial resolution, that hampered the damage detection (F/G 5 and A 7). An underestimation was observed for not completely crushed multi-storey houses (2 hits only) (F 6/7 and B 7). As a general trend the highest density is found in the upper left, where the interpretation started. Evidently, within the time limit of one hour a relaxing attention shows the fatigue of the subjects. Regarding the top-down colour gradient there is not only a lower density, but also a higher misinterpretation which can be seen in the cells A/B 7/8 and C/D 9/10.

Regarding the evaluation of the interpretation results, with $R^2 = 0,952$ the coefficient of determination explains almost the entire variance of Figure 6.7. The background shows study results of the reference group analysis. The expected value amounts to 216 and is therefore 40.4 per cent of all 535 damaged buildings for all interpretations. The standard deviation is 49.78. For the team-based analysis the expected value is 245 which corresponds 45.8 per cent recognition. The respective standard deviation is 28.23. In case of single interpreter analysis the expected value is 184, the percentage of recognition achieves solely 34.4. In this the standard deviation amounts to 47.59. In comparison to the benchmark of the grid-based damage estimation of DLR-ZKI of 10.2 per cent detection of collapsed houses there is a remarkable difference. Regarding the sensor evaluation a damage recognition of 87.7 per cent was achieved by the author, what corresponds approximately 472 detected damages. As a result, one has to state that the time constraints are the main reason for the limited number of damage recognition, because almost half of the damages are overseen in a simulated emergency exercise. This also explains the lower detection rate in comparison to the study conducted by OGAWA ET AL. (2000), who utilised aerial photography. In addition, there was no time limit given.

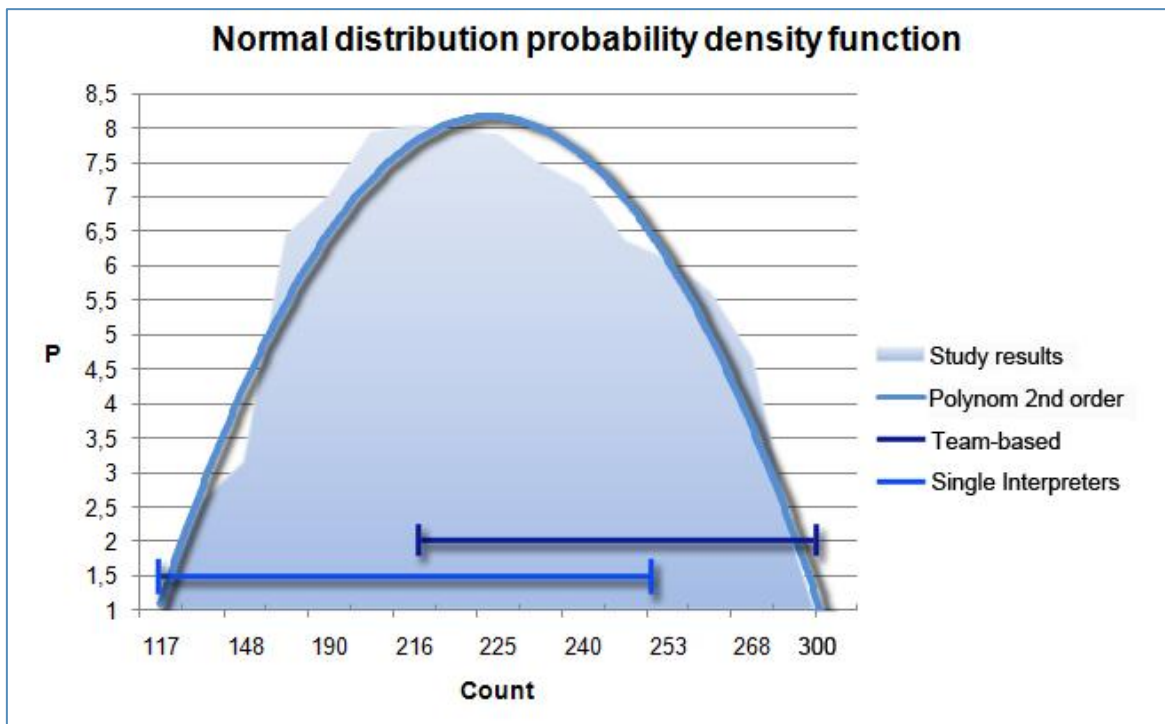


Figure 6.7: Normal distribution probability density function of visual interpretation results. The expected value amounts to 216. The variations of the single interpreters range from 117 to 250, for the team-based analysis from 216 to 301.

Source: Own illustration

The (co-) registration was applied on the pre- and post-disaster images and on the street data. These steps need much time in the proposed method but still this is essential for the multi-temporal analysis. Due to general limitations of EO data, independent of the spatial resolution, three classes of damage should be defined: 'no damage', 'damaged' and 'collapsed'. The distinction into these classes creates quantitative data. The strength of the quantitative data is an increase of quality, attributable to more detailed information. The weakness is the time consuming analysis because it is very complex and elaborative. Despite all this the multi-user approach is very time effective because of the contemporary editing in a single multi-user feature class. Hence, there is no post-processing, such as a union operation, needed. Briefing, gauging and twice checking as central aspects of a qualitative design are the main improvements in contrast to the single interpretation. This would also weaken the argument of KERLE AND WIDARTONO (2008) that the reliability of rapidly produced maps cannot be rated, because consistency is assured.

For the implementation in the operational ZKI environment the digitising should be made on a layer-file in a multi-user environment that all interpreters can access (see Figure 6.8).

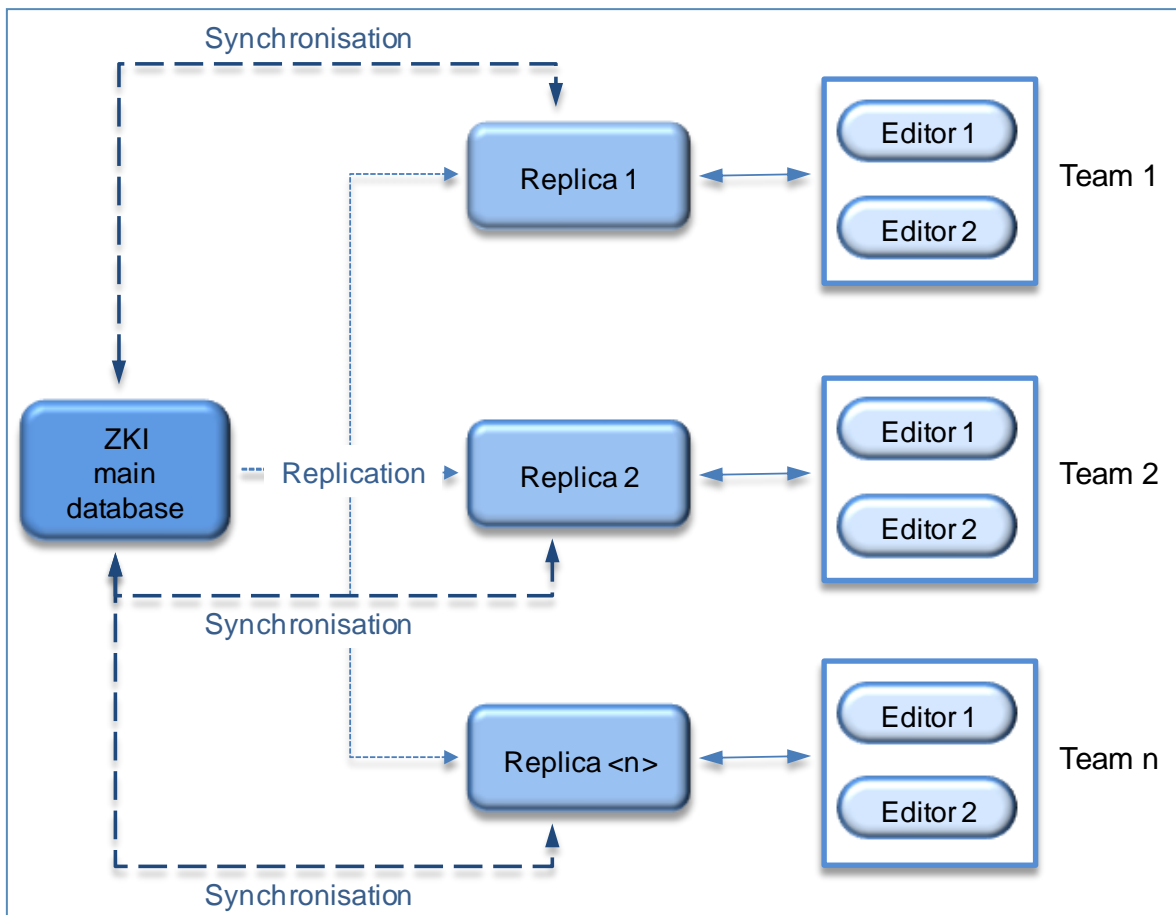


Figure 6.8: Multi-user data management for team-based damage assessment

Source: Own illustration, inspired by ZKI © S. Klett

Teams are digitising on two screens, whereas the first screen shows the image data and the second the attribute table. One team member should control the mouse and the other one handle the keyboard for data entry. Regular breaks should also be used to change roles within the teams. Several interpreters stated that during the iteration process (Figure 2.11) they became more familiar with the task. In conclusion, possible interpreters should get training in an emergency exercise, because this method needs some experience to get used to it. The exercises will increase individual knowledge on EQ damages and therefore increase product quality.

The proceeding for the information extraction in the proposed manner is about one hour per square kilometre. The medium capabilities of the operator (ZKI) amounts to four persons in 24/7 service, but in exceptional situations it is considerably more. The overall area covered by the damage assessment of DLR in the Haiti case was about 320 square kilometres. According to study results this would take 320 hours for a team of two interpreters. The maximum count of interpreters engaged in the Haiti case was 25. Altogether this is equivalent to 12 teams that could cover all the area performing a house-by-house damage assessment within approximately 27 hours of constant work. According

to Table 3.1 this would also accomplish the user requirements to deliver first damage assessment maps within 48 hours. The estimated accuracy, which could be stated on the map, is about 50 per cent. This value can be surpassed by appropriate teaching of the methodology during emergency exercises. In extraordinary damage extents the scale of 1:1,000 could be decreased to sacrifice detail in order to quicken the analysis.

It was discussed, that the final user of the method expects a process fast enough to quickly cover large areas, and at the same time, enough detail to provide useful information and reliable enough to take decisions based on it. As it was shown, the team-based method is qualified to fulfil expectations and, additionally, improve product quality. Consistency is ensured because a similar result can be achieved in reproduction (see Chapter 2.6). The results can be tested in coordination with the end-user and required modifications implemented in the guideline for the next events. In conclusion it is manifested, that the application of team-based methods improves the rapid mapping enormously. A standard operating procedure, as it was presented in this study, accounts for the fact that quality assurance is given.

6.3 Visualisation

As it was shown there exists a great variety in data representation. An unbiased visualisation is considered to ease interpretation and increase usability for the user. As a result, in dependency to different scales, different representations should be chosen. The colour indication of the damage classes should follow the advice of the 5th rapid mapping workshop of SAFER held in Madrid and utilise red, yellow and green for high middle and low damage numbers (oral communication: DR. TOBIAS SCHNEIDERHAN, 2011).

In conclusion to Chapter 5, hereafter some recommendations are made. For detailed maps, with a scale smaller than 1:10,000 a representation of single houses should favoured the interpolated surfaces, because it is more exact and better to grasp. The interpolated surfaces can hardly be interpreted, due to floating transitions. Since the survey objects are relatively small, a high scale is needed. However, according to settlement structure it is not always suitable, especially in shantytown regions of developing countries. In this area a block-based damage visualisation is recommendable, on condition that it is adjusted in order to avoid biases. Detail maps also contain specific information on points of interest. Considering the medium of delivery an interactive PDF-file was recognised to be very useful (see Figure 6.9). The solution enables the user pointed request for information. The interactive PDF contains layers that can be switched on and off, as liked. In addition, measuring, map coordinates and also attributes to single features are provided. The printing, as a consequence, is focused easily on the actual

information needed. Hence, an overload of the product is avoided, while detail richness is preserved. Maps that are designed in this manner apply the most suitable representation techniques according to the user requirements.

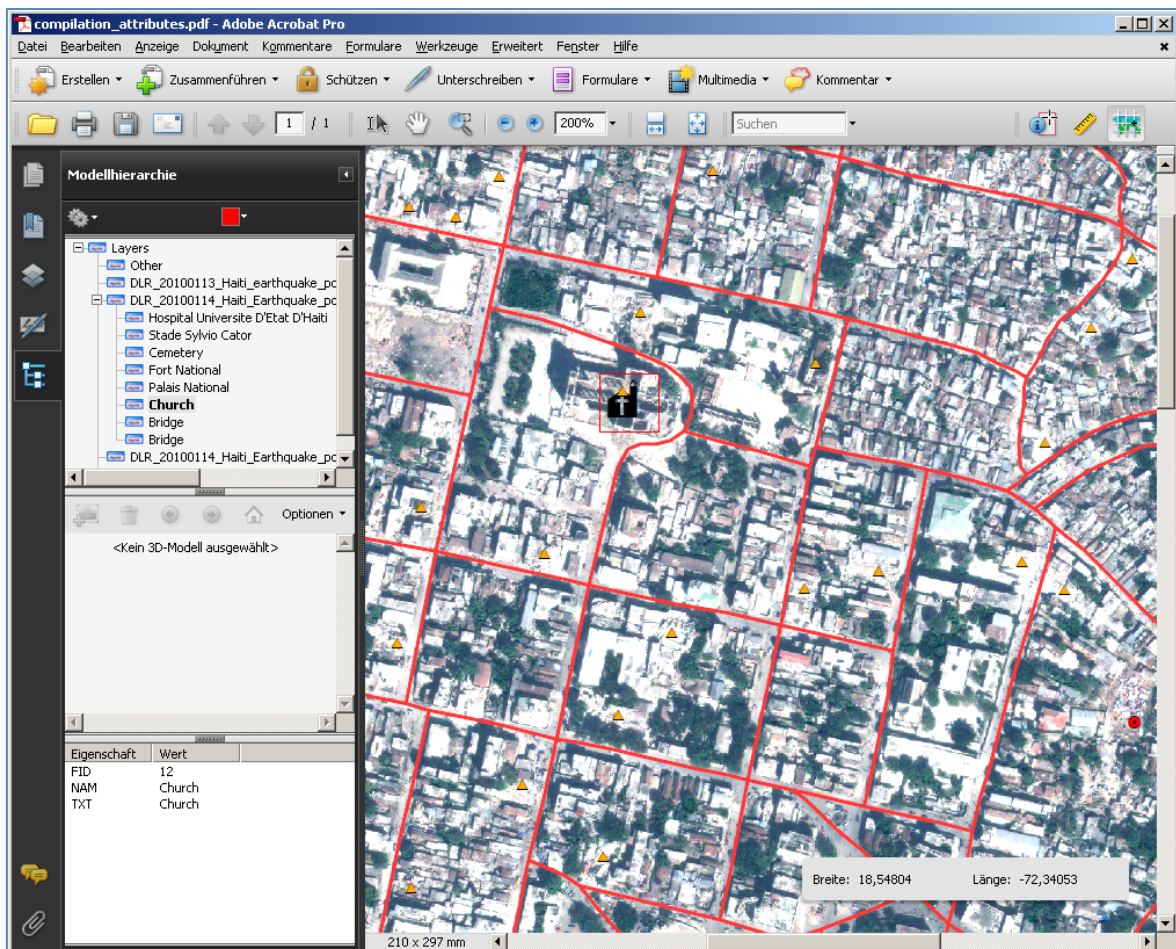


Figure 6.9: Presentation of single house damages in an interactive PDF

Source: Own Illustration © S. Klett

For overview maps with a scale larger than 1:10,000 other illustration facilities instead of the current grid-based visualisation should be considered. Since the data representation is artificial, without natural elements that ease comprehensibility, it is advisable to use the block-based visualisation (see Figure 6.10). The blocks are determined with aid of street data. A point in polygon analysis of the results gained by visual interpretation requires only a small computational effort.

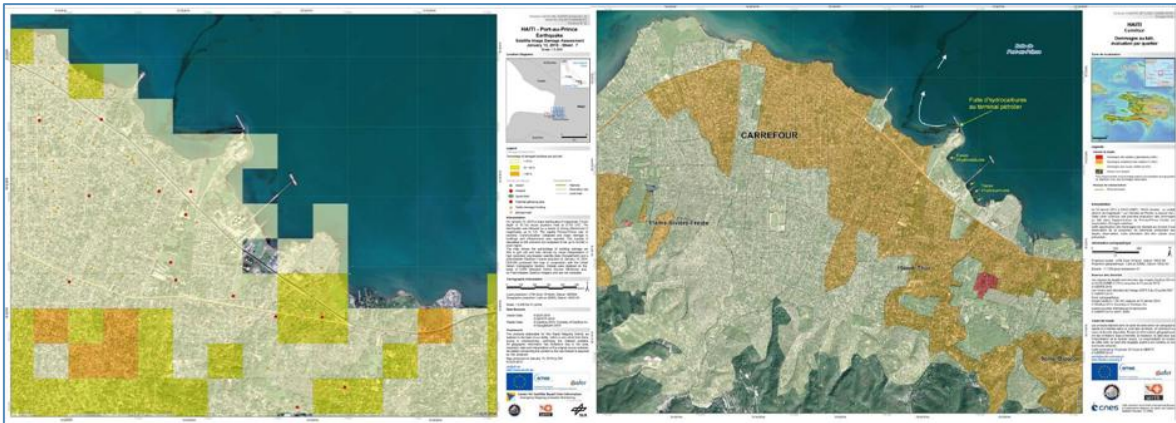


Figure 6.10: Comparison of grid-based and block-based damage assessment of Carrefour: map on the left shows grid-based damage assessment (DLR-ZKI), on the right a block-based damage assessment is presented (SERTIT)

Source: ZKI / RELIEFWEB (n.d.)

Additionally, for the final representation also supporting information was used. A merge operation with the class 'built-up' was deployed to alleviate biases in interpolated data representation. Untilled areas, such as parks or football stadiums are then excluded per se. This avoids overloading of the maps, because only needed information is transmitted. Figure 6.11 shows a block-based quantitative damage assessment of Carrefour, that also utilizes the supporting information.

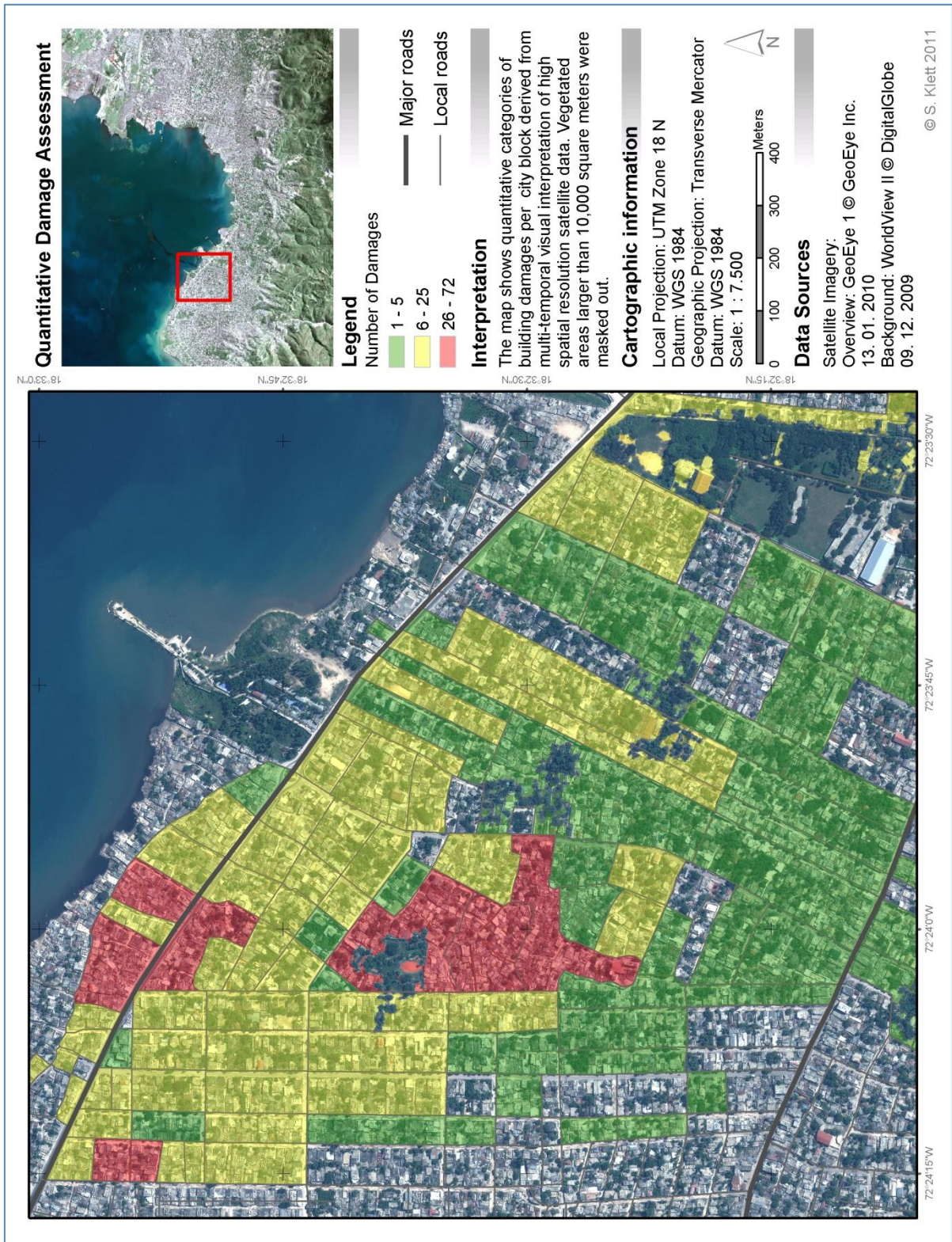


Figure 6.11: Block-based quantitative damage assessment of Carrefour.

Source: Own illustration © S. Klett

A further solution to reduce biases in interpolation is the three-dimensional visualisation with extruded blocks in the ArcScene environment. As outlined in Chapter 5.2 the limitations of two-dimensional map products cause biases. Therefore the decided advantage is the extended transmission of information. The height of the extruded blocks symbolises the count of damaged buildings per block. Facing one another the advanced three-dimensional rendering represents the absolute number whereas the traditional map product withholds this information. To avoid occluded areas in the shadow of highly extruded blocks at least two viewing directions are needed (see Figure 6.12). To circumvent shading the rendering of a video is the most appropriate solution. An example can be found on the compact disc attached to this thesis (Appendix 5). The main advantage is the very detailed and close to reality impression transmitted to the beholder. A weakness is the extra work which is intensified by occasional bugs. The medium used for viewing the video can be a website or a map server because of the size of approximately 55 megabytes. This, unfortunately, can cause problems in some parts of the world with lacking internet infrastructure.

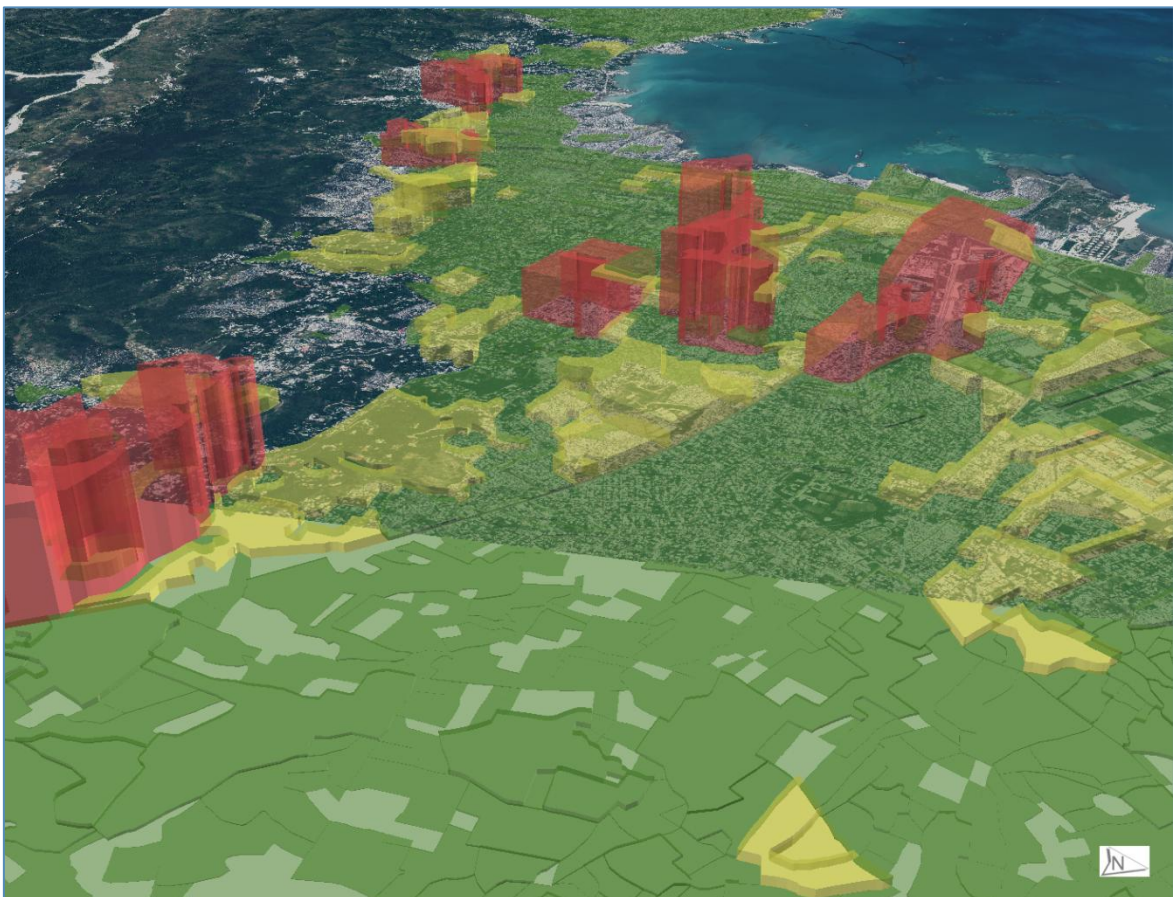


Figure 6.12: Combined qualitative and quantitative representation of damage numbers utilising three-dimensional extrusion of city blocks

Source: Own illustration © S. Klett

Extensive maps of scales larger than 1:50,000 should keep the grid-based representation, which is appropriate for this level of generalisation, even if biases remain and natural borders are neglected. Additionally the main streets should be represented.

7 Conclusion and Outlook

The main objective of this thesis was to develop a team-based method for visual damage assessment using optical VHSR satellite data in the context of rapid mapping in the aftermath of earthquake disasters. To seize the research challenges and main objectives, this Chapter initially presents the major conclusions and afterwards outlines further research needs and recommendations in the field of rapid damage assessment.

7.1 Conclusions

With regard to the main goal the thesis investigated the conditions of rapid mapping to provide a deeper understanding of the potential of very high resolution optical data for damage derivation. As it was shown the potential of VHSR satellite data is not yet exhausted. In this context it was demonstrated that the application of team-based visual interpretation is capable of increasing not only product quality but also consistency and thus reliability of the extracted information. It is concluded that under the premise of time pressure a resolution dependent procedure was developed. The process of development revealed the following key findings:

- (1) The method enables the user to define a certain degree of thematic quality within a limited timeframe.
- (2) The provided guideline and the respective briefing should be improved during emergency exercises and real disaster events. The experiences gained compel subjective decisions to create rational and reproducible results.
- (3) With respect to the iteration and learning process within the visual interpretation conducted in teamwork, the procedure is designed in a manner that takes (1) and (2) into consideration.
- (4) The current user requirements encompass only map content, but disregard its respective representation. Accordingly, harmonisation with the users has to be intensified as well as the development of application-oriented prototypes and standards. Since the content can be delivered, the focus should be in particular on data representation. The block-based quantitative representation Figure 6.11, that utilises also the supporting information in combination with the interactive PDF format is a first step towards meeting future challenges.

In addition to the key findings it is stated, that from a remote sensing point of view the earthquake in Haiti is a difficult context, especially the urban morphology. The spectral homogeneity of the image objects is considered as the main limitation for both the machine based analysis (supporting information) and the manual interpretation. However, an important advantage of the presented approach over conventional classification

techniques is the robust design that assures transferability of the OBIA solution. As a consequence an area covering application was developed that combines a faster, because of teamwork, and more detailed, for the reason of supporting information, analysis result.

The in-line design of data extraction and representation are further aspects that increase the value of the team-based method. The application of three-dimensional visualisation techniques is capable of not only delivering a qualitative assertion, but also a quantitative information. In conclusion, this reduces the current biases in data representation enormously.

Summing up, it may be said that the standardised team-based visual interpretation is a powerful tool to improve the quality of information delineation from EO data. The team-based approach increases product reliability if representation follows close upon. Finally, there is a gain not only for the users, moreover for the ones potentially being rescued.

7.2 Outlook

The methodology was made transferable to a large extent, since building geometries and construction standards differ worldwide. Further investigations are needed to estimate the degree of accuracy in other parts of the world. Especially if the maximum size of buildings is significantly increasing as is the case for Munich or Berlin. To face expected problems a slim and fast performing algorithm for segmentation optimisation needs to be developed.

Further harmonisation of value adders and users, that also takes into consideration the final data representation, allows striving for specific visualisation. A further step should be the implementation of mobile solutions for emergency response. Utilisation of handhelds and mobile GIS would enable the rescue teams to use routing datasets and location based services. Accordingly more targeted actions by the rescue teams would be possible.

DLR presently delivers only printable maps to the users. Currently there is a discussion about future data delivery of additional file formats. A direct transmission of the extracted digital geo-data is only provided on request of certain entities. In principle it is intended to deliver also digital geo-data, but there exists not yet any license agreement to consolidate DLR's copyright. The copyright implies metadata compliant with INSPIRE, ISO and OGC standards. The data provision then occurs via web-mapping servers and contain three-dimensional representation techniques.

Lastly, an international entity should be embodied which's duty is the passing on of products that fulfil agreed upon standards and user requirements. An overflow of products

could be limited since this entity could screen the maps on best practice solutions. A mapping guideline, developed by this entity, should consider different aspects for a cultural and case sensitive visualisation, such as scale, complexity and most suitable symbology.

References

- AL-KHUDHAIRY, D.H. A., CARAVAGGI, I., GIADA, S.** (2005): Structural damage assessments from Ikonos data using change detection, object-oriented segmentation, and classification techniques, in: *Photogrammetric Engineering and Remote Sensing*, Vol. 71 (5), 825-837.
- ALBERTZ, J.** (⁴2009): Einführung in die Fernerkundung. Grundlagen der Interpretation von Luft- und Satellitenbildern. 254 p., Darmstadt.
- ALBRECHT, F. LANG, S., & HÖLBLING, D.** (2010): Spatial Accuracy assessment of object boundaries for object-based image analysis, in: *The International Archives of the Photogrammetry, Remote Sensing and Spatial Information Sciences*, 38(4/C7), 6p.
- ALTAN, O.** (2005): Use of Photogrammetry, Remote Sensing and Spatial Information Technologies in Disaster Management, especially Earthquakes, in: Oosterom, P., Zlatanova, S., Fendel, E. M. (Eds.): *Geo-information for Disaster Management*, Berlin, 311-322.
- ANDRIENKO, N. & ANDRIENKO, G.** (2007): Intelligent Visualisation and Information Presentation for Civil Crisis Management, in: *Transactions in GIS*, 2007, 11(6): 889–909.
- AYDONER, C. & MAKTAV, D.** (2009): The role of the integration of remote sensing and GIS in land use/land cover analysis after an earthquake, in: *International Journal of Remote Sensing*, Vol. 30 (7), 1697-1717.
- BAATZ, M., SCHÄPE, A.** (2000): Multi-resolution Segmentation: an optimization approach for high quality multi-scale image segmentation, in: *Beiträge zum XII. AGIT-Symposium Salzburg*. Strobel, J., Blaschke, T.; Griesebner, G. (Eds.), 12-23.
- BACHOFER, F., ESCH, T., KLEIN, D.** (2009): Ableitung von Versiegelungsgraden basierend auf hochaufgelösten Fernerkundungsdaten mittels Support Vector Machines, in: *Angewandte Geoinformatik 2009*, 432-441.
- BAHRENBERG, G., GIESE, E., MEVENKAMP, N. & NIPPER, J.** (⁵2010): *Statistische Methoden in der Geographie 1: Univariate und Bivariate Statistik*, 282 p., Stuttgart
- BELL, P.** (2010): Content Analysis of visual images, in: Leeuwen, T. v. and Jewitt, C. (Eds.): *Handbook of Visual Analysis*, London, UK, 10-34.
- BENZ, U., HOFMANN, P., WILLHAUCK, G., LINGENFELDER, I. HEYNEN, M.** (2004): Multi-resolution, object-oriented fuzzy analysis of remote sensing data for GIS-ready information, in: *ISPRS Journal of Photogrammetry and Remote Sensing* 58(3-4), 239-258.
- BRUNNER, D., LEMOINE, G., & BRUZZONE, L.** (2010): Earthquake damage assessment of buildings using VHR optical and SAR imagery, in: *IEEE Transactions on Geoscience and Remote Sensing*, 48(5), 2403-2420.
- BUEHLER, Y. A., KELLENBERGER, T. W.** (2007): Development of processing chains for rapid mapping with satellite data, in: Li, J., Zlatanova, S., Fabbri, A. (Eds.): *Geomatics solutions for disaster management*, Berlin, 49-60.
- CAREY, J. & GELAUDE, D.** (2008): Systematic methods for Collecting and analyzing Multidisciplinary Team-based Qualitative Data, in: Guest, G. & MacQueen, K. (Eds.): *Handbook for Team-based Qualitative Research*, Plymouth, UK, 227-274.

- CASTOLDI, R., BROGLIA M. & PESARESI, M.** (2010): Image interpreters/interpreted images, study of recognition mechanisms: experiment setting at the JRC, in: Corbane, C., Carrion, D., Broglia M., and Pesaresi, M. (Eds.): Conference proceedings of the 2nd international Workshop on validation of geo-information products for crisis management (VALgEO), 13-15 October 2010, Ispra, Italy, 122-125.
- CHEN, C.-M., HEPNER, G. F. & FORSTER, R. R.** (2003): Fusion of hyperspectral and radar data using the IHS transformation to enhance urban surface features, in: ISPRS Journal of Photogrammetry and Remote Sensing, 58(1-2), 19-30.
- CHINI, M., PIERDICCA, N., EMERY, W. J.** (2009): Exploiting SAR and VHR Optical Images to Quantify Damage Caused by the 2003 Bam Earthquake, in: IEEE Transactions on Geoscience and Remote Sensing 47(1), 145-152.
- COLLIER, M.** (2010): Approaches to analysis in visual anthropology, in: Leeuwen, T. v. and Jewitt, C. (Eds.): Handbook of Visual Analysis, London, UK, 35-60.
- CONGALTON, R. & GREEN, K.** (2009): Assessing the Accuracy of Remotely Sensed Data. Principles and Practices, 183, Boca Raton, FL.
- DEFINIENS AG** (2009): eCognition Developer 8 – User Guide, München.
- DONNER, R. U.** (2008): Die visuelle Interpretation von Fernerkundungsdaten, Habilitationsschrift, Freiberg, 175 p.
- DRAGUT, L., TIEDE, D. & LEVICK, S.** (2010): ESP: a tool to estimate scale parameters for multi-resolution image segmentation of remotely sensed data, in: International Journal of Geographical Information Science, Vol. 24 (6), 859-871.
- EBERHARD, M.O., BALDRIDGE, S., MARSHALL, J., MOONEY, W. & RIX, G.J.** (2010): The MW 7.0 Haiti earthquake of January 12, 2010, in: USGS/EERI Advance Reconnaissance Team report: U.S. Geological Survey Open-File Report 2010-1048, 58 p.
- EERI – EARTHQUAKE ENGINEERING RESEARCH INSTITUTE** (2010): The 12 January 2010 Haiti Earthquake: Emerging Research Needs and Opportunities Report from Workshop held September 30 and October 1 2010. 43 p., Oakland, California.
- EGUCHI, R. T., HUYCK, C. K., GHOSH, S., ADAMS, B. J. & McMILLAN, A.** (2010): Utilizing new Technologies in Managing Hazards and Disasters, in: Showalter, P., Lu, Y. (Eds.): Geotechnologies and the Environment: Geospatial Techniques in Urban Hazard and Disaster Analysis, Dordrecht, Netherlands, 295-232.
- EHLERS, M.** (2010): Unsere Augen im All – Möglichkeiten und Grenzen moderner Fernerkundung, in: Arbeitskreis Fernerkundung (Vortrag) Heidelberg, Germany, 07-08 Oktober 2010.
- EHLERS, M., KLONUS, S.** (2004): Erhalt der spektralen Charakteristika bei der Bildfusion durch FFT basierte Filterung. – In: Photogrammetrie, Fernerkundung, Geoinformation 6, S. 495-506.
- ESCH, T., THIEL, M., BOCK, M., ROTH, A., DECH, S.** (2008): Improvement of Image Segmentation Accuracy Based on Multiscale Optimization Procedure, in: IEEE Geoscience and Remote Sensing Letters, Vol. 5 (3), 463-467.
- ESRI** (2009): ArcGIS Desktop Help, Redlands, CA, USA.

- GAMBA, P., ALDRIGHI, M. & STASOLLA, M.** (2010): Robust extraction of urban area extents in HR and VHR SAR images. – *IEEE Journal of Selected Topics in Earth Observations and Remote Sensing*, in press.
- GAMBA, P., DELL'ACQUA, F., LISINI, G. & TRIANNI, G.** (2007): Improved VHR Urban Area Mapping Exploiting Object Boundaries, in: *IEEE Transactions on Geoscience and Remote Sensing*, Vol. 45, no. 8, 2676–2682.
- GREY, W., LUCKMAN, A., HOLLAND, D.** (2003): Mapping urban change in the UK using satellite radar interferometry, in: *Remote Sensing of Environment* 87 (2003), 16–22.
- GRÜNEWALD, F., BINDER, A. GEORGES, Y.** (2010): Inter-agency real-time evaluation in Haiti: 3 Months after the earthquake, Final Report, Plaisians/Berlin, 93p.
- GRÜNTAL, G.** (1998): European Macroseismic Scale 1998 (EMS-98). *Cahiers du Centre Européen de Géodynamique et de Séismologie* 15, Centre Européen de Géodynamique et de Séismologie, Luxembourg, 99 p.
- GUO, H., LU, L., MA, J., PESARESI, M., YUAN, F.** (2009): An improved automatic detection method for earthquake-collapsed buildings from ADS40 image, in: *Chinese Science Bulletin*, Vol. 54 (18), 3303-3307.
- HAGENLOCHER, M.** (2010): Assessing the impact of IDP / Refugee Camps on the State of the Environment – An indicator-based approach utilizing high-resolution satellite time series of ZamZam, northern Dafur. Diploma thesis, Tübingen, 227 p.
- HEYWOOD, I., CORNELIUS, S., CARVER, S.** (2006): *An Introduction to Geographical Information Systems*, 426 p., Essex, GB.
- HOMMEL, M.** (2009): Verification of a building damage analysis and extension to surroundings of reference buildings, in: *Proceedings of the ISPRS Workshop 'Laserscanning' 09, The International Archives of the Photogrammetry, Remote Sensing and Spatial Information Sciences*, September 1-2, Paris, France, Vol. XXXVIII, Part 3/W8, 18-23.
- KAMPOURAKI, M. & WOOD, G.A.** (2006): The application of remote sensing to identify and measure sealed areas in urban environments, in: *ISPRS 1st International Conference on Object-based Image Analysis (OBIA 2006)*, July 2006, Salzburg, Austria. Vol. 36 4/C42, 5p.
- KERLE, N. & WIDARTONO, B.** (2008): Geoinformation-Based Response to the 27 May Indonesia Earthquake – an Initial Assessment, in: *Nayak, S., Zlatanova, S. (Eds.): Environmental Science and Engineering: Remote Sensing and GIS Technologies for Monitoring and Prediction of Disasters*, Berlin 11-23.
- KOEHLER, P.** (2005): User oriented Provision of Geo-Information in Disaster Management: Potentials of Spatial Data Infrastructures considering Brandenburg / Germany as an Example, in: *Oosterom, P., Zlatanova, S., Fendel, E. M. (Eds.): Geo-information for Disaster Management*, Berlin, 171-179.
- KRANZ, O., LANG, S., TIEDE, D., ZEUG, G., KEMPER, T., CASPARD, M. & CLANDILLON, S.** (2010): GMES Services for Conflict Prevention and Mitigation: Supporting the DG RELEX in Mission Planning, in: *Konecny, M., Zlatanova, S., Bandrova, T.L. (Eds.) Geographic Information and Cartography for Risk and Crisis Management*, New York, 179-196.

- LANG, S.** (2008): Object-based image analysis for remote sensing applications: modeling reality - dealing with complexity. In: Blaschke, T. Lang, S. Hay, T.J.(Eds.): Object-Based Image Analysis: Spatial concepts for knowledge-driven remote sensing applications. New York, 3-28.
- LANG, S. & BLASCHKE, T.** (2007): Landschaftsanalyse mit GIS. 404 p, UTB.
- LANG S., TIEDE D., ALBRECHT F. & FÜREDER P.** (2010): Automated techniques in rapid geospatial reporting - issues of object validity, in: Corbane, C., Carrion, D., Broglia M., and Pesaresi, M. (Eds.): Conference proceedings of the 2nd international Workshop on validation of geo-information products for crisis management (VALgEO), 13-15 October 2010, Ispra, Italy, 65-75.
- LEMOINE, G.** (2010): Validation of building damage assessments based on post-Haiti 2010 earthquake imagery using mutli-source reference data in: Corbane, C., Carrion, D., Broglia M., and Pesaresi, M. (Eds.): Conference proceedings of the 2nd international Workshop on validation of geo-information products for crisis management (VALgEO), 13-15 October 2010, Ispra, Italy, 33-34.
- LI, Y., LI, J. & CHAPMAN, M.A.** (2005): Automatically Extracting Manmade Objects from Pan-Sharpned High-Resolution Satellite Imagery Using a Fuzzy Segmentation Method, in: Oosterom, P., Zlatanova, S., Fendel, E. M. (Eds.): Geo-information for Disaster Management, Berlin, 641-653.
- LILLESAND, T. KIEFER, R. & CHIPMAN, J.** (2008): Remote sensing and image interpretation. 756 p., Hoboken, NJ.
- LÖFFLER, E., HONECKER, U., STABEL, E.** (2005): Geographie und Fernerkundung. Eine Einführung in die geographische Interpretation von Luftbildern und Fernerkundungsdaten. 287 p., Berlin/Stuttgart.
- MACQUEEN, K. M., MCLELLAN, E., KAY, K., MILSTEIN, B.** (1998): Codebook Development for Team-Based Qualitative Analysis, in: Field Methods 10 (1998), 31-36.
- MATSUOKA, M. & YAMAZAKI, F.,** (2004): Use of satellite SAR intensity imagery for detecting building areas damaged due to earthquakes, in: Earthquake spectra, 20 (3), 975-994.
- MEINEL, G. & HEROLD, M.** (2006): Automatische Ableitung siedlungsstruktureller Grundlegendaten auf Basis digitaler Bildverarbeitung, GIS und räumlicher Statistik, in: Strobl, J., Blaschke, T., Griesebner, G. (Eds.):Angewandte Geoinformatik 2006. Beiträge zum 18. AGIT-Symposium Salzburg, 423-429.
- MEINEL, G., HEROLD, H. & HECHT, R.** (2007). Gebäudebasierte, vollautomatische Erhebung und Analyse der Siedlungsstruktur - Grundlage für ein Monitoring und die Bewertung der Siedlungsentwicklung, in: Schrenk, M.; Popovich, V. V.; Benedikt, J. (Eds.): REAL CORP 2007, Proceedings / Tagungsband 18, Vienna, 815-824.
- MITCHELL, J.K.** (1999): Megacities and natural disasters: a comparative analysis, in: GeoJournal 49: 137-142.
- NAGA JYOTHI, B., BABU, G., MURALI KRISHNA, I.** (2008): Object Oriented and Multi-Scale Image Analysis: Strengths, Weaknesses, Opportunities and Threats – A Review, in: Journal of Computer Science 4 (9), 706-712.

- NAMEY E., GUEST, G. THAIRU, L. & JOHNSON, L.** (2008): Data Reduction Techniques for Large Qualitative Data Sets, in: Guest, G. & MacQueen, K. (Eds.): Handbook for Team-based Qualitative Research, Plymouth, UK, 137-161.
- NEUBERT, M.** (2006): Bewertung, Verarbeitung und segmentbasierte Auswertung sehr hoch auflösender Satellitenbilddaten vor dem Hintergrund landschaftsplanerischer und landschaftsökologischer Anwendungen. Dissertation, Institut für Photogrammetrie und Fernerkundung Universität Dresden. 172 p, Dresden.
- NIESYTO, H.** (2006): Bildverstehen als mehrdimensionaler Prozess. Vergleichende Auswertung von Bildinterpretationen und methodische Reflexionen, in: Marotzki, W., Niesyto, H. (Eds.): Bildinterpretation und Bildverstehen – Methodische Ansätze aus sozialwissenschaftlicher, kunst- und medienpädagogischer Perspektive. 286p, Wiesbaden.
- OGAWA, N. & YAMAZAKI, F.** (2000): Photo-Interpretation of building damage due to earthquakes using aerial photographs. Proceedings of the 12th World Conference on Earthquake Engineering, 01 January – 04 February, Auckland, New Zealand, 8p.
- OK, A. Ö.** (2008): Robust detection of buildings from a single color aerial image, in: ISPRS 2nd International Conference on Object-based Image Analysis (GEOBIA 2008), 04-09 August, Calgary, Canada Vol. XXXVII 4-C1, 6 p.
- PILZ, H. & STROBL, J.** (2002): Versiegelungsanalyse auf Basis digitaler Farbbathofotos mittels objektorientierter Bildverarbeitung, in: Blaschke, T. (Hrsg.): Fernerkundung und GIS - Neue Sensoren – innovative Methoden, Wichmann Verlag Heidelberg.
- PRESS, F. & SIEVER, R.** (2003): Allgemeine Geologie, Einführung in das System Erde, 723p, Heidelberg/Berlin.
- QUATTROCHI, D.A. & RIDD, M.K.** (1994): Measurement and analysis of thermal energy responses from discrete urban surfaces using remote sensing data, in: International Journal of Remote Sensing 15(10), 1991-2022.
- ROUSE, J. W., HAAS, R. H., SCHELL, J. A. & DEERING, D. W.** (1973): Monitoring vegetation systems in the Great Plains with ERTS, in: Third ERTS Symposium, NASA SP-351 I, 309-317.
- SAFER** (2010): Project User Board (WP40000), working paper for the internal agreement of user interests within the SAFER project, 11p.
- SCHÖPFER, E., LANG, S.,** (2006): Object-fate analysis – A virtual overlay method for the categorization of object transition and object-based accuracy assessment, in: ISPRS 1st International Conference on Object-based Image Analysis (OBIA 2006), July 2006, Salzburg, Austria. Vol. 36 4/C42, 4p.
- SCHÖPFER, E., LANG, S., ALBRECHT, F.** (2008): Object-fate analysis: Spatial relationships for the assessment of object transition and correspondence, in: Blaschke, T., Lang, S., Hay, G. J. (Eds.), Object-Based Image Analysis: Spatial Concepts for Knowledge-Driven Remote Sensing Applications, New York 785-802.
- SHANKAR, R. BJORGO, E. & DELL'ORO, L.** (2010): Accuracy assessment of post-earthquake building damage classification in Haiti, in: Corbane, C., Carrion, D., Broglia M., and Pesaresi, M. (Eds.): Conference proceedings of the 2nd international Workshop on validation of geo-information products for crisis management (VALgEO), 13-15 October 2010, Ispra, Italy, p. 21.

- SHINOZUKA, M., REJAIE, S.** (2000): Analysis of remotely sensed pre-and post-disaster images for damage detection, in: Society of Photo-Optical Instrumentation Engineers proceeding series, 5-9 March 2000, 13p.
- STEVENS, D.** (2008): Increasing the Use of Geospatial Technologies for Emergency Response and Disaster Rehabilitation in developing Countries, in: Nayak, S., Zlatanova, S. (Eds): Environmental Science and Engineering: Remote Sensing and GIS Technologies for Monitoring and Prediction of Disasters, Berlin, 57-71.
- STRAMONDO, S., BIGNAMI, C., CHINI, M., PIERDICCA, N., TERTULLIANI, A.** (2006): Satellite radar and optical remote sensing for earthquake damage detection: results from different case studies, in: International Journal of Remote Sensing, Vol. 27 (20), 4433-4447.
- SUMER, E., TURKER, M.** (2008): Building detection from high-resolution satellite imagery using adaptive fuzzy-genetic approach, in: ISPRS 2nd International Conference on Object-based Image Analysis (GEOBIA 2008), 04-09 August, Calgary, Canada Vol. XXXVII 4-C1, 6 p.
- TAHAYT, A., FEIGL, K.L., MOURABIT, T., RIGO, A., REILINGER, R., MCCLUSKY, S. FADIL, A., BERTHIER, E., DORBATH, L., SERROUKH, M., GOMEZ, F., BEN SARI, D.** (2009): The Al Hoceima (Morocco) earthquake of 24 February 2004, analysis and interpretation of data from ENVISAT ASAR and SPOT5 validated by ground-based observations, in: Remote Sensing of Environment, 113 (2), 306-316.
- TAUBENBÖCK, H.** (2008): Vulnerabilitätsabschätzung der erdbebengefährdeten Megacity Istanbul mit Methoden der Fernerkundung. Dissertation, Geographisches Institut, Universität Würzburg. 178 p., Würzburg.
- TAUBENBÖCK, H. , ESCH, T. , WURM, M. , ROTH, A. & DECH, S.** (2010a): Object-based feature extraction using high spatial resolution satellite data of urban areas, in: Journal of Spatial Science, 55: 1, 117-132.
- TAUBENBÖCK, H. , HELDENS, W., HEIDEN, U. & WURM, M.** (2010b) Physische Indikatoren für die Stadtplanung, in: Taubenböck, H., Dech, S. (Eds.) Fernerkundung im urbanen Raum, Darmstadt, 86-93.
- THIEL, M., ESCH, T., SCHENK, A.** (2008): Object-Oriented Detection of Urban Areas from TerraSAR-X Data, in: Proceedings of ISPRS 2008 Congress, Volume XXXVII, Part B8, Commission VIII, 23-27.
- TIEDE, D., HOFFMANN, C., FÜREDER, P., LANG, S.** (2010a), Machine-based damage assessment for rapid geospatial reporting: First experiences from the Haiti earthquake 2010, in: GI_Forum 2010 (Presentation), Salzburg, Austria, 6-9 July 2010.
- TIEDE, D., LANG, S., HÖLBLING, D., FÜREDER, P.** (2010b), Transferability of obia rule-sets for IDP camp analysis in Darfur. The International Archives of the Photogrammetry, Remote Sensing and Spatial Information Sciences, 38(4), 6p.
- TOMOWSKI, D., KLONUS, S., EHLERS, M., MICHEL, U. & REINARTZ, P.** (2010), Visualisierung von Veränderungen in Katastrophengebieten mittels texturbasierter Auswerteverfahren. Zipf, A., Behncke, K., Hillen, F. & Schaefermeyer, J. (Eds.), GEOINFORMATIK 2010 - "Die Welt im Netz", 164-171.
- TURKER, M. & CETINKAYA, B.** (2005): Automatic detection of earthquake-damaged buildings using DEMs created from pre- and post-earthquake stereo aerial photographs, in: International Journal of Remote Sensing, Vol. 26 (4), 823-832.

- TURKER, M. & SAN, B. T.** (2004): Detection of collapsed buildings caused by the 1999 Izmit, Turkey earthquake through digital analysis of post-event aerial photographs, in: *International Journal of Remote Sensing*, Vol. 25 (21), 4701-4714.
- TURKER, M. & SUMER, E.** (2008): Building-based damage detection due to earthquake using the watershed segmentation of the post-event aerial images, in: *International Journal of Remote Sensing*, Vol. 29 (11), 3073-3089.
- THIEL, M. & ESCH, T.** (2008): Object-Oriented Detection of Urban Areas from TerraSAR-X Data, - ISPRS Congress, Beijing.
- VEGA EZQUIETA, P., GONZÁLEZ JIMENEZ, A., GRANDONI, D., DI FEDERICO, A.** (2010): Product Design, the in-line quality control in the context of rapid geospatial reporting, in: Corbane, C., Carrion, D., Broglia M., and Pesaresi, M. (Eds.): *Conference proceedings of the 2nd international Workshop on validation of geo-information products for crisis management (VALgEO)*, 13-15 October 2010, Ispra, Italy, 53-61.
- VOIGT, S., KEMPER, T., RIEDLINGER, T., KIEFEL, R., SCHOLTE, K. & MEHL, H.** (2007): Satellite Image analysis for disaster and crisis-management support, in: *Transactions on Geoscience and Remote Sensing*, Vol. 25 (6), 1520-1528.
- VOIGT, S., RIEDLINGER, T., REINARTZ, P., KÜNZER, C., KIEFL, R., KEMPER, T. & MEHL, H.** (2005): Experience and Perspective of Providing Satellite Based Crisis Information, Emergency Mapping & Disaster Monitoring Information to Decision Makers and Relief Workers, in: Oosterom, P., Zlatanova, S., Fendel, E. M. (Eds.): *Geo-information for Disaster Management*, Berlin, 519-531.
- VOIGT, S., SCHNEIDERHAN, T., TWELE, A., GÄHLER, M., STEIN, E., MEHL, H.** (IN PRESS), Rapid Damage Assessment and Situation Mapping – Learning from the 2010 Haiti Earthquake, in: *Photogrammetric Engineering and Remote Sensing*, 24p.
- VU, T., T., MATSUOKA, M., YAMAZAKI, F.** (2004): Shadow analysis in assisting damage detection due to earthquakes from Quickbird imagery, in: *Proceedings of the 10th international society for photogrammetry and remote sensing congress*, 607-611.
- WALTER, V.** (2005): Object-based classification of integrated multispectral and LIDAR data for change detection and quality control in urban areas, in: *Proceedings of the 3rd international Symposium on Remote Sensing and Data Fusion Over Urban Areas (URBAN 2005)*, Phoenix, Arizona, 6p.
- WORLD BANK & UNITED NATIONS** (2010): *Natural Hazards, UnNatural Disasters: The Economics of Effective Prevention*, 276 p., Washington DC.
- WURM, M., TAUBENBÖCK, H., ROTH, A., DECH, S.** (2009): Urban structuring using multisensoral remote sensing data. By the example of the German cities Cologne and Dresden. – In: *Urban Remote Sensing Joint Event*, Shanghai, China. 8 pp.
- YAMAZAKI, F. AND KOUCH, K.** (2006) Machine-based Damage Detection of Buildings from High-Resolution Satellite Images, in: *Proceedings of the First European Conference on Earthquake Engineering and Seismology*, Geneva, Switzerland, 3-8 September 2006, 7p.
- YANO, Y., YAMAZAKI, F.** (2004): Building damage detection of the 2003 Bam, Iran earthquake using Quickbird images based on object-based classification, in: *25th Asian Conference on Remote Sensing*, Vol. 1, 624-629.
- ZHOU, W., HUANG, G., TROY, A., CADENASSO, M.L.,** (2009): Object-based land cover classification of shaded areas in high spatial resolution imagery of urban areas: A comparison study, in: *Journal of Remote Sensing of Environment*, 113, 1769-1777.

Internet Resources

ALERTNET (2011): Haiti earthquake 2010: Haiti's biggest tremor in 200 years

http://www.alertnet.org/db/crisisprofiles/HT_QUAKE.htm (10.03.2011)

CRED – CENTRE FOR RESEARCH ON THE EPIDEMIOLOGY OF DISASTERS (2009): Annual Disaster Statistical Review 2009: The numbers and trends

http://cred.be/sites/default/files/ADSR_2009.pdf (10.03.2011)

DIGITAL GLOBE CORP. (no date): Standard Satellite Imagery

http://www.digitalglobe.com/index.php/48/Products?product_id=2 (07.03.2011)

OAK RICH NATIONAL LABORATORY (no date): LandScan™

<http://www.ornl.gov/sci/landscan/> (02.04.2011 – login required)

GMES – GLOBAL MONITORING FOR ENVIRONMENT AND SECURITY (no date): Emergency Management

<http://www.gmes.info/pages-principales/services/emergency-management/> (11.03.2011)

LGR / AFP / REUTERS (2010): Brotpreis in Russland steigt kräftig an

<http://www.spiegel.de/wirtschaft/unternehmen/0,1518,711296,00.html> (11.08.2010)

KAUFMANN, M. (2010): Deutsche Industrie warnt vor Rohstoff-Engpass

<http://www.spiegel.de/wirtschaft/unternehmen/0,1518,711559-2,00.html> (15.08.2010)

OCHA – UNITED NATIONS OFFICE FOR THE COORDINATION OF HUMANITARIAN AFFAIRS (2010): A country should not depend on the international community.

<http://www.irinnews.org/Report.aspx?ReportID=89831> (10.03.2011)

RELIEFWEB (no date): Map Centre Haiti

<http://www.reliefweb.int/rw/rwb.nsf/doc404?OpenForm&rc=2&cc=hti> (07.12.2010)

RESPOND – GMES SERVICES SUPPORTING HUMANITARIAN RELIEF, DISASTER REDUCTION & RECONSTRUCTION (2008): About Respond

<http://www.respond-int.org/respondlive/> (16.01.2011)

STROHMEYER, H. (2010): Krisenprävention dient auch unserer Sicherheit

<http://www.zeit.de/politik/ausland/2010-09/Millenniumsgipfel-Nothilfe> (22.10.2010)

THW (no date): Einheiten und Technik

http://www.thw.de/cln_172/DE/Einheiten-Technik/einheiten-technik_node.html (07.03.2011)

UNEP / GRID-ARENDAL (2005): Trends in natural Disasters

<http://maps.grida.no/go/graphic/trends-in-natural-disasters> (16.11.2010)

USGS - U.S. GEOLOGICAL SURVEY (2010): Magnitude 7.0 – Haiti Region.

<http://earthquake.usgs.gov/earthquakes/eqinthenews/2010/us2010rja6/> (14.01. 2011)

ZKI – Zentrum für Satellitengestützte Kriseninformation (no date): About ZKI

<http://www.zki.dlr.de/> (03.08.2010)

Declaration

I hereby declare that this thesis was carried out on my own accord without third party assistance and without using further than the cited sources and auxiliaries. All quotations are marked adequately. This thesis was not submitted to another examination board and was not published.

Ich erkläre hiermit, dass ich diese Diplomarbeit selbstständig ohne Hilfe Dritter und ohne Benutzung anderer als der angegebenen Quellen und Hilfsmittel verfasst habe. Alle den benutzten Quellen wörtlich oder sinngemäß entnommenen Stellen sind als solche einzeln kenntlich gemacht. Diese Arbeit ist bislang keiner anderen Prüfungsbehörde vorgelegt worden und auch nicht veröffentlicht worden.

Tübingen,

den 20. Juni 2011

Stefan Klett

Appendix

Appendix 1	Focus group damage assessment guideline
Appendix 2	eCognition process tree
Appendix 3	Maps
Appendix 4	SOP
Appendix 5	Compact disc

Appendix 1

Visuelle Interpretation von Fernerkundungsdaten zur Schadensabschätzung nach Erdbeben

1	Einlesen der Daten.....	2
1.1	Darstellung der Daten	3
2	Schaden erkennen	3
2.1	Vergleich der pre- und post-disaster Bilder	4
3	Schaden digitalisieren	5
3.1	Editieren des Shapefiles collapse	5
4	Dokumentation	5
5	Speichern der Ergebnisse	5

2 Einführung

Am Beispiel des Erdbebens von Haiti im Januar 2010 wird mittels einer empirischen Untersuchung eine Methodik zur visuellen Interpretation von hochaufgelösten Fernerkundungsdaten getestet. Im Folgenden wird eine Einführung in die Schadenserkenkung sowie eine Anleitung in die Methodik gegeben. Das Ziel ist eine schnelle und einfache Erkennung von beschädigten und eingestürzten Gebäuden. Dies soll anhand von zweier Teams geschehen, da somit in einem kurzen Zeitraum jedes Gebiet doppelt analysiert wird. Die erkannten Schäden sollen durch Punkte digitalisiert und als .shp Datei gespeichert werden. Der Zeitaufwand beträgt eine Stunde. Um eine realitätsnahe Stresssituation zu simulieren sollten Sie die Zeitvorgabe einhalten.



Abb.1: Haiti. Quelle: Google Earth.

1. Einlesen der Daten

Zu Beginn der Auswertung starten Sie bitte ArcGIS. Anschließend öffnen Sie die bereitgestellten Daten aus dem Ordner ‚Vergleichsgruppenanalyse‘. Dieser enthält neben dem Skript folgende Dateien:

- Collapse
- Grid
- Footprint
- Geoeye_post
- Geoeye_pre

Bringen Sie die Daten per drag&drop in die hier angegebene Reihenfolge. Dies ist wichtig für die spätere Analyse.

1.1 Darstellung der Daten

Um eine optimale Darstellung für die Interpretation zu erhalten ist es notwendig die eingelesenen Daten anzupassen. Durch klicken auf das jeweilige Symbol im ‚table of content‘ können die Darstellungsweisen angepasst werden. Verwenden Sie die folgenden Symbole:

- Collapse:** Rotes Dreieck, Größe 14
- Grid:** Hellgrün (ohne Füllung), Strichstärke 1,5
- Footprint:** Hollow, Strichstärke 1
- Geoeye_post:** Kanalkombination 1-2-3
- Geoeye_pre:** Kanalkombination 3-2-1

2. Schaden erkennen

Im Vergleich zu intakten Gebäuden weisen eingestürzte bzw. beschädigte Häuser unterschiedliche Merkmale auf. Als solche sind unter anderen sehr kleinräumige Schattenanteile, Schutt und wenig klare Konturen zu erkennen. Die Gebäude sind also nicht scharf von der Umgebung abgetrennt oder leicht verdreht.



Abb. 3: Pre-/Post-disaster Vergleich eines Gebäudes. Quelle: Digital Globe
(World View II Daten vom 13.12.2009 und 03.02.2010)



Abb. 3: Im linken Bild ist ein zerstörtes Haus zu sehen. Im Bild rechts sieht man den Vergleich von zerstörter zu intakter Siedlung. Quelle: Google Earth (13. Januar 2010)

Aufgabe 1:

Suchen Sie folgende Gebäude mit den dazugehörigen Koordinaten in Google Earth (UTM):

- Casernes Dessalines: 18.541829°, -72.339752°
- Palais National: 18.543128°, -72.338825°
- Administration Générale des Contributions: 18.545073°, -72.340024°
- Cathédrale Notre-Dame de L'Assomption: 18.549070°, -72.338529°

Welche typischen Erscheinungsbilder an und um die beschädigten Gebäude erkennen Sie?

Vergleichen Sie die Bilder mit denen vom 13. Januar 2010 und 26. August 2009

Tipp: Im Menü unter ‚Ansicht: Historisches Bildmaterial‘ aktivieren.

2.1 Vergleich der pre- und post-disaster Bilder

Öffnen Sie unter View:Toolbars die Menüleiste ‚Effects‘. Aktivieren Sie das Swipe-Tool und legen Sie als Ziel das Bild ‚geoeye_post‘ fest. Nun können Sie mit einem Click den Pfeil bewegen und das darunter liegende pre-Bild erscheint.

!! Achtung: Ein leichter Versatz der beiden Bilder resultiert aus den verschiedenen Aufnahmewinkeln !!

3. Schaden digitalisieren

Orientieren Sie sich an den Gridzellen. Beginnen Sie an einer Ecke und untersuchen Sie jede einzelne Zelle. Wenn Sie einen Schaden erkennen setzen Sie einen Punkt. Die Layer ‚footprint‘ dient als visuelle Hilfe zur Erkennung von Schaden. Sollten Sie unsicher sein, ob ein Schaden vorliegt, können Sie die Layer aktivieren um beispielsweise Drehungen oder Änderungen an der Grundform eines Gebäudes festzustellen. Deaktivieren Sie die Layer, wenn Ihnen zu viele Informationen angezeigt werden. Ein geeigneter Maßstab für die Analyse liegt bei etwa 1:1.000.

3.1 Editieren des Shapefiles „collapse“

Das Shapefile „collapse“ dient der Visualisierung der beschädigten Häuser. Dies geschieht mittels der Edit-Funktion. Öffnen Sie unter View:Toolbars die Menüleiste ‚Editor‘. Wählen Sie ‚collapse‘ als Ziel aus. Mit dem Sketch-Tool (Bunstift) können Sie die beschädigten Häuser mit einem Punkt markieren. Vergessen Sie nicht ihre Ergebnisse zu speichern (Editor: Save Edits).

!! Achtung: Um keine Gridzelle auszulassen ist es bei der Digitalisierung sinnvoll Reihe für Reihe zu betrachten !!

4. Dokumentation

Während der Schadensanalyse wird es in Ihrem zweier Team zu unterschiedlichen Einschätzungen kommen. Daher ist es von großem Interesse weshalb es zu Unterschieden kommt und wie Sie in Ihrem Team damit umgegangen sind. Bitte beantworten Sie die folgenden Fragen:

1. Wo kam es zu Abweichungen bei der visuellen Interpretation?
2. Wie oft kamen Abweichungen vor und wie wurden diese gelöst?

5. Speichern der Ergebnisse

Erstellen Sie einen Ordner und legen Sie darin die Ergebnisse ab. Dieser sollte alle 6 Files mit dem Namen collapse.* und ein Textfile mit der Dokumentation beinhalten. Bitte schicken Sie diesen Ordner gezippt per Mail an:

Stefan.Klett@dlr.de

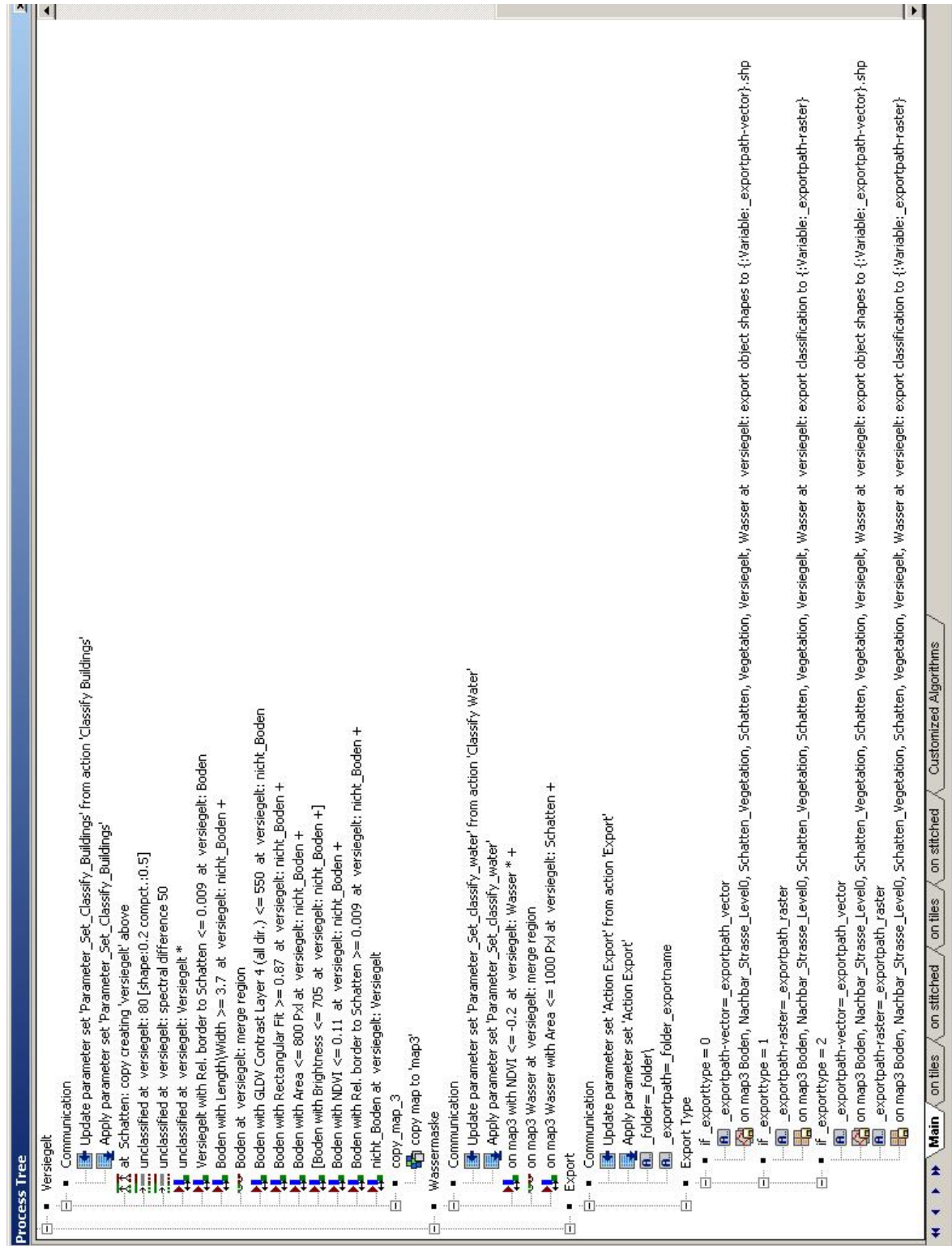
Vielen Dank für Ihre Unterstützung!

Appendix 2

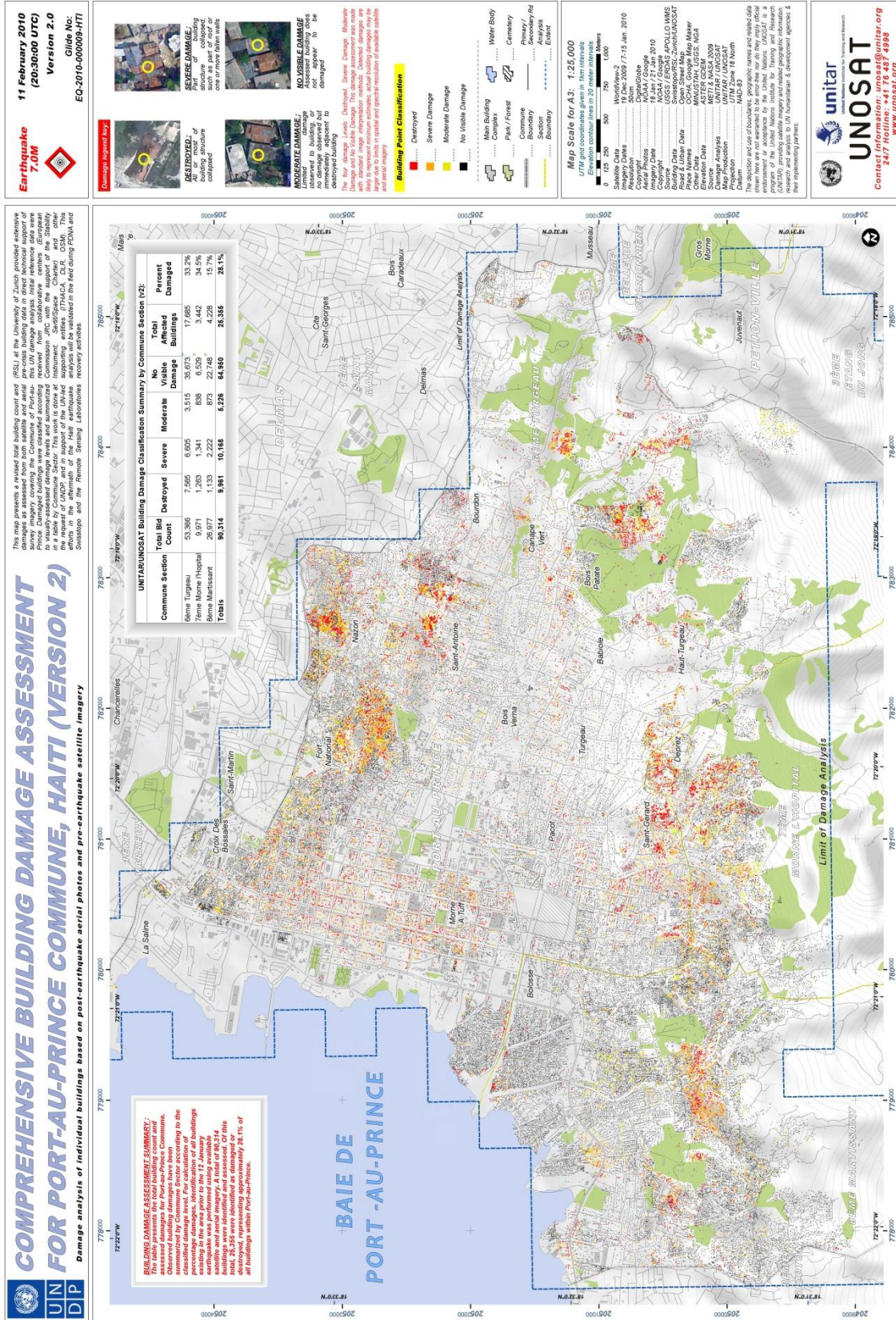
Process Tree

- create project
 - command ID(57600)
 - copy_map
 - copy map to 'map_street'
 - Strassenmaske
 - Communication
 - Update parameter set 'Parameter_Set_Classify_Streets' from action 'Strassenmaske'
 - Apply parameter set 'Parameter_Set_Classify_Streets'
 - Segmentierung_L1
 - Segmentierung_Strasse_L1
 - Klassifikation_Strasse
 - Segmentierung_L0
 - on map_street at L1: copy creating 'L1' below
 - Segmentierung_L0
 - Nachbar_Strasse
 - on map_street at L0: copy creating 'L0' below
 - Klassifikation_Strasse
 - on map_street with Rel. border to street > 0 at L0: Nachbar_Strasse_Level0
 - [on map_street with NDVI >= 0.29 at L0: unclassified]
 - on map_street Nachbar_Strasse_Level0 at L0: merge region
 - minimize_neighbours
 - on map_street Nachbar_Strasse_Level0 at L0: 20 [shape:0.9 compact:-0.0] creating 'L3'
 - on map_street unclassified at L3: spectral difference 40
 - Klassifikation_Strasse (*)
 - on map_street with Rel. border to street > 0 at L3: Nachbar_Strasse_Level3
 - on map_street Nachbar_Strasse_Level0 at L3: Nachbar_Strasse_Level3
 - on map_street Nachbar_Strasse_Level3 with Length\Width <= 3.8 at L3: unclassified
 - Klassifikation_Strasse (*)
 - on map_street Nachbar_Strasse_Level3, street at L3: merge region
 - Klassifikation_Strasse (*)
 - loop: on map_street street at L3: grow into all where rel. area of object pixels in (5 x 5) > 0.5
 - Vegetationsmaske
 - Segmentierung_NDVI
 - Communication
 - Update parameter set 'Parameter_Set_Classify_Vegetation' from action 'Classify_Vegetation'
 - Apply parameter set 'Parameter_Set_Classify_Vegetation'
 - Klassifikation_Vegetation
 - on main Vegetation at L2: merge region
 - Schatten
 - Communication
 - Update parameter set 'Parameter_Set_Classify_Shadow' from action 'Classify_Shadow'
 - Apply parameter set 'Parameter_Set_Classify_Shadow'
 - Brightness_Shadow_2 = [Brightness_Shadow]+160
 - Vegetation at L2: copy creating 'Schatten' above
 - unclassified at Schatten: 20 [shape:0.6 compact:0.5]
 - unclassified at Schatten: Schatten *
 - Schatten with Area >= 650 Pxl at Schatten: unclassified +
 - Schatten with Rel. border to Vegetation > 0.25 and NDVI > 0.1 at Schatten: Schatten_Vegetation * +
 - Versiegelt

Main | on files | on stitched | on tiles | on stitched | Customized Algorithms



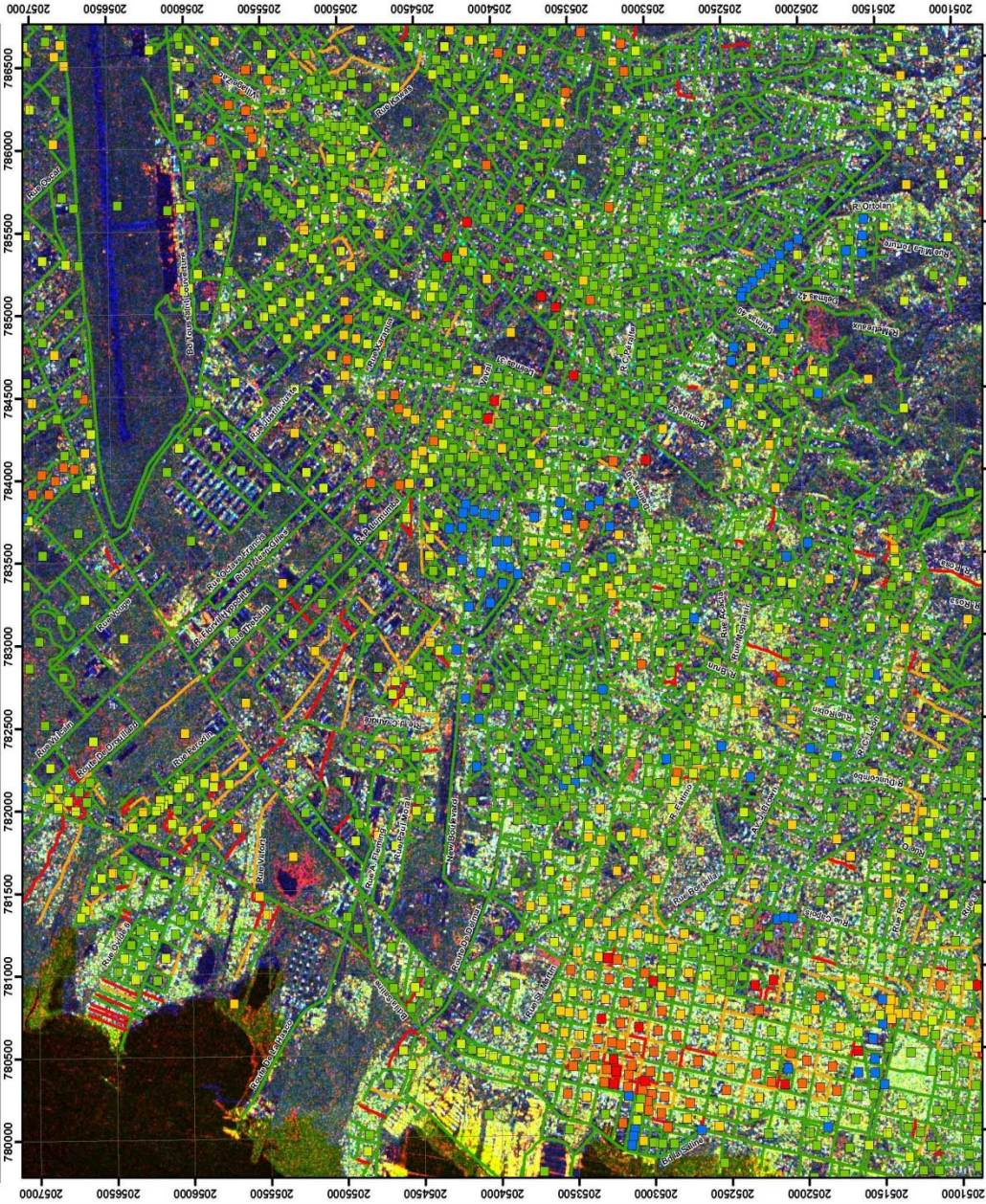
Appendix 3



UNCLASSIFIED,
For Official Use Only

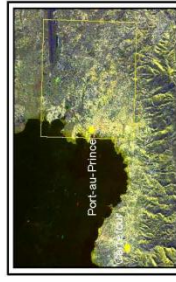
18/01/2010

DAMAGE ASSESSMENT FOR THE HAITI EARTHQUAKE, 12th January 2010



UNCLASSIFIED,
For Official Use Only

RGR001-MTC-01



Projection: Universal Transverse Mercator
Zone: 18N
Datum: WGS84

G-mesaic's services are certified by UNOSG, Cartographic Section, Spanish Road Corps. The road assessment was produced by the G-Mesaic Road Geospatial Information System (G-Mesaic Road Network) using the Esri Image Analysts. The Esri Image Analysts were performed by the Esri Image Analysts. The Esri Image Analysts were performed by the Esri Image Analysts. The Esri Image Analysts were performed by the Esri Image Analysts.

Block Damage Assessment

- Out of the optical image
- No visible damage from above
- Suspicion of small damages
- Slight visible damages
- Substantial damages, partial collapse
- Facility destroyed

Roads Condition

- Free of obstacles
- Transit is very limited
- Street is totally blocked
- Not available

Cosmo-SkyMed Interferom. Land Use

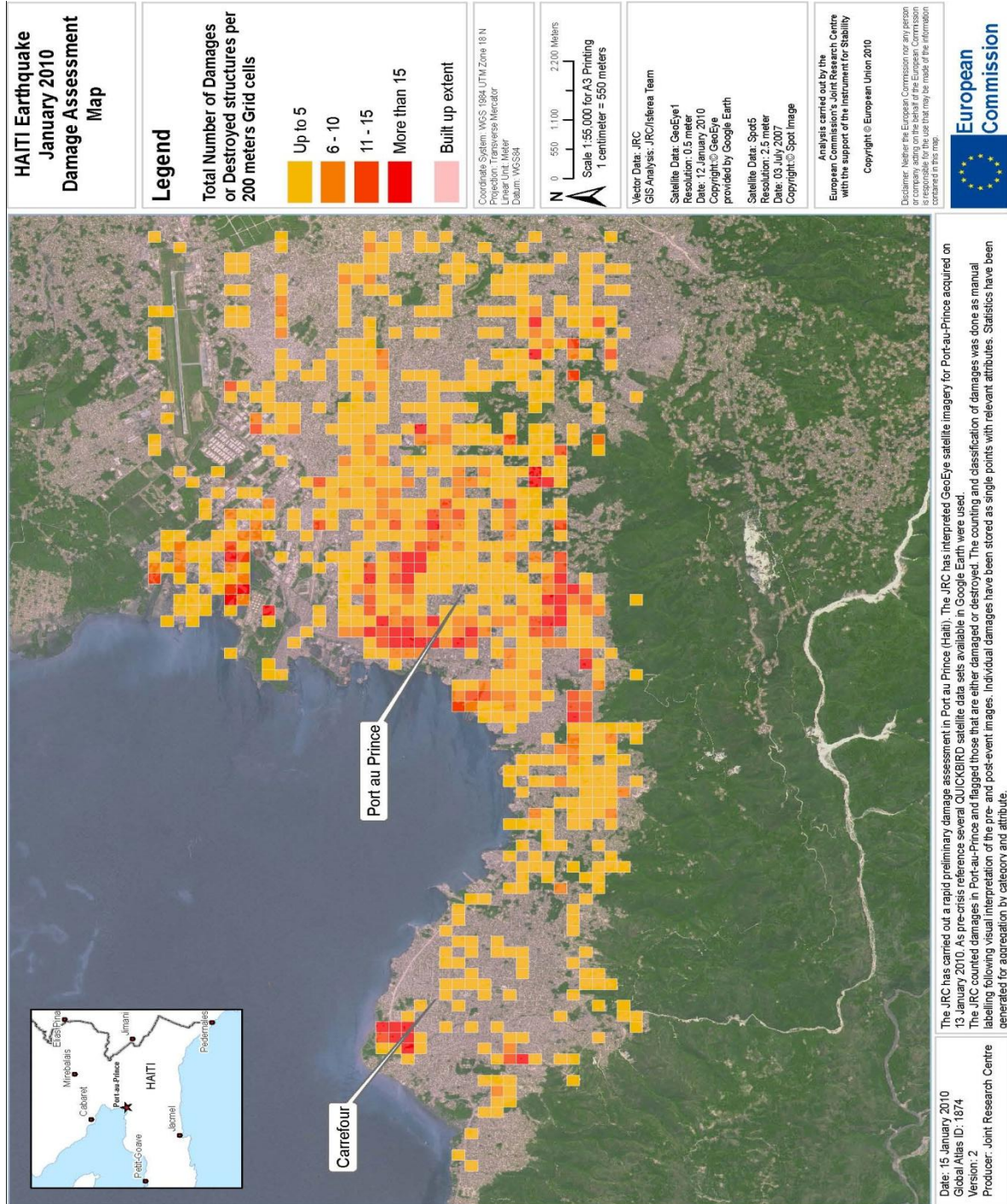
- RGB
- Abs value pre-post difference
- Mean value pre/post
- Interferom. coherence pre-post

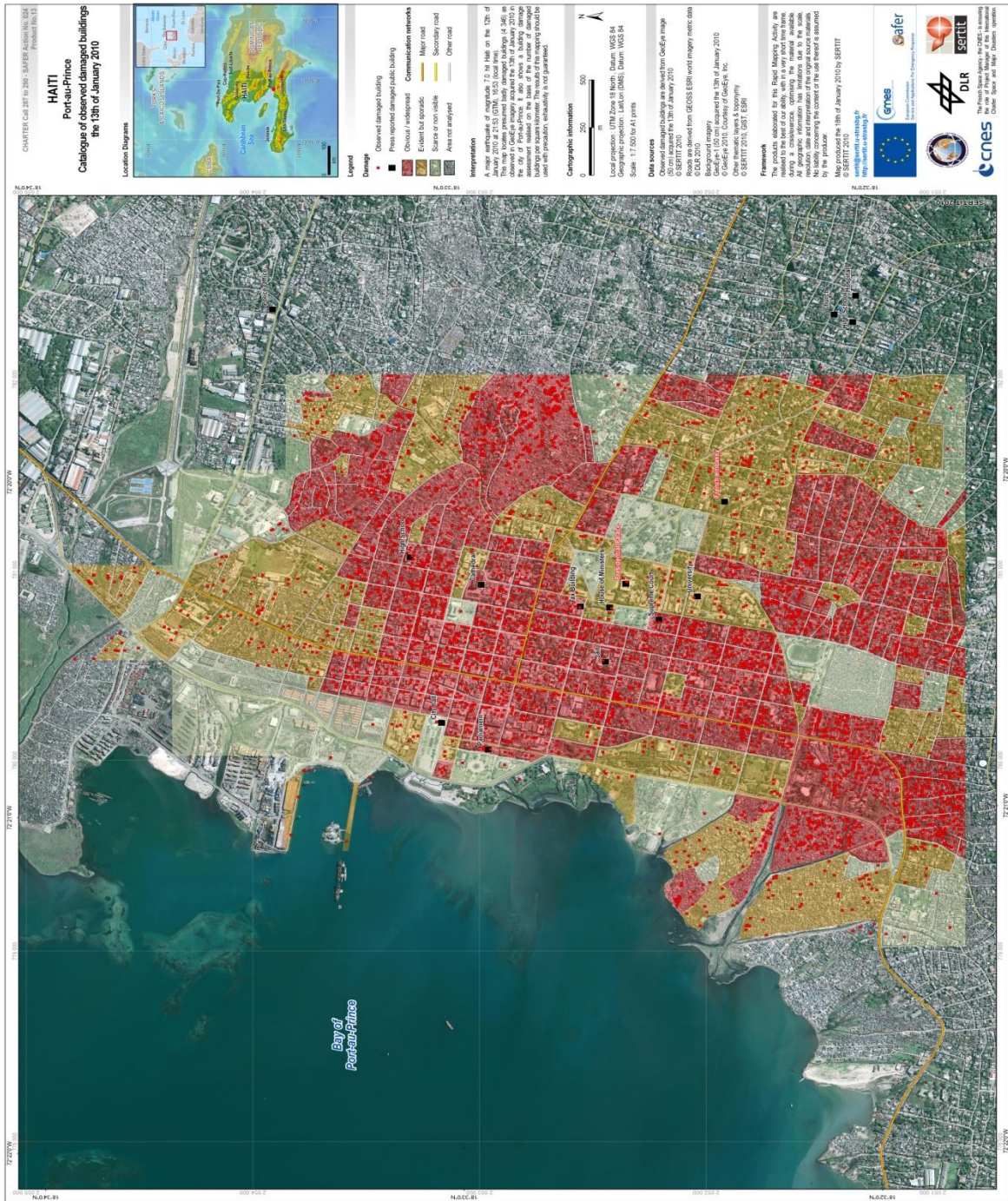
Scale: 1 centimeter = 250 meters

This product is covered by the EU Security Regulation 2007/24/EC. Boundary of the information model is not endorsed from the producer. The producer accepts no legal responsibility or liability whatsoever with regard to the use of this product.

egebos

European Union Satellite Centre, Avenida de Corcova 60174, 010 0006
28000 Torrejón de Ardoz, Madrid, España Tel: (+34) 91 621 6000 Fax: (+34) 91 621 6008





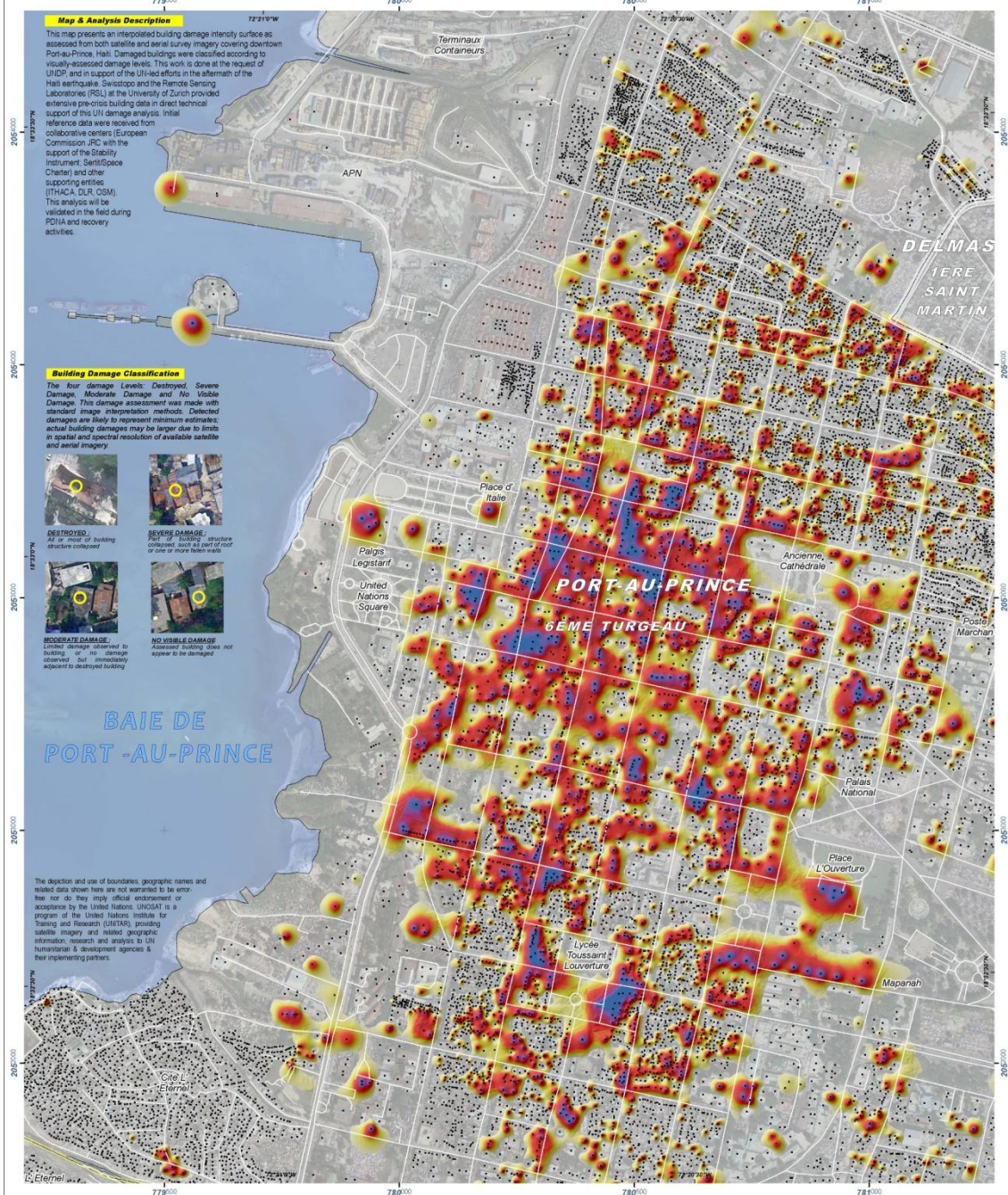


INTENSITY OF BUILDING DAMAGES IN DOWNTOWN PORT-AU-PRINCE, HAITI

Earthquake
7.0M

15 February 2010
(19:30:00 UTC)
Version 2.0
Glide No:
EQ-2010-000009-HTI

Damage analysis of individual buildings based on post-earthquake aerial photos and pre-earthquake satellite imagery



Map & Analysis Description

This map presents an interpolated building damage intensity surface as assessed from both satellite and aerial survey imagery covering downtown Port-au-Prince, Haiti. Damaged buildings were classified according to visually-assessed damage levels. This work is done at the request of UNDP, and in support of the UN-led efforts in the aftermath of the Haiti earthquake. SwissTopo and the Remote Sensing Laboratory (RSU) at the University of Zurich provided extensive pre-earthquake building data in direct technical support of this UN damage analysis. Initial reference data were received from collaborative centers (European Commission JRC with the support of the Stability Instrument, SeritSpace Charter) and other supporting entities (ITHACA, DLR, OSM). This analysis will be validated in the field during PDIA and recovery activities.

Building Damage Classification

The four damage levels: Destroyed, Severe Damage, Moderate Damage and No Visible Damage. This damage assessment was made with standard image interpretation methods. Deleted damages are likely to represent minimum estimates; actual building damages may be larger due to limits in spatial and spectral resolution of available satellite and aerial imagery.



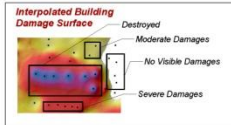
DESTROYED: All or most of building structure collapsed.

SEVERE DAMAGE: Part of building structure collapsed, such as part of roof or one or more balconies.

MODERATE DAMAGE: Limited damage observed to building, or no damage observed but immediately adjacent to destroyed building.

NO VISIBLE DAMAGE: Assessed building does not appear to be damaged.

The depiction and use of boundaries, geographic names and related data shown here are not warranted to be correct nor do they imply official endorsement or acceptance by the United Nations. UNOSAT is a program of the United Nations Institute for Training and Research (UNITAR), providing satellite imagery and related geographic information research and analysis to UN humanitarian & development agencies & their implementing partners.



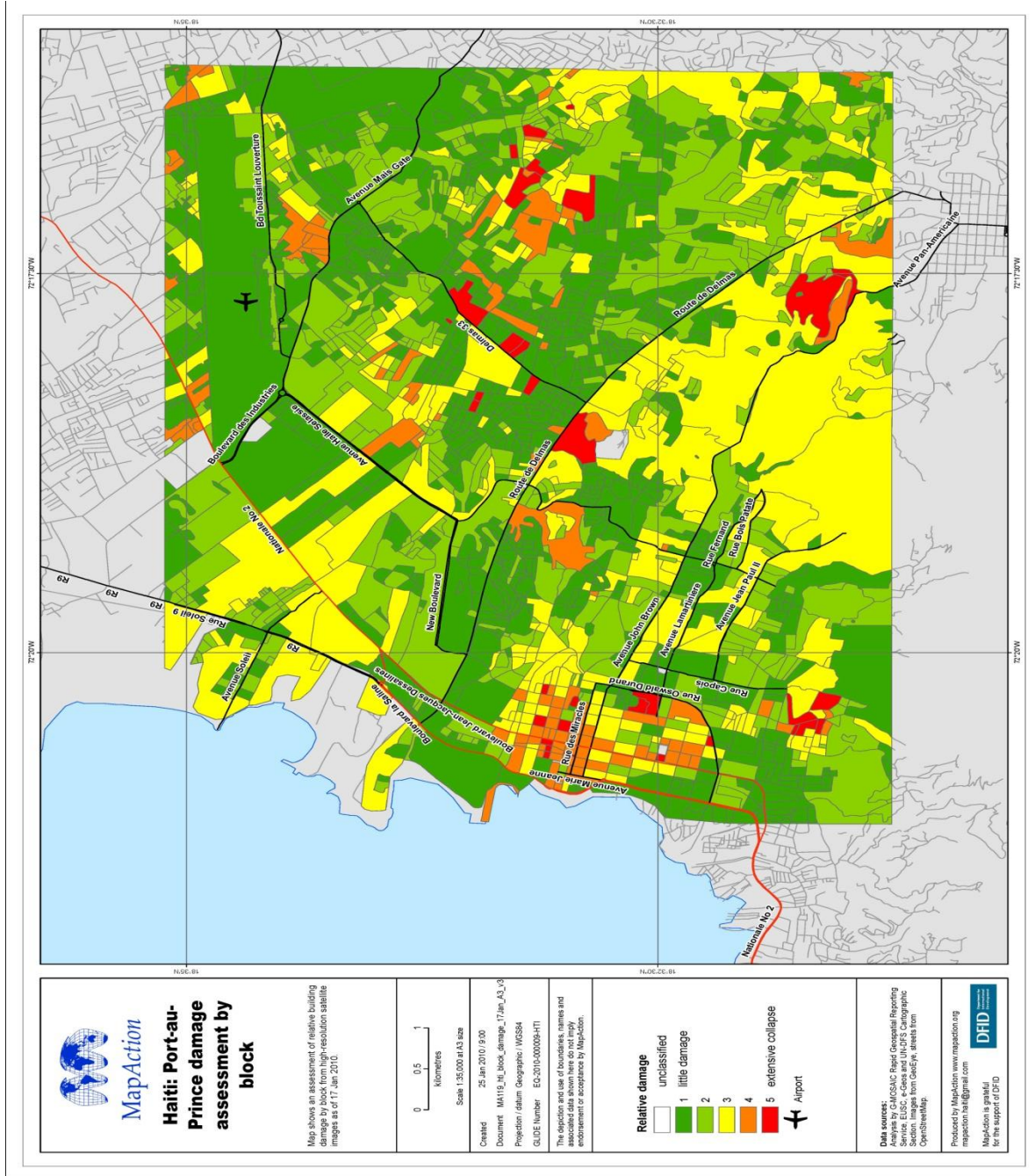
Commuune Boundary	Primary / Secondary Rd
Section Boundary	Analysis Extent

Satellite Data	WorldView-2	Copyright	NOAA / Google	Other Data	MINUSTAH, USGS, NGA
Imagery Dates	19 Dec 2009 / 7-15 Jan 2010	Source	USGS / ERDAS APOLLO WMS	Elevation Data	ASTER GDEM
Resolution	50cm	Source	SwissTopo/RSU, Zurich/UNOSAT	Source	METI & NASA 2009
Copyright	DigitalGlobe	Landcover Data	CNIGS, Informa, OSM, OCHA	Damage Analysis	UNITAR / UNOSAT
Aerial Photos	NOAA / Google	Road & Urban Data	Open Street Map	Map Production	UNITAR / UNOSAT
Imagery Date	16 Jan / 21 Jan 2010	Place Names	OCHA, Google Map Maker	Projection	UTM Zone 18 North - NAD-83

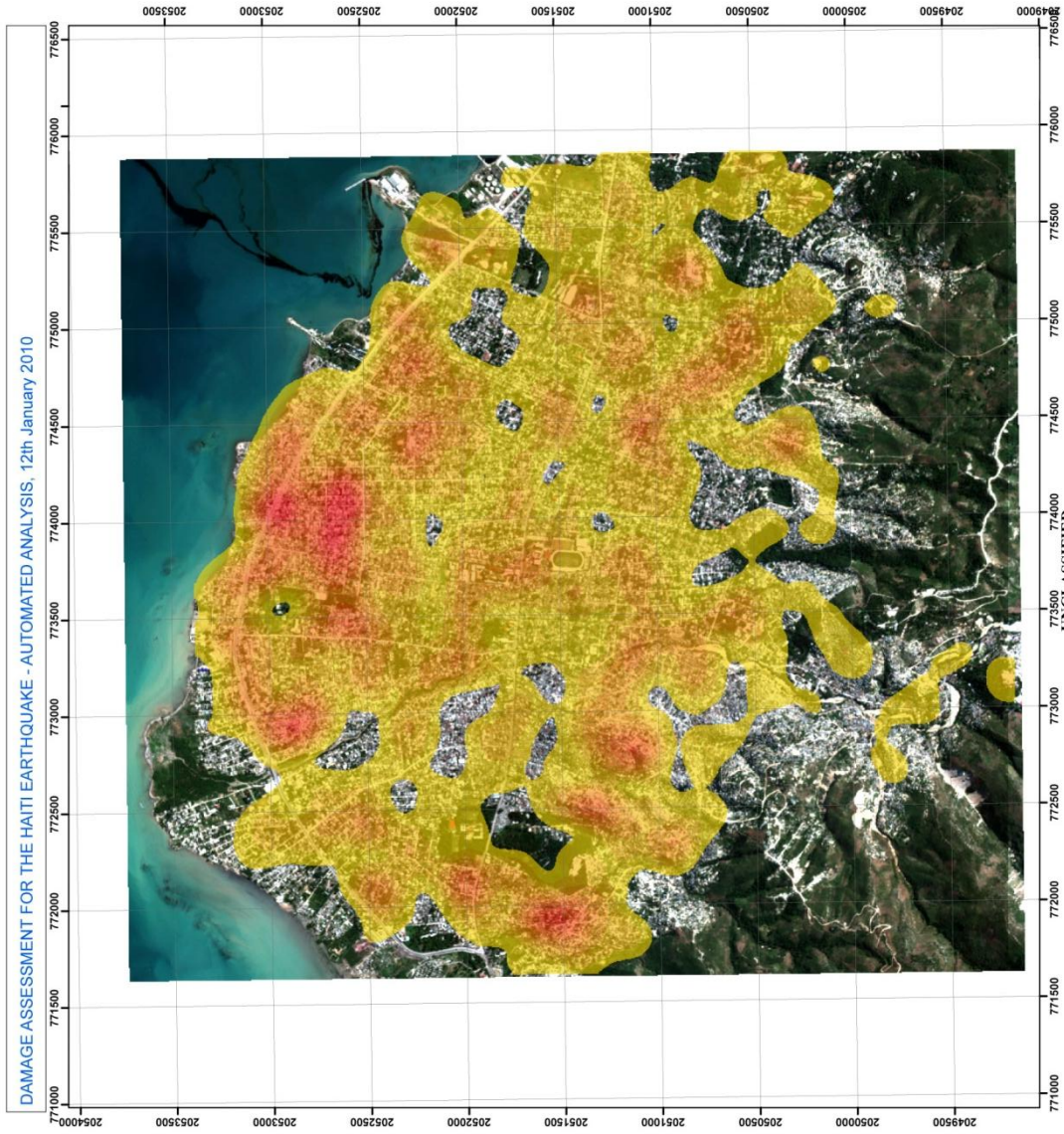
Map Scale for A3: 1:7,500 (A4 Print Scale 1:10,500)
UTM grid coordinates given in 500m intervals

unitar
United Nations Institute for Training and Research

UNOSAT
Contact Information: unosat@unitar.org
24/7 Hotline: +41 76 487 4998
www.unosat.org



19/01/2010
 UNCLASSIFIED,
 For Official Use Only
 DAMAGE ASSESSMENT FOR THE HAITI EARTHQUAKE - AUTOMATED ANALYSIS, 12th January 2010



Projection: Universal Transverse Mercator
 Zone: 18N
 Spheroid: WGS84
 Datum: WGS84
 Image: Geo-Eye
 Date: 19/01/2010

GIMOSAIC FOR version acquired by:
 UN
 Spanish Red Cross
 This information has been made available to the public
 was produced by the G-MOSAIC Report Generator
 Object based: Reporting Service
 Produced by: Geo-Information Systems, Salzburg University
 (supported by DEFENSE)

Density of damaged buildings

Appendix 4



QMH Cluster AF Band 3 – Produktrealisierung

Image Analysis - EQ-Damage Assessment

Document ID: QMH-CAF-E.ZKI-E.RM-EP XX.XX
Issue: 1.00
Date: 04.04.2011

Author: gez. Stefan Klett
04.04.2011, Stefan Klett

Reviewed: _____

Approved: _____

Released: _____



Image Analysis - ClassificationEQ-Damage
Assessment

QM/CAF-E.ZKI-E.RM-EP2.03.03 XXXXX

Issue 5.00

Date 04.04.2011

Page 2 of 5

Changes to this document

Issue	Date	Chapter	Change
1.00	04.04.2011	All	First release



Entity Name & Entity Path

Entity Name:	Entity Rapid Mapping (E.RM)
Entity Path:	Entity ZKI (E.ZKI) - Entity Rapid Mapping (E.RM)

Process Identification

Process Name	Image Analysis - Earthquake Damage Assessment
Process ID	QMH-CAF-E.ZKI-E.RM-EP XX.XX
Process Manager	Tobias Schneiderhan

Purpose of Process

Team-based visual interpretation of earthquake damages in urban areas from image data into semantic classes which can be of use for further assessments and maps.

Responsibility: Image Processing Manager, supported by OP-Service

Product In

- Remote sensing data (multispectral optical satellite data) from [\\MappingServer\mapping\YYYY\activation_folder\isat_data\sensor\sensor_in](#) or [\\MappingServer\mapping\YYYY\activation_folder\isat_data\sensor\sensor_proc](#)
- Auxiliary data for classification and validation purposes (very high resolution data, street data)

Process

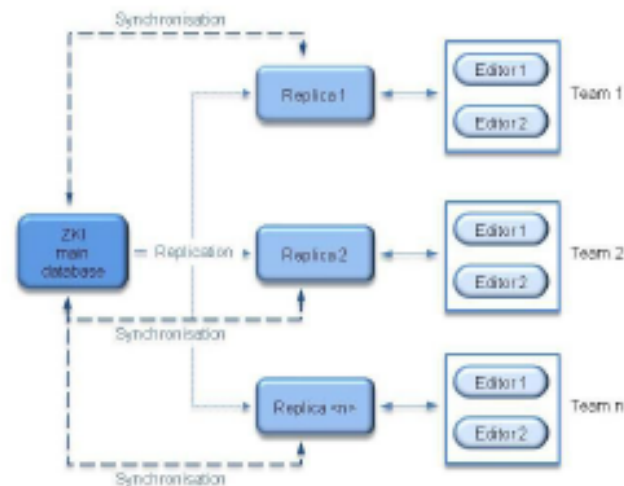
Comment: Damage assessment for earthquake disasters is the process of team-based visual interpretation of optical very high resolution data. After an initial introduction and gauging of the teams a multi-temporal analysis of pre- and post-disaster data is carried out in a multi-user GIS environment. With assistance of supporting information teams of two interpreters digitize visual detected damages, classifying them into different classes on screen. Regular breaks can be used for further adjustment of the classification process, depending on the area of investigation and available data. Short moderated discussion ensure consistency of interpretation results. According to the damage extent the final interpretation results are represented grid-based, block-based or for single buildings. If necessary, the aggregated visualisation ensues with a point-in-polygon analysis.

Recommended software packages:

- DEFINIENS Developer for object based classification to extract GIS ready supporting information, classes depending on neighbourhood or object structures, etc.



- ArcGIS for digitizing damages on multi-user layer files, buffering streets, create city blocks, perform point-in-polygon analysis, etc.



Process Steps:

- Start norming and gauging
- Buffer street data according to road function type
- Dissolve buffered street data and save in
[\\MappingServer\mapping\YYYY\activation_folder\gis_data_DLR\roads\DLR_YYYYMMDD_COUNTRY_Earthquake_CITY_roads_PROJECTION_.shp](#)
- Run eCognition architect solution 'EQ_action_library'
 - Define thematic layer (street data)
 - Define thresholds for predetermined classes
 - save output in
[\\MappingServer\mapping\YYYY\activation_folder\gis_data_DLR\obla\DLR_YYYYMMDD_COUNTRY_Earthquake_CITY_OBIACLASSNAME_PROJECTION_VERSION.shp](#)
- Produce Grid of 100 m x 100m
- Perform team-based visual interpretation according to manual described in
[\\MappingServer\mapping\YYYY\activation_folder\log\EQ_mapping_gludeline.doc](#)
- Save all temporary results in
[\\MappingServer\mapping\YYYY\activation_folder\gis_data_DLR\temp](#)



Image Analysis - ClassificationEQ-Damage
Assessment

QMH-CAF-E.ZKJ-E.RM-EP2.03.03 XX.XX

Issue 5.00

Date 04.04.2011

Page 5 of 5

- Save all final outputs in `\\MappingServer\mapping\YYYY\activation_folder\gis_data_DLR\` according to nomenclature described in `\\MappingServer\mapping\YYYY\activation_folder\log\nomenclature.doc`

Product Out

- Classified data (raster file or Shapefile) in `\\MappingServer\mapping\YYYY\activation_folder\gis_data_DLR\DLR_YYYYMMDD_COUNTRY_Earthquake_CITY_damageassessment_PROJECTION_VERSION.shp`

Appendix 5

